

ADVANCES IN LIQUID CHROMATOGRAPHY AND LIQUID CHROMATOGRAPHY-
MASS SPECTROMETRY FOR THE CHIRAL ANALYSIS OF AMINO ACIDS AND
DIFFERENTIATION OF ISOMERIC AMINO ACID RESIDUES IN PEPTIDES/PROTEINS
FROM COMPLEX MATRICES

by

SIQI DU

Presented to the Faculty of the Graduate School of
The University of Texas at Arlington in Partial Fulfillment
of the Requirements
for the Degree of

DOCTOR OF PHILOSOPHY

THE UNIVERSITY OF TEXAS AT ARLINGTON

December 2019

Copyright © by Siqi Du 2019

All Rights Reserved



Acknowledgements

Firstly, I would like to express my sincere gratitude to my advisor Prof. Daniel Armstrong for his excellent mentorship and support during my graduate studies. As my teacher and mentor, he has provided a working environment that allowed me to grow exponentially. His guidance has aided me in acquiring problem solving capabilities and critical thinking skills.

I want to say thanks to Prof. Saiful Chowdhury for his introduction of mass spectrometry when I first joined the analytical chemistry program. I would also like to express my appreciation to Prof. Kevin Schug for his support on my research and the efforts on bringing the state-of-the-art mass spectrometry instrumentations to us. I am truly thankful to Prof. Subhrangsu Mandal for his support and help during my Ph.D program.

I also sincerely thank Dr. Choyce Weatherly who led me into the world of chromatography when I first joined Dr. Armstrong's group. It is an enjoyable experience working with him and I learned so much and got a lot of help from him. I would like to give my special thanks to my best friend Dr. Yadi Wang. She always encouraged and helped me when I was under a lot of pressure or felt frustrated about research. It is her who makes me never feel alone when working in the lab on weekends and late night.

I would like to thank my roommate, Beth, and my friends Michael and Sam. We worked on a few projects together and brainstormed ideas. Also, they cooked for me a lot this semester so that I can focus on my research in the lab. I also thank my friend Fang and Chuchu, who were always there whenever I needed help. I appreciated the help and assistance from our group members: Zach, Darshan, Chandan, Rahul, Mohsen, Rasangi, Garrett, Roy, Nimish, Abuid, Dr. Farooq Wahab, Dr. Diego Lopez, Dr. Lee, Angel and Barbara. Special thanks should go to department staff: Jill, Debbie, Roy, and Beth.

I owe a lot of thanks to my beloved parents and family. To my parents, thanks for supporting me for higher education in the US. To my uncle and aunt, thanks for your help when I first came to the US. To my husband, Andy, thanks for always being there for me, loves me and supports all my decision.

October 28, 2019

Abstract

ADVANCES IN LIQUID CHROMATOGRAPHY AND LIQUID CHROMATOGRAPHY- MASS SPECTROMETRY FOR THE CHIRAL ANALYSIS OF AMINO ACIDS AND DIFFERENTIATION OF ISOMERIC AMINO ACID RESIDUES IN PEPTIDES/PROTEINS FROM COMPLEX MATRICES

Siqi Du, PhD

The University of Texas at Arlington, 2019

Supervising Professor: Daniel W. Armstrong

Amino acids are essential building blocks in all living organisms. Initially it was believed that only L-amino acids were relevant in higher organisms, and D-amino acids were laboratory artifacts. Today, various D-amino acids have been detected in different organisms, including humans, and some even play essential roles in biological processes. In addition, abnormal D-amino acid levels have been reported in patients with different diseases. The variations in D-amino acid levels might be of some diagnostic value. However, our knowledge of D-amino acids remains limited and most of the D-amino acids are not well investigated due to the lack of a comprehensive analytical platform. Analysis of D-amino acids in biological samples is challenging, because of the interference of large amounts of L-amino acids and a plethora of other indigenous compounds. The complete analysis of all D-amino acids requires a long period of time. Therefore, the goals of this dissertation are to 1) enhance current analytical methods for analyzing D-amino acids in biological samples, and 2) provide information that further studies can reference in finding functions related to pathology and potentially other unexplored D-amino acids processes.

Novel methodologies, based on high performance liquid chromatography-paired ion electrospray ionization mass spectrometry (HPLC-PIESI-MS), two dimension-HPLC (2D-HPLC), and HPLC-tandem mass spectrometry (HPLC-MS/MS), were developed and evaluated for the analysis of free L- and D-amino acids and peptides-containing isomeric amino acid residues from complex matrices. For the achiral analysis of amino acids, an ultrasensitive detection method using PIESI-MS was developed for the analysis of Fmoc-amino acids in urine samples. This method showed improved detection sensitivity down to sub-pg level. A 2D-HPLC chiral separation method with high sensitivity and selectivity was developed for the comprehensive baseline study of L- and D-amino acids in mouse brain and blood. A simple, rapid and sensitive chiral analysis method was developed using HPLC-MS/MS for the simultaneous analysis of 20 common amino acids and their enantiomeric compositions in wild-type mice and mutant mice lacking D-amino acid oxidase activity. Also, the intracellular and extracellular profiles of L- and D-amino acids in human breast cancer cells (MCF-7) and non-tumorigenic epithelial breast cells (MCF-10A) were reported for the first time using this HPLC-MS/MS method. We have also developed the first comprehensive analytical platform that can separate all 20 possible β -amyloid peptides containing Asp, isoAsp, and Ser isomers. Using this simple and high-throughput separation method, we will be able to identify and quantify Asp, isoAsp, and Ser isomers at every position of the β -amyloid peptides from Alzheimer's patients simultaneously.

Table of Contents

Acknowledgements	iii
Abstract	v
List of Illustrations	xii
List of Tables	xiv
Chapter 1 Introduction.....	1
1.1 L- and D-Amino acids	1
1.1.1 Discovery of L- and D-amino acids	1
1.1.2 Regulatory enzymes for D-amino acids in mammals.....	1
1.1.3 Significance of D-amino acids in mammals	2
1.2 Analysis of D-amino acids	3
1.2.1 Commonly used analytical techniques	3
1.2.2 Amino acids derivatization in HPLC methods	3
1.2.3 Chiral stationary phases in HPLC methods	4
1.3 Research objectives and organization of the thesis	5
Chapter 2 D-Amino Acid Levels in Perfused Mouse Brain Tissue and Blood:	
A Comparative Study	7
2.1 Introduction	8
2.2 Methods	10
2.2.1 Materials	10
2.2.2 Derivatization of amino acid standards	11
2.2.3 Mouse brain non-perfused tissues	11
2.2.4 Mouse brain perfused tissue	12
2.2.5 Blood samples	12
2.2.6 Animal subjects	13

2.2.7 Free amino acid extraction	13
2.2.8 Two dimension HPLC instrumentation and method	14
2.3 Results and discussion	17
2.3.1 Broad trend	22
2.3.1.1 Effect of perfusion	22
2.3.1.2 Amino acid levels: homeostasis?	22
2.3.1.3 Cortex vs. hippocampus amino acid levels	22
2.3.1.4 Percent D-amino acid levels	24
2.3.2 Specific amino acids	25
2.3.2.1 D-Glutamic Acid (glutamate) and D-glutamine	25
2.3.2.2 D-Aspartic acid (aspartate) and D-serine	27
2.3.2.3 D-Branched chain amino acids (D-leucine, D-valine, D- isoleucine, and D-allo-isoleucine)	28
2.3.2.4 D-Phenylalanine, D-alanine, and D-asparagine	28
2.4 Conclusions	33
Chapter 3 Sensitive Analysis of N-blocked Amino Acids Using High- Performance Liquid Chromatography with Paired Ion Electrospray Ionization Mass Spectrometry	
Abstract	35
3.1 Introduction	36
3.2 Experimental	37
3.2.1 Reagents and materials	37
3.2.2 Paired ion ESI analysis	39
3.2.3 Linear ion trap and triple-quadrupole mass spectrometer conditions	41

3.2.4 Preparation and separation of calibration standards.....	42
3.2.5 Urine sample preparation and analysis.....	44
3.3 Results and discussion.....	44
3.3.1 Mechanism for the improved performance of ion-pairing reagents for Fmoc amino acids	44
Sample injected: 100 ng/mL of Fmoc-Ile. The dicationic ion-pairing reagent used in the PIESI analysis is 40 μ M C ₅ (bpyr) ₂	47
3.3.2 Selection of the ion-pairing reagent.....	47
3.3.3 Limit of detection of Fmoc amino acids.....	49
3.3.4 Comparison of the performance of PIESI on linear ion trap versus triple-quadrupole mass spectrometer.....	51
3.4 Application	53
3.4.1 Chromatographic separation of amino acids.....	53
3.4.2 Recovery Studies	55
3.4.3 Determination of free amino acids in human urine.....	56
3.5 Conclusions	58
Chapter 4 Variations of L- and D-Amino Acid Levels in the Brain of Wild-Type and Mutant Mice Lacking D-Amino Acid Oxidase Activity	59
Abstract.....	59
4.1 Introduction.....	60
4.2 Materials and Methods	62
4.2.1 Chemicals.....	62
4.2.2 Animals.....	63
4.2.3 Stock solutions and standards	63
4.2.4 Sample preparation and derivatization procedure	63

4.2.5 Instrumentation and chromatographic conditions	64
4.3 Results and discussion	68
(see Materials and methods for exact conditions). Note the opposite enantioselectivity to that shown in Figure 4-2.	68
4.3.1 L-Amino acid levels in mouse whole brain	69
4.3.2 D-amino acid levels in mouse whole brain	72
4.4 Conclusions	74
Chapter 5 Altered Profiles and Metabolism of L- and D-Amino Acids in Cultured Human Breast Cancer Cells vs. Non-tumorigenic Human Breast Epithelial Cells.....	
Abstract.....	76
5.1 Introduction	77
5.2 Materials and methods	78
5.2.1 Chemicals and reagents.....	78
5.2.2 Cell lines and culture conditions.....	79
5.2.3 Cell counting.....	79
5.2.4 Intracellular and extracellular amino acids extraction and analysis	79
5.3 Results and Discussion	83
5.3.1 Free L-Amino Acid Profiles in MCF-7 and MCF-10A Cells.....	83
5.3.1.1 Intracellular and extracellular free L-amino acid levels	83
5.3.1.2 Altered L-amino acid profiles and metabolism for MCF-7 breast cancer cells	87
5.3.2 Free D-amino acid profiles in MCF-7 and MCF-10A cells	88
5.3.2.1 Intracellular and extracellular free D-amino acid levels.....	88

5.3.2.2 Altered D-amino acid profiles and metabolism for MCF-7 breast cancer cells	92
5.3.3 L-Asn and D-Asn may both serve as exchange currency during breast cancer cell proliferation	94
5.3.4 Malignancy indicators may be used to indicate the presence of cancer	95
5.3.5 Effect of glucose concentration on MCF-7 cell proliferation and amino acid levels	96
5.4 Conclusions	97
Chapter 6 Simultaneous Identification of the Isomeric Amino Acid Residues in β -Amyloid: A Remarkable Piece of the Alzheimer's Puzzle	99
Abstract	99
6.1 Experimental	104
6.1.1 Materials and chemicals	104
6.1.2 Instruments and stationary phases	104
6.2 Results and discussion	105
6.3 Conclusions	108
Chapter 7 General Summary	109
Appendix A Publication Information and Contributing Authors	112
Appendix B Copyright and Permissions	114
References	117
Biographical Information	134

List of Illustrations

Figure 1-1 Structure of the chiral stationary phase used (a) teicoplanin (b) quinine	5
Figure 2-1 Representative chromatograms of the first and second dimension separations of standard Fmoc amino acids.	16
Figure 2-2 The average value of A) total amino acid levels and B) D-amino acid levels (ug/mg) in blood, non-perfused cortex, and non-perfused hippocampus.	30
Figure 2-3 Linear plots of the total amino acid levels in perfused and non-perfused samples and normalized data (with respect to glutamic acid) in comparison to raw data.	31
Figure 2-4 A) Comparison of total amino acid levels in the cortex vs. hippocampus. B) Comparison of D-amino acid levels in the cortex vs. hippocampus,	32
Figure 2-5 A) Plot of hippocampus %D amino acid levels vs. total amino acid levels. B) Plot of cortex %D amino acid levels vs. total amino acid levels.	33
Figure 3-1 The instrument set up of HPLC-PIESI-MS.	41
Figure 3-2 (a) Fmoc-derivatization reaction. (b) Structure of all the amino acids studied in this paper.	43
Figure 3-3 Representative full-scan MS spectra of Fmoc-Ile with and without ion-pairing reagent (IPR).....	46
Figure 3-4 Chromatographic profile of signal-to-noise ratio at positive SIM mode, negative SIM mode, PIEESI-SIM mode, and PIEESI-SRM mode.	47
Figure 3-5 The ESI signal-to-noise (S/N) improvement factor for each amino acid is calculated as the S/N value at the PIEESI mode over the negative SIM mode.....	49
Figure 3-6 Total ion chromatogram (EIC) and extracted ion chromatogram (TIC) of the separation of 22 Fmoc-AAAs with HPLC-PIESI-MS.	54
Figure 3-7 HPLC-PIESI-MS analysis of urine sample.	55

Figure 3-8 Analysis of amino acid concentrations in the urine sample with HPLC-PIESI-MS.....	58
Figure 4-1 HPLC-MS/MS chromatogram of the separation of AQC-amino acid standards on the quinine SPP chiral stationary phase	68
Figure 4-2 HPLC-MS/MS chromatogram of the separation of AQC-amino acid standards on TeicoShell chiral stationary phase	69
Figure 4-3 L-Amino acid levels in mice whole brain.	70
Figure 4-4 D-Amino acid levels in mice whole brain.....	74
Figure 5-1 Representative chromatograms of AQC derivatized amino acids in MCF-7 cancer cells after 48-hour growth in high glucose medium.....	82
Figure 5-2 Intracellular L-amino acid profiles.....	84
Figure 5-3 Extracellular L-amino acid profiles.	86
Figure 5-4 Intracellular D-amino acid profiles.	89
Figure 5-5 Intracellular percent D-amino acid levels.	90
Figure 5-6 Extracellular D-amino acid profiles.....	91
Figure 6-1 Separation of A β (1-5) peptide epimers on modified Q-Shell chiral stationary phase (3 x 150 mm, 2.7 μ m).....	106
Figure 6-2 Separation of A β (6-16) peptide epimers on NicoShell chiral stationary phase (3 x 150 mm, 2.7 μ m).....	106
Figure 6-3 Separation of A β (7-28) peptide epimers on modified Q-Shell chiral stationary phase (3 x 150 mm, 2.7 μ m).....	107

List of Tables

Table 2-1 Second dimension chiral chromatography conditions for the separation of Fmoc amino acids	15
Table 2-2 Total amino acid and D-amino acid level in non-perfused cortex and hippocampus	19
Table 2-3 Total amino acid and D-amino acid levels in perfused cortex and hippocampus	20
Table 2-4 Total amino acid and D-amino acid levels in blood	21
Table 3-1 Abbreviation, exact mass and structure of the ion pairing reagent used in this study.....	39
Table 3-2 Limit of detection values of Fmoc-AAs at negative mode and PIESI SIM/SRM mode obtained with linear ion trap mass analyzer.....	50
Table 3-3 Limit of detection values of Fmoc-AAs at negative mode and PIESI SIM/SRM mode obtained with triple quadrupole MS analyzer.....	52
Table 3-4 Recovery values at urine sample with different dilution factor.	57
Table 4-1 L-Amino acid levels in mice whole brain ^a (ng/mg wet tissue).....	66
Table 4-2 D-Amino acid levels in mice whole brain ^a (ng/mg wet tissue)	67
Table 5-1 Malignancy indicators for breast cancer	96
Table 6-1 Amino acid sequence of the three groups of A β peptide epimers with Asp and Ser isomeric residues.....	104
Table 6-2 Results of MRM optimization and LODs for tryptic A β peptides on LCMS-8060	107

Chapter 1

Introduction

1.1 L- and D-Amino acids

1.1.1 Discovery of L- and D-amino acids

Amino acids are indispensable molecules in all living organisms given their fundamental roles as building blocks of proteins, intermediates of metabolic processes, and cell-cell signaling. In 1806, the first amino acid was isolated from asparagus, hence the name asparagine [1]. Subsequently the rest of the proteinogenic amino acids were discovered. Proteinogenic amino acids are alpha amino acids as their stereogenic center is at the alpha carbon. All proteinogenic amino acids can exist in either L- or D-form, except for glycine due to its lack of chiral center. Initially it was believed that only L-amino acids were relevant in higher organisms, while D-amino acids were thought to be absent. In the mid-20th century, D-amino acids, *i.e.*, D-Ala and D-Glu, were found to be present in the bacterial peptidoglycan, which is a major component of the bacterial cell wall [2]. With the development of sensitive analytical techniques, separation and detection of D-amino acids led to the discovery of free and peptide-bound D-amino acids in plants, invertebrates, vertebrates, and mammals [3-6].

1.1.2 Regulatory enzymes for D-amino acids in mammals

One of the important enzymes that are involved in the synthesis of D-amino acids are amino acid racemases, which catalyze the conversion of L-amino acids to D-amino acids. As bacteria are the most important D-amino acid source in nature, free D-amino acids found in higher organisms were originally assumed to originate from bacterial sources, external racemization and food. In 1999, serine racemases, which catalyzes the formation of D-Ser from L-Ser, were found in mammalian tissues, indicating that mammals are able to synthesize D-amino acids [7]. The enzymes that are involved in the

degradation of D-amino acids are D-amino acid oxidases and D-aspartate oxidases, which are flavoproteins that are responsible for the oxidation of neutral and acidic D-amino acids, respectively [8]. They catalyze the oxidative deamination of D-amino acids to give α -keto acids and ammonia. Both enzymes were discovered by H. A. Krebs in the 1930s, which was considerably earlier than the discovery of D-amino acids in animals [9]. Altered D-Ser, D-Pro, and D-Leu levels have been detected in mutant mice lacking DAO activity, suggesting that DAO is important for regulating D-amino acid levels in mammals [10, 11].

1.1.3 Significance of D-amino acids in mammals

Among all the D-amino acids studied, D-Ser has drawn the most attention and interest due to its important physiological role. D-Ser is a co-agonist of N-methyl-D-aspartate (NMDA) receptor and can occupy the glycine binding site [12, 13]. Low D-Ser levels in cerebrospinal fluid and serum were detected in schizophrenia patients and it is believed that decreased D-Ser levels resulted in the hypofunction of NMDA receptors [14]. It is now considered as one of the most plausible causes of schizophrenia [15]. In addition to D-Ser, D-Ala and D-Asp have been reported to act as co-agonists of NMDA receptors occupying the glutamate binding site [16, 17]. D-Asp levels in the white matter of Alzheimer brains were found to be half of that in normal subjects.[18] The reduction of NMDA receptors was also reported in Alzheimer brains [19, 20]. NMDA receptors have been implicated in learning and memory processes.[21] Therefore, it was proposed that the decreased D-Asp levels caused the reduction of NMDA receptors, which contributed to the memory deficits in Alzheimer's patients [22]. Recently, D-Leu treatment was found to be effective for suppressing ongoing seizures in mice, although the mechanism remains unclear [23]. It has been found that NMDA receptors are widely present not only in the central nervous system, but also in a variety of cancer cell lines and tumors with

functions in regulating cancer cell growth and division [24]. This means specific D-amino acids, *i.e.*, D-Ser, D-Asp, and D-Ala, may play important roles in the metabolism and proliferation of cancer cells.

1.2 Analysis of D-amino acids

1.2.1 Commonly used analytical techniques

Various methods have been reported on the enantiomeric analysis of amino acids in physiological samples, including capillary electrophoresis (CE), gas chromatography (GC), and high performance liquid chromatography (HPLC) [25]. Concerning CE, one widely used chiral separation method for amino acids is cyclodextrin-mediated capillary zone electrophoresis (CD-CZE) that can be coupled with a variety of detection methods, *e.g.* UV, mass spectrometry (MS) or laser-induced fluorescence (LIF) [26]. However, it is well known that CE has poor quantitative reproducibility mainly due to the irreproducible electroosmotic flow rate and inconsistent injection volumes [27]. GC methods provide high separation efficiency with commercially available chiral capillary columns [28]. Among the current GC methods, enantiomeric separation of derivatized amino acids on a Chirasil-(L- or D)-Val column, together with flame ionization or MS detection, has been most widely used [28]. Nevertheless, the main drawback of GC-MS for enantiomeric analysis is its restriction to volatile and thermostable molecules [25]. Over the years, HPLC with diverse types of chiral stationary phases and fluorescence or MS detection has become the preferred approach to study amino acid enantiomers in biological samples [29].

1.2.2 Amino acids derivatization in HPLC methods

HPLC analysis for underivatized amino acids coupled with UV or MS always encounter selectivity and sensitivity problems [30]. For example, UV detection for most underivatized amino acids requires using the absorption of carboxylic group in the 200 to

210 nm range, where increased background interference is observed due to the mobile phase absorption [31]. When MS/MS is used as the detection method, the amino acids are typically in a low mass range, in which high noise is more often observed.

Derivatization brings several advantages to HPLC amino acids analysis. First, derivatization of amino acids improves chromatographic properties, e.g., improved retention and resolution, especially in reversed-phase HPLC. Second, better detection limits have been achieved for derivatized amino acids when UV, fluorescence, or MS detection is employed. Furthermore, ionization efficiency can be significantly improved by derivatization in LC-MS and LC-MS/MS [32]. There are various derivatization reagents which have been applied to the analysis of amino acids enantiomers. The most common ones include 5-dimethylamino-1-naphthalenesulphonyl-chloride (Dansyl), o-phthalaldehyde (OPA), 9-fluorenylmethyl chloroformate (FMOC), 7-fluoro-4-nitrobenzo-2-oxa-1,3-diazole (NBD-F), and 6-aminoquinolyl-N-hydroxysuccinimidyl (AQC) [33]. The advantages of AQC derivatization over other reagents are 1) short derivatization time, 10 min at 55 °C; 2) stable adducts, stable for at least a week at room temperature; 3) high derivatization efficiency; 4) no need to add quenching reagent to remove excess reagent [33, 34].

1.2.3 Chiral stationary phases in HPLC methods

Macrocyclic antibiotics (vancomycin, teicoplanin, ristotecin A, etc.) have been widely used as chiral selectors in HPLC, since they were first introduced in 1994 [35]. The structure of teicoplanin indicates a variety of possible mechanisms for enantioselectivity, including ionic interaction, π - π stacking, hydrogen bonding, inclusion complexation, hydrophobic and steric effects, etc. [36]. Teicoplanin-based chiral stationary phase has shown excellent selectivity for a number of classes of molecules, especially underivatized amino acids, N-derivatized amino acids and small peptides [35-36].

37]. Quinine based chiral stationary phase also showed enantiomeric selectivity to N-blocked amino acids [38]. Interestingly, these two stationary phases provide complementary selectivity for the enantioseparation of amino acids. L-amino acids elute earlier than their corresponding D-enantiomers on the teicoplanin stationary phase except for Pro; While on quinine stationary phase, D-amino acids elute earlier than their corresponding L-enantiomers except for Pro. The use of these two chiral stationary phases provides more accurate and robust peak identification as well as quantitation. The structures of chiral stationary phases used in this dissertation are shown in Figure 1-1.

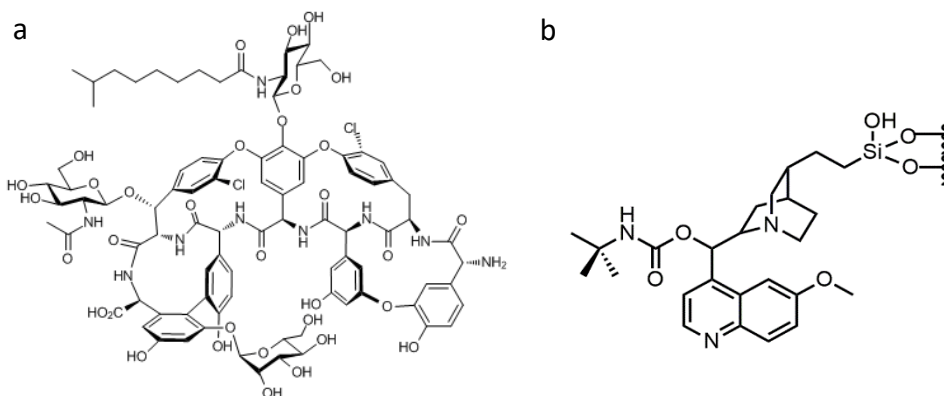


Figure 1-1 Structure of the chiral stationary phase used (a) teicoplanin (b) quinine

1.3 Research objectives and organization of the thesis

This dissertation focuses on advancing HPLC and LC-MS/MS techniques and applying them to bioanalysis. Chapter 2 describes the baseline study of L- and D-amino acid levels in mouse brain and blood using heart-cutting 2D-HPLC. Chapter 3 focuses on the evaluation and application of paired ion electrospray ionization (PIESI) for the sensitive detection of FMOc-amino acids from biological samples. Chapters 4 and 5 describe the development and validation of a rapid and sensitive method for the analysis of L- and D-amino acids in biological samples using HPLC-MS/MS. Chapter 4 examines

the profiles of L- and D-amino acid in mouse whole brain of wild-type mice and mutant mice lacking D-amino acid oxidase activity. Chapter 5 focuses on the L- and D-amino acid profiles in cultured breast cancer cells and the comparison to non-tumorigenic human breast epithelial cells.

Chapter 2

D-Amino Acid Levels in Perfused Mouse Brain Tissue and Blood: A Comparative Study

Abstract

The L-enantiomer is the predominant type of amino acid in all living systems. However, D-amino acids, once thought to be “unnatural”, have been found to be indigenous even in mammalian systems and increasingly appear to be functioning in essential biological and neurological roles. Both D- and L-amino acid levels in the hippocampus, cortex, and blood samples from NIH Swiss mice are reported. Perfused brain tissues were analyzed for the first time, thereby eliminating artifacts due to endogenous blood, and decreased the mouse-to-mouse variability in amino acid levels. Total amino acid levels (L- plus D-enantiomers) in brain tissue are up to 10 times higher than in blood. However, all measured D-amino acid levels in brain tissue are typically ~10 to 2000 times higher than blood levels. There was a 13% reduction in almost all measured D-amino acid levels in the cortex compared to those in the hippocampus. There is an approximate inverse relationship between the prevalence of an amino acid and the percentage of its D-enantiomeric form. Interestingly, glutamic acid, unlike all other amino acids, had no quantifiable level of its D-antipode. The bioneurological reason for the unique and conspicuous absence/removal of this D-amino acid is yet unknown. However, results suggest that D-glutamate metabolism is likely a unidirectional process and not a cycle, as per the L-glutamate/glutamine cycle. The results suggest that there might be unreported D-amino acid racemases in mammalian brains. The regulation and function of specific other D-amino acids are discussed.

2.1 Introduction

Amino acids are among the most important molecules in nature. The first discovered amino acid was asparagine, which was isolated from asparagus extract in 1806 [39]. Subsequently the analysis of protein hydrolysates revealed additional analogous compounds that are now referred to as amino acids [40]. In 1851 Louis Pasteur revealed the optical activity of asparagine and aspartic acid [41], leading to the realization that most common amino acids have optical activity arising from their differing orientation around the α -carbon [42]. The initial discovery and configurational assignment of amino acids led to the opinion that L-configuration amino acids were solely found in nature, and D-amino acids were laboratory artifacts [43, 44].

Dispelling the notion that D-amino acids are “unnatural” or not biologically relevant began in the mid-20th century with the report that D-amino acids were an integral part of the bacterial peptidoglycan [2]. It was the first report that D-amino acids, specifically D-alanine and D-glutamic acid, were appurtenant biological entities. Subsequent evidence began to emerge supporting the notion that D-amino acids were not uncommon in living systems. In 1969 J. Corrigan published a review with 30 examples of D-amino acids found in invertebrates [43]. In some cases a functional role was implied while in many others it was unknown. By the end of the last century with the advent of new bioanalytical techniques, scientists were able to easily isolate and identify D-amino acids in a greater variety of biological samples and in particular, vertebrates [6, 5, 45-47]. In 1986 free D-aspartic acid was found in human and animal tissue [47]. Subsequently, free L- and D- amino acids were reported in pathologically relevant human urine, plasma, cerebrospinal fluid, and amniotic fluid [6, 5]. A nonproteinic amino acid, D-pipecolic acid, was found to be an indicator of the severity of a neurological genetic disease [48]. Additional reports showed that D-amino acid containing peptides had

distinct functions including binding to specific opiate receptors and acting as neurotoxins blocking voltage-sensitive calcium channels [49, 50]. Since the early 2000s, there have been additional reports of free D-amino acids in various mammalian tissues [51-53].

Investigations into the role and function of specific D-amino acids in mammalian systems is an intriguing but relatively neoteric. D-serine is a co-agonist of the N-methyl-D-aspartate (NMDA)-type glutamate receptor, and it can occupy the glycine binding site [54, 13]. Free D-serine has been determined to be localized primarily in the mammalian forebrain, where the highest concentrations for NMDA receptors is found [55-57]. In cases with treatment-resistant depression, D-serine has been used as potential biomarker of ketamine antidepressant response [58]. Recently, D-leucine has been applied as an effective treatment for seizures in mice [23]. However, the exact mechanism through which D-leucine acts to inhibit seizure activity remains unknown. D-serine and D-leucine are two of the more prominent examples of D-amino acids found in brain tissues. Most D-amino acids are metabolized by either D-amino acid oxidase (DAO) or D-aspartic acid oxidase. It is thought D-amino acid oxidase is important for regulating levels of select D-amino acids and is crucial to help control levels of D-serine, which is known to have function at the NMDA-type glutamate receptor[54, 13].

As evidence accrues on the unique biological roles of D-amino acids, it has become evident that there are limited fundamental studies on normal, baseline levels of most L- and D- amino acids in the brain and blood of any mammalian entity. The few limited studies may not have had sufficient sensitivity [59, 60]. Hippocampus and cortex regions of the brain are two of the most common anatomical sources of epilepsy [23]. Examination of these tissues to determine baseline levels of D-amino acids will aid in establishing essential normative data that further studies can reference in finding function(s) relating to neurological pathology and potentially, other unexplored D-amino

acid processes. In this work, we provide the most complete characterization of brain and blood amino acid levels in mice. Further, the levels are examined in terms of anomalies, trends and possible relevance to the limited existing data on mammalian D-amino acids.

Transcardial perfusion is a standard technique involving vascular perfusion of anesthetized animals for preservation of tissues for analysis [61]. It is unclear how much of each amino acid is in the intravascular and extravascular spaces, which could provide useful information about their potential physiological roles. Regarding D-amino acid analyses, perfusion has only been applied to the determination of D-serine and its function in the activity of D-amino acid oxidase (DAO) in the human central nervous system [62]. The effect of perfusion in the analysis of a spectrum of L and D-amino acids in brain tissues has not been examined.

2.2 Methods

2.2.1 Materials

All amino acid standards, teicoplanin, fluorenylmethyloxycarbonyl chloride, amantadine hydrochloride, and boric acid were purchased from Sigma-Aldrich (St. Louis, MO). High performance liquid chromatography (HPLC) grade acetonitrile and methanol were purchased from Sigma-Aldrich, and deionized water was obtained from a Milli-Q water system (Millipore, Bedford, MA). An octadecylsilane derivatized superficially porous particle (SPP) based HPLC column (Poroshell 120 EC-C18, 4.6 x 150 mm i.d. 2.7 μ m particles) was purchased from Agilent Technologies (Wilmington, DE). Another HPLC column was prepared in-house utilizing teicoplanin covalently bonded to SPPs and slurry packed into a 4.6 x 100 mm i.d stainless steel column (IDEX Health and Science, Oak Harbor, WA).

2.2.2 Derivatization of amino acid standards

Fluorenylmethyloxycarbonyl chloride (FMOC) was used as a fluorescent reagent for amino acid derivatization in this study. FMOC amino acids have been reported to be stable [63]. Other fluorescent reagents for precolumn derivatization such as *o*-phthaldialdehyde (OPA) and 7-fluoro-4-nitrobenzo-2-oxa-1,3-diazol (NBD-F) have been reported to form unstable amino acid adducts [63]. The derivatization of standards was performed in autosampler vials. Standard L- and D- amino acids were prepared in deionized water at concentrations around 0.03 M. Into the autosampler vial 50 μ L of amino acid standards was pipetted. A 0.8 M borate buffer was prepared with boric acid and potassium chloride. The borate buffer pH was adjusted with 0.8 M NaOH to pH 9. Into the autosampler vial 400 μ L of borate buffer was pipetted. In addition, 500 μ L of acetonitrile was pipetted into the autosampler vial. A FMOC solution was prepared by dissolving 0.13 g in 5 mL acetonitrile (0.1 M), and 50 μ L of the FMOC solution was pipetted into the autosampler vial. The mixture was then allowed to react at room temperature after the addition of the FMOC solution for 20 minutes. After the reaction was completed, 50 μ L of 0.8 M amantadine solution was added to the autosampler vial to quench the remaining FMOC reagent. The 0.8 M amantadine solution was prepared with acetonitrile and water, 1:1, mixture. All standards, reagents, and solutions were stored at 4 °C while not in use.

2.2.3 Mouse brain non-perfused tissues

The study was carried out under experimental protocols approved by the Johns Hopkins Animal Care and Use Committee (ACUC). Reporting of this work complies with ARRIVE guidelines. All efforts were made to minimize animal suffering. In all experiments NIH Swiss mice (NCI, Frederick, MD, U.S.A.) aged 5-6 weeks (body weight 25-30 g) were used. The mice were housed 3-5 per cage, with a simulated 14-hour light/10-hour

dark cycle. The mice were fed a rodent chow diet (Teklad Global 2018SX, Madison, WI) and tap water *ad lib*.

Mice were sacrificed by rapid cervical dislocation. Surgical scissors were used to remove the head and to complete the brain dissection. The hippocampus and cortex were dissected using a dissecting microscope. All samples were stored at -80 °C until analyzed.

2.2.4 Mouse brain perfused tissue

Mice were anesthetized lightly with carbon dioxide. A midline incision was made at the thoracic costal margin, followed by visualization and incision of the right atrium. Heparin/saline (APP Pharmaceuticals, LLC 1,000 USP Units/mL, Schaumburg, IL) was injected using a 25-gauge butterfly needle (BD Vacutainer, Four Oaks, NC) into the apex of the left ventricle until a swelling of the heart was observed. The injection was thereafter continued at a low rate. The proximal end of the collection set was removed from the flush syringe when the effluent was clear. A 20 mL syringe was used to slowly inject a 10% neutral buffered formalin (NBF) solution (Sigma Life Science, St. Louis, MO) and when cardiac muscle contraction stopped, perfusion was complete. A 3 mL syringe and 25 gauge one-inch needle were used to infuse the intestines and lungs with 10% NBF, working from the proximal to distal end. Brains were then dissected rapidly according to the procedure previously described. All samples were stored at -80 °C until analyzed.

2.2.5 Blood samples

Mice were anesthetized with carbon dioxide and blood was collected rapidly by a cardiac puncture technique using a 22-gauge needle. The blood was collected and stored at -80 °C until analyzed.

2.2.6 Animal subjects

A total of nineteen male mice (NIH Swiss) were utilized for the analysis of 12 free amino acids in hippocampus tissue, cortex tissue, and blood samples. This strain of mice was used in parallel with other experiments on the efficacy of D-leucine in treating epilepsy. Male mice were only analyzed for L- and D- amino acids because the parallel experiments on the efficacy of D-leucine in treating epilepsy showed some adverse effects in female mice. Seven mice were utilized for the non-perfused tissue analysis of the hippocampus and cortex. Another seven mice were utilized for the perfused tissue analysis of the hippocampus and cortex. The last five mice were used for the blood analysis (blood was not collected from mice sacrificed for brain tissue because of the need for very rapid tissue/blood acquisition in order to minimize D-amino acid degradation). A total of fourteen samples were used for tissue analysis from both perfused and non-perfused mice (seven hippocampus tissue samples and seven cortex tissue samples).

2.2.7 Free amino acid extraction

The hippocampus, cortex, and blood samples obtained from the dissection and collection processes were weighed and placed into micro centrifugation tubes. To all samples 100 μ L of an internal standard was added. The internal standard consisted of 8.38 mM racemic norleucine in water. Next, 1 mL of 0.1 N perchloric acid was pipetted into the tube. Then the samples were homogenized for 30 seconds (three 10 seconds pulses) with a Q-Sonica CL-18 probe (Newtown, CT). The samples were placed on ice during the homogenization process. After the homogenization, the samples were centrifuged at 13,000 RPM for 20 minutes at 4 °C. The supernatant was removed and stored at - 80 °C while not in use. 100 μ L aliquots of supernatant was derivatized by following the derivatization procedure described for the amino acid standards.

2.2.8 Two dimension HPLC instrumentation and method

The chromatography system consisted of an Agilent 1200 HPLC system (Santa Clara, CA) and an LC system consisting of a Shimadzu LC-6A pump, RF-10A fluorescence detector, and CR-6A integrator (Kyoto, Japan). A Rheodyne 7000 six port stream switching valve (Rohnert Park, CA) was used for the heart-cut from the first dimension to the second dimension. The first dimension utilized a C18 SPP column, and the second dimension utilized an in house constructed chiral teicoplanin SPP column. Both columns were described in the material section. First dimension signal monitoring was done using ChemStation software from Agilent, and the second-dimension signal was monitored by a CR-6A integrator from Shimadzu. Two reverse phase HPLC gradients for individual amino acid isolation was performed in the first dimension. The first gradient consisted of mobile phase A (20 mM H₂PO₄ buffer adjusted to pH 2.5 with H₃PO₄) and mobile phase B (acetonitrile). The gradient method began with 5% B (0-2 min) followed by a linear ramp from 15-80% B (2.01-35 min) then 80-95%B (35-38 min). Finally, the gradient concluded with a 2-minute ramp down to 5% B. The flow rate was 0.75 mL/min. For the second reverse phase gradient, mobile phase A was 0.025 M sodium acetate, and mobile phase B was a 23/22 (v/v) mixture of 0.05 M sodium acetate/acetonitrile. The gradient method began with a ramp from 30-37% B (0-3.75 min) followed by a ramp from 37-73% B (3.75-26.25 min) and finally brought to 100% B over the concluding 5 min. For the first dimension a diode array detector (DAD) monitored signals at 254 nm and the detector outlet was connected to the six-port switching valve. Effluent bands were manually cut or redirected to the second-dimension column. Manual cuts lasted approximately 0.1 to 1 seconds. In the second dimension, amino acid enantiomers were separated on the teicoplanin SPP column using isocratic reverse phase methods. Table 2-1 lists the conditions for the separation of each chiral amino acid

in the second dimension. For the second dimension, fluorometric detection of FMOC-amino acids was conducted using excitation wavelength of 254 nm and an emission wavelength of 313 nm. Figure 2-1 shows typical results obtained from the chromatographic separations from the first and second dimensions.

The method described was able to evaluate 16 amino acids. The levels of 12 free amino acids were reported in the blood and brain tissues. Four of the amino acid levels were below the detection limits (LODs) of our method and therefore could not be reported. Other methods also reported low detection levels for similar amino acids in rat brains (e.g. cysteine, tyrosine, methionine, and D-glutamate) [64, 65].

Amino Acid	Mobile Phase	Column
Leucine	60/40 0.1% TEAA (pH=4.1)/MeOH	4.6 x 100 mm SPP Teicoplanin
Valine	70/30 0.1% TEAA (pH=4.1)/MeOH	4.6 x 100 mm SPP Teicoplanin
Serine	70/30 0.1% TEAA (pH=4.1)/MeOH	4.6 x 100 mm SPP Teicoplanin
Isoleucine	55/45 0.1% TEAA (pH=4.1)/MeOH	4.6 x 100 mm SPP Teicoplanin
Phenylalanine	55/45 0.1% TEAA (pH=4.1)/MeOH	4.6 x 100 mm SPP Teicoplanin
Alanine	70/30 0.1% TEAA (pH=4.1)/MeOH	4.6 x 100 mm SPP Teicoplanin
Glutamic Acid	70/30 0.1% TEAA (pH=4.1)/MeOH	4.6 x 100 mm SPP Teicoplanin
Tryptophan	70/30 0.1% TEAA (pH=4.1)/MeOH	4.6 x 100 mm SPP Teicoplanin
Threonine	70/30 0.1% TEAA (pH=4.1)/MeOH	4.6 x 100 mm SPP Teicoplanin
Methionine	60/40 0.1% TEAA (pH=4.1)/MeOH	4.6 x 100 mm SPP Teicoplanin
Aspartic Acid	70/30 0.1% TEAA (pH=4.1)/MeOH	4.6 x 100 mm SPP Teicoplanin
Arginine	100/0.1 (w/w %) MeOH/NH ₄ TFA	4.6 x 100 mm Chirobiotic R
Lysine	100/0.1 (w/w %) MeOH/NH ₄ TFA	4.6 x 100 mm Chirobiotic R
Tyrosine	100/0.02 (w/w %) MeOH/NH ₄ OAc	4.6 x 100 mm Chirobiotic R
Asparagine	60/40 0.1% TEAA (pH=4.1)/MeOH	4.6 x 100 mm SPP Teicoplanin
Glutamine	60/40 0.1% TEAA (pH=4.1)/MeOH	4.6 x 100 mm SPP Teicoplanin

Table 2-1 Second dimension chiral chromatography conditions for the separation of FMOC amino acids

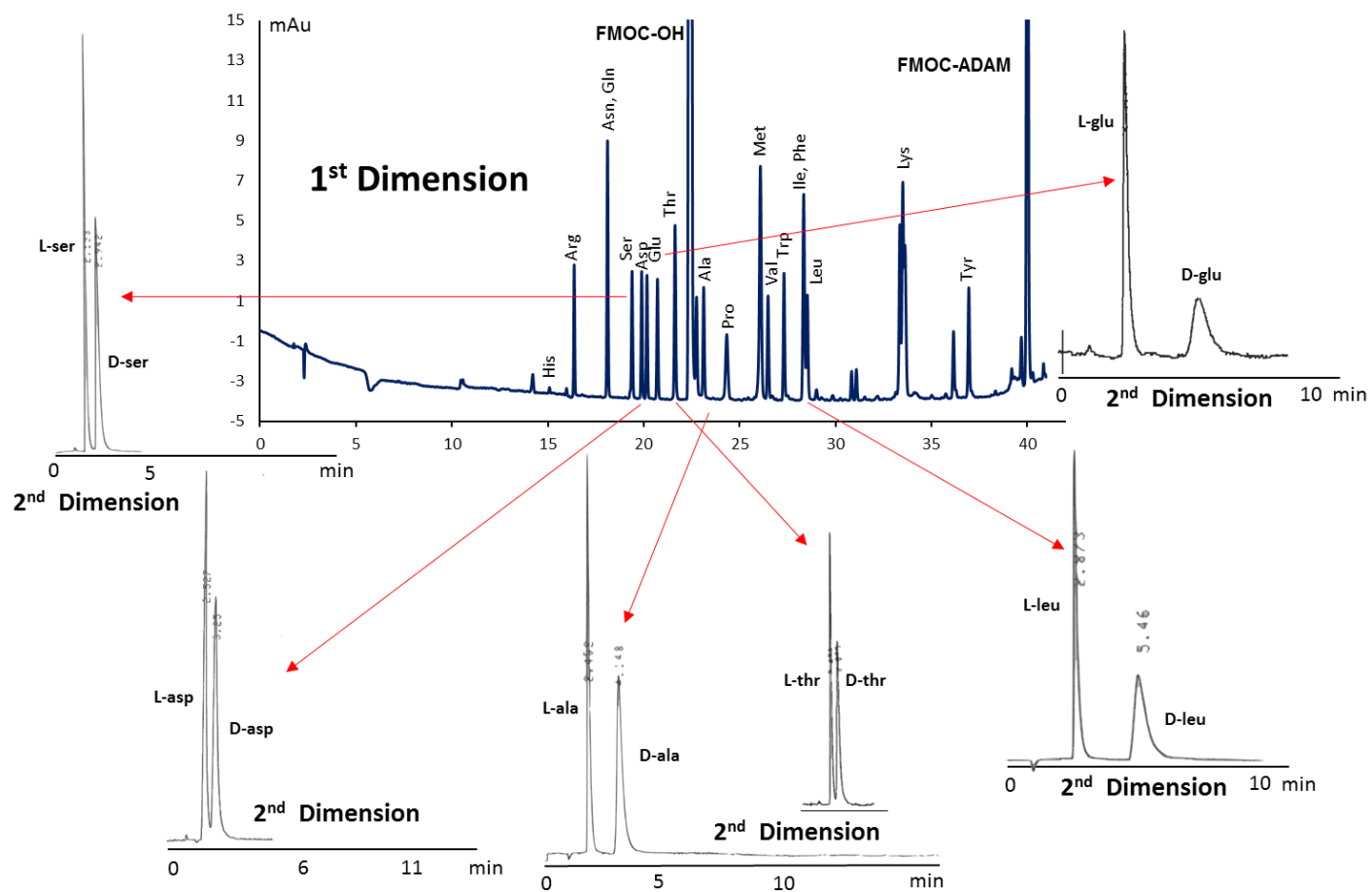


Figure 2-1 Representative chromatograms of the first and second dimension separations of standard Fmoc amino acids.

2.3 Results and discussion

Tables 2-2 and 2-3 provide the amino acid data for both the cortex and hippocampus of non-perfused and perfused mice, respectively. Table 2-4 shows both the total and D-amino acid levels in the blood. Both the total amino acid and especially D-amino acid levels are usually lower in the blood (often by an order of magnitude). Figure 2-2A shows 12 averaged concentration levels of total amino acids (i.e. D- plus L-amino acids). The three amino acids with the highest levels in brain tissues are glutamic acid, glutamine, and aspartic acid. Figure 2-2B shows 12 averaged concentration levels of D-amino acids. Concentrations of D-glutamine, D-aspartic acid, and D-serine have the highest values. Interestingly, no detectable amount of D-glutamic acid was found. This was unexpected because the concentration of total glutamic acid is significantly higher than all other amino acids, and all other amino acids detected have significant levels of their D-enantiomers present. Concentrations of D-amino acid levels are almost always lower than the corresponding L-amino acid levels (Figure 2-2A vs. Figure 2-2B). For example, concentrations of D-glutamine in the non-perfused cortex and concentrations of D-isoleucine in the non-perfused hippocampus are approximately four times less than their total amino acid values. Concentrations of D-phenylalanine, D-leucine, D-isoleucine, and D-allo-isoleucine are among the lowest values. Distinct from other amino acids, the ratio of blood to non-perfused cortex or hippocampus levels of branched chain amino acids, particularly leucine, is closer to unity than other amino acids (Figure 2-2A). However, the level of their D-amino acid antipodes remains elevated in brain tissue compared to blood.

Free amino acid concentrations obtained from perfused tissue may yield a more accurate measurement of cellular and extracellular/extravascular levels. Table 2-3 lists

the amino acid values obtained from the perfused tissues and Figure 2-3 shows the effect of perfusion on the amino acid levels measured in the cortex and hippocampus. A plot of the average amino acid values of perfused tissue vs. non-perfused tissue is linear (see Figure 2-3). Each data point is an amino acid, and the measure of R^2 (how close the data are fitted to the regression line) represents the uniformity of the effect of perfusion. In the raw data of Figure 2- 3B for the hippocampus tissues and Figure 2-3D for the cortex tissues, the slope of the line is approximately 0.85. This represents an average 15% decrease in total amino acid levels in both the perfused cortex and hippocampus relative to the non-perfused samples. In terms of reproducibility, mouse-to-mouse variations in total amino acid levels is less for perfused mice (see y-axis or ordinate range) than non-perfused mice (see x-axis or abscissa range).

The hippocampus tissue values in Figure 2-3B and cortex tissue values in Figure 2-3D have a high amount of mouse to mouse variation. To reduce this variation, a normalization technique was applied to the data. The hippocampus tissue values in Figure 2-3A and cortex tissue values in Figure 2-3C show the normalized data. Glutamic acid, the highest concentration amino acid, was used to normalize the data. Normalization considerably reduces the mouse to mouse variation in amino acid values in the perfused and non-perfused tissues (see Figures 2-3A and 2-3C vs. Figures 2-3B and 2-3D). However, the average values of all the amino acid levels (defined by the slope of the lines) show no significant change.

Mouse whole brain samples also were analyzed. It was found that the total amino acid levels were within the same range as those reported for cortex and hippocampus tissues. Whole brain D-amino acid levels were 10 – 70% lower, except for D-aspartic acid which was similar. It also indicates that that total amino acid values do not appear to change due to dissection.

	Cortex					Hippocampus				
	Total amino acid (µg/mg)		D-amino acid (µg/mg)		D%	Total amino acid (µg/mg)		D-amino acid (µg/mg)		D%
	Range	Average	Range	Average		Range	Average	Range	Average	
Leu	0.02 - 0.05	0.04	0.0005 - 0.007	0.004	12.1	0.03 - 0.14	0.08	0.002 - 0.053	0.013	16.3
Ser	0.11 - 0.49	0.25	0.034 - 0.139	0.076	30.9	0.11 - 0.6	0.28	0.04 - 0.163	0.095	34.2
Ala	0.18 - 0.34	0.25	0.0003 - 0.019	0.010	3.9	0.17 - 0.51	0.32	0.003 - 0.079	0.031	9.7
Asp	0.46 - 1.82	0.94	0.003 - 0.283	0.115	12.2	0.36 - 1.58	0.77	0.005 - 0.042	0.036	4.6
Thr	0.04 - 0.20	0.10	0.0023 - 0.022	0.007	7.6	0.05 - 0.31	0.14	0.003 - 0.050	0.017	12.1
Glu	1.57 - 8.10	3.90	<0.1 - <0.1	<0.1	<0.1	1.37 - 8.69	3.50	<0.1 - <0.1	<0.1	<0.1
Val	0.02 - 0.12	0.05	0.0003 - 0.027	0.011	21.0	0.04 - 0.22	0.11	0.005 - 0.061	0.023	21.3
Asn	0.02 - 0.09	0.04	0.0004 - 0.011	0.004	10.5	0.02 - 0.33	0.11	0.001 - 0.091	0.014	12.2
Gln	0.81 - 2.5	1.48	0.001 - 0.330	0.117	7.9	0.67 - 3.09	1.43	0.00002 - 0.032	0.012	0.8
Ile	0.001 - 0.03	0.01	0.0002 - 0.005	0.003	26.1	0.002 - 0.09	0.03	0.0004 - 0.027	0.007	22.9
Allo-Ile	0.0004 - 0.005	0.003	0.0002 - 0.0007	0.001	16.9	0.0002 - 0.032	0.01	0.0001 - 0.005	0.004	47.0
Phe	0.02 - 0.05	0.03	0.0003 - 0.019	0.005	15.1	0.01 - 0.3	0.09	0.0007 - 0.050	0.021	22.8

Table 2-2 Total amino acid and D-amino acid level in non-perfused cortex and hippocampus

	Cortex					Hippocampus				
	Total amino acid (µg/mg)		D-amino acid (µg/mg)		D%	Total amino acid (µg/mg)		D-amino acid (µg/mg)		D%
	Range	Average	Range	Average		Range	Average	Range	Average	
Leu	0.02 - 0.05	0.04	0.002 - 0.009	0.006	16.4	0.02 - 0.08	0.04	0.002 - 0.030	0.009	20.4
Ser	0.08 - 0.25	0.15	0.024 - 0.073	0.047	32.0	0.09 - 0.28	0.17	0.029 - 0.078	0.053	30.4
Ala	0.16 - 0.38	0.25	0.006 - 0.053	0.025	9.8	0.17 - 0.37	0.26	0.003 - 0.063	0.034	13.0
Asp	0.41 - 1.40	0.79	0.039 - 0.080	0.106	13.5	0.34 - 1.19	0.65	0.030 - 0.097	0.064	9.8
Thr	0.02 - 0.10	0.05	0.002 - 0.007	0.006	11.3	0.04 - 0.17	0.08	0.001 - 0.018	0.007	8.4
Glu	2.08 - 5.02	3.34	<0.1	<0.1	<0.1	1.71 - 4.40	2.96	<0.1	<0.1	<0.1
Val	0.02 - 0.03	0.02	0.001 - 0.005	0.003	12.3	0.02 - 0.05	0.05	0.005 - 0.011	0.009	20.9
Asn	0.01 - 0.05	0.03	0.001 - 0.014	0.007	23.3	0.03 - 0.11	0.05	0.001 - 0.053	0.014	25.6
Gln	0.65 - 1.86	1.19	0 - 0.149	0.048	4.1	0.62 - 1.73	1.11	0 - 0.123	0.058	5.2
Ile	0.001 - 0.02	0.01	0.00003 - 0.004	0.001	14.8	0.003 - 0.016	0.01	0.0004 - 0.006	0.002	24.2
Allo-Ile	0.001 - 0.004	0.002	0.00004 - 0.0009	0.0005	23.4	0.0002 - 0.004	0.002	0.0001 - 0.001	0.001	50.1
Phe	0.01 - 0.05	0.03	0.001 - 0.015	0.005	19.1	0.02 - 0.04	0.03	0.003 - 0.013	0.008	27.3

Table 2-3 Total amino acid and D-amino acid levels in perfused cortex and hippocampus

	Total Amino acid (µg/mg)		D-Amino Acid (µg/mg)		D%	
	Range	Average	Range	Average	Range	Average
Leu	0.034 - 0.039	0.04	0.00005 - 0.0001	0.0001	0.1 - 0.4	0.3
Ser	0.010 - 0.020	0.01	0.001 - 0.001	0.001	4.1 - 7.7	5.8
Ala	0.033 - 0.065	0.05	0.000005 - 0.00009	0.00005	0.008 - 0.2	0.09
Asp	0.157 - 0.29	0.19	0.03 - 0.04	0.04	15.3 - 26.2	18.9
Thr	0.083 - 0.104	0.10	0.0002 - 0.003	0.002	0.2 - 4.0	2.0
Glu	0.17 - 0.22	0.19	<0.00001 - <0.00001	<0.00001	<0.01 - <0.01	<0.01
Val	0.025 - 0.032	0.03	0.00007 - 0.0009	0.0003	0.3 - 3.6	1.1
Asn	0.009 - 0.018	0.01	0.0003 - 0.0006	0.0004	2.8 - 4.9	3.6
Gln	0.104 - 0.125	0.12	0.00001 - 0.0001	0.00005	0.004 - 0.1	0.04
Ile	0.01 - 0.012	0.01	0.00002 - 0.0003	0.0001	0.1 - 2.8	0.8
allo-Ile	0.0002 - 0.001	0.0004	0.00001 - 0.0005	0.0001	2.1 - 60.0	26.1
Phe	0.014 - 0.019	0.02	0.001 - 0.006	0.003	2.9 - 34.1	15.6

Table 2-4 Total amino acid and D-amino acid levels in blood

2.3.1 *Broad trend*

2.3.1.1 Effect of perfusion

Because of interorganism anatomical variation in vascular anatomy, the presence of blood in brain tissue is an additional variable that affects any study of blood-based analyte in tissue. As a result, the cerebral blood volume (CBV) varies between mice [66]. Perfusion largely corrects this source of interorganism variation, representing a significant technical advance. This technical issue may, in turn, have an impact on the interpretation of the importance of D-amino acids (and other analytes) in normal physiology and disease. Limiting this source of variation also may make the detection of differences between normal and abnormal physiology easier to detect, particularly in the context of subtle findings.

2.3.1.2 Amino acid levels: homeostasis?

D-Amino acids are introduced into biological systems from food, bacterial sources, and indigenous biological processes [6, 67, 40]. As D-amino acids are introduced to biological systems, a variety of processes must be present to regulate D-amino acid levels. Both D-amino acid oxidase (see Introduction) and amino acid racemases [68, 69] affect the levels of their substrates in biologically unspecified ways. Other processes also must be operative (*vide infra*). Biological processes must be present to effect control of the highly elevated brain levels of most D-amino acids as well as the anomalously low level of D-glutamic acid therein. Linking specific D-amino acids and their levels to biological function and/or disease is the ultimate challenge.

2.3.1.3 Cortex vs. hippocampus amino acid levels

A plot of the cortex and hippocampus total amino acid levels is linear with a slope of 1, indicating that there is little difference between the total amino acid levels in

the cortex and hippocampus (Figure 2-4A). In contrast, a similar plot of D-amino acid levels showed a slope of 0.87, indicating that on average, levels of D-amino acids are 13% lower in the cortex (Figure 2-4B), which points to the need for further characterization of the effects of D-amino acid function in the hippocampus. The only exception is D-aspartic acid, which is 2 times higher in the cortex. As noted previously, D-aspartic acid has the highest concentration of any D-amino acid in blood, and there is more D-aspartic acid in blood than all the other D-amino acids combined.

One process for the control of multiple D-amino acids levels is the expression or activity of D-amino acid oxidase (DAO) [70]. D-amino acid oxidase oxidizes D-amino acids, except for aspartic acid and glutamic acid, to the corresponding imino acids, producing ammonia and hydrogen peroxide [70]. Hydrogen peroxide is a reactive oxygen species associated with oxidative stress. In this report, baseline amino acid levels from healthy wild-type mice exhibited unique regional discrepancies between the hippocampus and cortex tissues. The approximate 13% decrease in D-amino acid levels in the cortex is an indication that there may be regional differences in D-amino acid synthesis and degradation. DAO might be one of the enzymes responsible for this difference. However, immunoblot and immunocytochemical studies in rodent and human tissue have not shown a difference in immunoreactivity or protein levels between hippocampus and cortex [71, 14]. Prior work examining endogenous enzyme activity levels in rodent brain subregions was not sensitive enough to show DAO activity in either cortex or hippocampus, despite DAO immunoreactivity and mRNA expression in both areas [72]. Nonetheless, differences in enzyme activity between these regions might account for some of the 13% decrease [73]. These findings also may support the hypothesis that additional processes exist other than DAO to control levels of D-amino acids in brain tissues. In fact, it has been shown that formation of D-serine from L-serine, via a serine

racemase enzyme, is one process that both synthesizes and degrades D-serine in rat brain [68].

In contrast to most of the other D-amino acids, the outlier D-aspartic acid (see Figure 2-4B) is not oxidized by DAO but rather, by D-aspartate oxidase [74, 75]. D-aspartic acid has a 2 times higher concentration in the cortex tissues (Figure 2-4B). This suggests the activity (or expression) of D-aspartate oxidase is less in cortex tissues. It was found D-aspartate oxidase, visualized by enzyme histochemistry, was present in cortex and hippocampus tissues of rats [74]. However, D-aspartate oxidase was almost two times more concentrated in the hippocampus [74]. Other processes may contribute to D-aspartic acid metabolism in the cortex relative to the hippocampus.

2.3.1.4 Percent D-amino acid levels

Figure 2-5 shows plots of % D-amino acids versus total amino acids in the hippocampus and cortex. Such plots of % D-amino acid levels allow for a deeper analysis of our findings and detection of interesting relationships and possible anomalies. These plots indicate that there is an approximate inverse relationship between the prevalence of an amino acid and its percent D-enantiomeric form. With the exception of allo-isoleucine in the hippocampus tissues, all % D-amino acid levels are similar between the two tissues. There are at least two additional highly interesting features revealed in these data. First, glutamic acid, the most prevalent of all free amino acids, had no quantifiable level of its D-antipode, the only amino acid where this was noted. This may reflect D-glutamic acid metabolism and the biological relevance of this finding is interesting but unknown. Second, the least prevalent of the measured amino acids, allo-isoleucine, was found to have approximately equal amounts of its D- and L- antipodes in the hippocampus (discussed below).

High % D-serine was observed in both brain regions (see Figure 2-5). As noted previously, D-serine plays a role in NMDA-type glutamate receptor function [54, 13]. D-amino acid oxidase only affects D-serine, but D-serine racemase, a reversible enzyme, affects levels of both L- and D- isomers of serine [68, 14, 76, 77]. Formation of D-serine from L-serine, via serine racemase, is an important mechanism for maintaining the levels of D-serine in rat brain [68]. Ratios of D- to L- amino acid interconversion rates (reported as %D-amino acid values) may be an indication of racemase activity. Currently serine and aspartate racemases are the only D-amino acid racemases reportedly found in mammalian brains [68, 69]. Our results suggest that there might be other D-amino acid racemases in mammalian brains that cause high levels of % D-amino acid values in Figure 2-5 (e.g., phenylalanine, asparagine, isoleucine, etc.). This does not exclude the probability that other biological processes affect levels of L- and D-amino acid racemization.

2.3.2 *Specific amino acids*

2.3.2.1 D-Glutamic Acid (glutamate) and D-glutamine

At physiological pH, L- and D- glutamic acid exist as their carboxylate anion, L- and D-glutamate. L-glutamate is the most abundant and principal excitatory neurotransmitter in the brain [78]. Given its importance, it is not surprising that L-glutamate has a well-known regulatory pathway, the glutamate-glutamine cycle [78]. In this cycle, L-glutamate is supplied to the central nervous system from L-glutamine [79, 80]. Astrocytes convert L-glutamate to L-glutamine via glutamine synthetase [79]. L-glutamine is then released into the extracellular space [79]. Conversely, L-glutamine is metabolized into L-glutamate in presynaptic terminals by the mitochondrial enzyme glutaminase [79]. The levels of L-glutamate and L-glutamine found in the hippocampus and cortex of NIH Swiss mice were not only higher than any of the other amino acids, but

they were also an order of magnitude higher than the blood levels (Figure 2-2A). Only serine had comparably elevated levels in brain tissues relative to blood levels. More surprisingly, D-glutamic acid was the only D-amino acid not found (i.e., below quantitation limits) in either the brain or blood. Conversely, D-glutamine was the most prevalent D-amino acid in the cortex with hippocampus levels about 10 times lower and blood levels 100 times lower (Figure 2-2B).

The relative lack of D-glutamic acid is the one of the more intriguing results in this study, particularly since L-glutamic acid is the most prevalent amino acid and all other lower abundance amino acids show appreciable levels of their D-antipodes. D-glutamic acid is enzymatically converted to D-pyrrolidone carboxylic acid (in rat liver and kidney), then excreted [81]. The concurrent high level of D-glutamine may indicate that it is a product of an active D-glutamate reaction or removal pathway. However, unlike the L-glutamate to L-glutamine cycle, this D-glutamate to D-glutamine pathway is largely a unidirectional process.

D-glutamate and D-aspartate also are metabolized by D-aspartate oxidase (DDO) in mammals [65]. However, in the present work, D-aspartate levels are high even though DDO is more selective to D-aspartate than to D-glutamate. Therefore, it is likely that the additional processes that involve D-glutamine are limiting D-glutamate levels in the hippocampus and cortex tissues. D-glutamate is taken up by glial cells and converted via glutamine synthetase to D-glutamine [82]. Glutamine synthetase is not enantiospecific and can catalyze aminations of both L- and D- glutamate [82]. However, there are no reports showing that glutaminase, which converts L-glutamine into L-glutamate, is permissive for D-glutamine. This supports the conclusion that the D-glutamate pathway is largely a unidirectional process and not part of a cycle, like the L-glutamate - L-glutamine cycle. The relevance/importance of having low D-glutamate levels is unclear. D-

glutamine is a biomarker for kidney injuries [83]. In the brain D-glutamine increased the uptake of tryptophan [84]. D-glutamine also appeared to produce retrograde amnesia and seizures [85]. Further work is needed to delineate the impact of errors in endogenous metabolism of D-glutamate.

2.3.2.2 D-Aspartic acid (aspartate) and D-serine

Levels of D-aspartate and D-serine in the mouse hippocampus and cortex tissues are high compared to all measured D-amino acids, except for D-glutamine (see Figure 2-2B). The high levels of D-serine and D-aspartate are assumed to be due to their function as neurotransmitters [53, 13]. D-serine is probably the most studied D-amino acid. Reviews by Wolosker and Schell thoroughly discuss D-serine function in regard to the NMDA receptor [86, 87]. High blood levels of D-aspartate may indicate the need for different tissues to have ready access to this amino acid for a variety of metabolic or signaling processes (and perhaps, inefficiency of its intracellular synthesis). D-aspartate has different properties as a neurotransmitter, compared to D-serine [53]. D-aspartate is present in high concentrations in synaptic vesicles of axon terminals and the origin of D-aspartate occurs in neurons via D-aspartate racemases [53, 69]. D-aspartate is involved in synthesis and release of testosterone and luteinizing hormone in rat pituitary gland [88, 89]. In addition, free D-aspartic acid is found in white and gray matter in human brains, but free D-aspartic acid levels are twice as high in gray matter with subjects diagnosed with Alzheimer's disease [22, 18]. More recently, D-aspartate was found to regulate neuronal dendritic morphology, synaptic plasticity, gray matter volume, and brain activity in rats [90, 91].

2.3.2.3 D-Branched chain amino acids (D-leucine, D-valine, D-isoleucine, and D-allo-isoleucine)

The branched chain aliphatic amino acids leucine, isoleucine, allo-isoleucine, and valine all have low total amino acid levels but high % D-amino acid levels (Table 2-3 and Figure 2-5). Total levels of branched chain amino acids (BCAAs) are similar in blood compared to perfused and non-perfused tissues in most cases, but D-amino acid levels for BCAAs are significantly higher in hippocampus and cortex tissues than blood as are all the other amino acids in this study. No explanation of BCAA levels compared to other amino acids was found in the literature. Recently it has been discovered that D-leucine, but not D-valine, can be used to treat seizures in mice [23]. The levels of D-branched chain amino acids (D-BCAA) in the brain are fairly similar (Figure 2-2B). In view of D-leucine's use in the treatment of seizures, it may be worth examining the action of other D-BCAAs. Prolinase, which is present in brain tissue, is strongly inhibited by L-BCAAs [92]. Conversely, D-BCAAs enhance prolinase's function [92]. In glial-enriched cultures from mouse brain tissues, D-valine has been used in media to inhibit growth of fibroblasts, causing cultures to be characterized as over 80% astrocytic, and having suppressed growth rates [93]. The results of this experiment suggest that D-valine might have an influence on the growth of select non-glial cell populations in the brain. There are no reports for function of D-allo-isoleucine in mammalian tissues, but levels of L-allo-isoleucine are increased in patients suffering from maple syrup urine disease (the pathophysiological significance of this finding is unclear) [94, 95].

2.3.2.4 D-Phenylalanine, D-alanine, and D-asparagine

The % D-amino acid values of D-asparagine and D-phenylalanine in brain tissues were relatively high (~ 10 – 30% range), even though their total amino acid concentrations were comparatively low (Table 2-3). D-asparagine and D-phenylalanine

exhibited similar concentrations. D-phenylalanine may alleviate neurological stress through trapping of reactive oxygen species in neurological tissue [96]. D-phenylalanine also may treat emotional stress [97]. Free D-asparagine has not been reported to be involved in any neurological process. However, hydrolysis converts D-asparagine to D-aspartate. D-aspartate function has been reported in brain tissue. A D-asparagine to D-aspartate cycle analogous to the glutamate to glutamine cycle has not been identified. D-alanine showed moderate levels of total amino acid, D-amino acid, and %D-amino acid values in this study. D-alanine levels were found to be the same in brain white matter of tissue from normal patients and those with Alzheimer disease but D-alanine levels were twice as high in Alzheimer gray matter compared to normal gray matter [18]. D-alanine administration can lead to hypofunction of NMDA neurotransmission, and it has been used as a potential approach for the pharmacotherapy of schizophrenia [16].

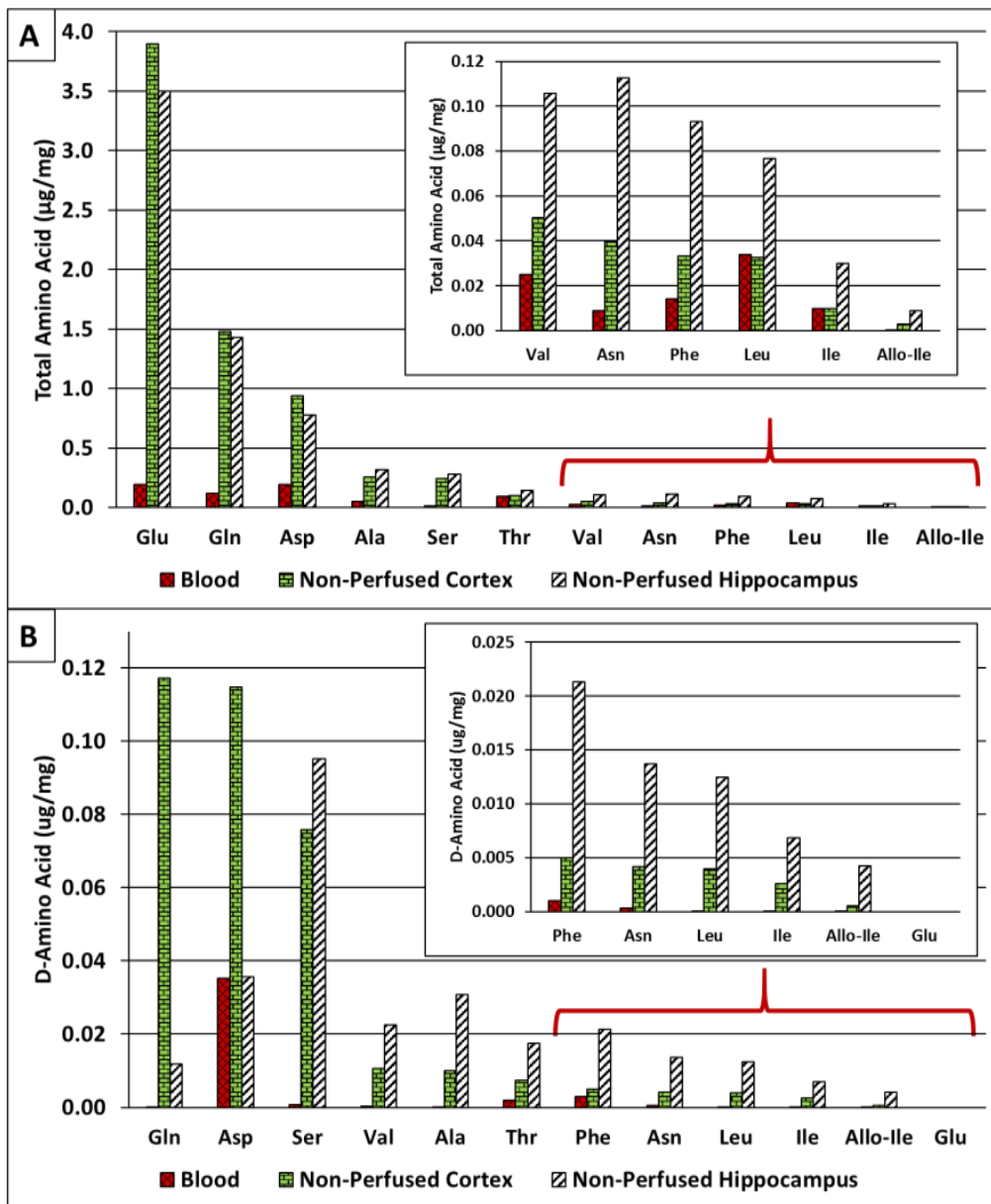


Figure 2-2 The average value of A) total amino acid levels and B) D-amino acid levels (ug/mg) in blood, non-perfused cotex, and non-perfused hippocampus.

The range of the average values can be seen in Table 2-1. Average value for blood with n = 5. Average value for non-perfused cortex with n = 7. Average value for non-perfused hippocampus with n = 7

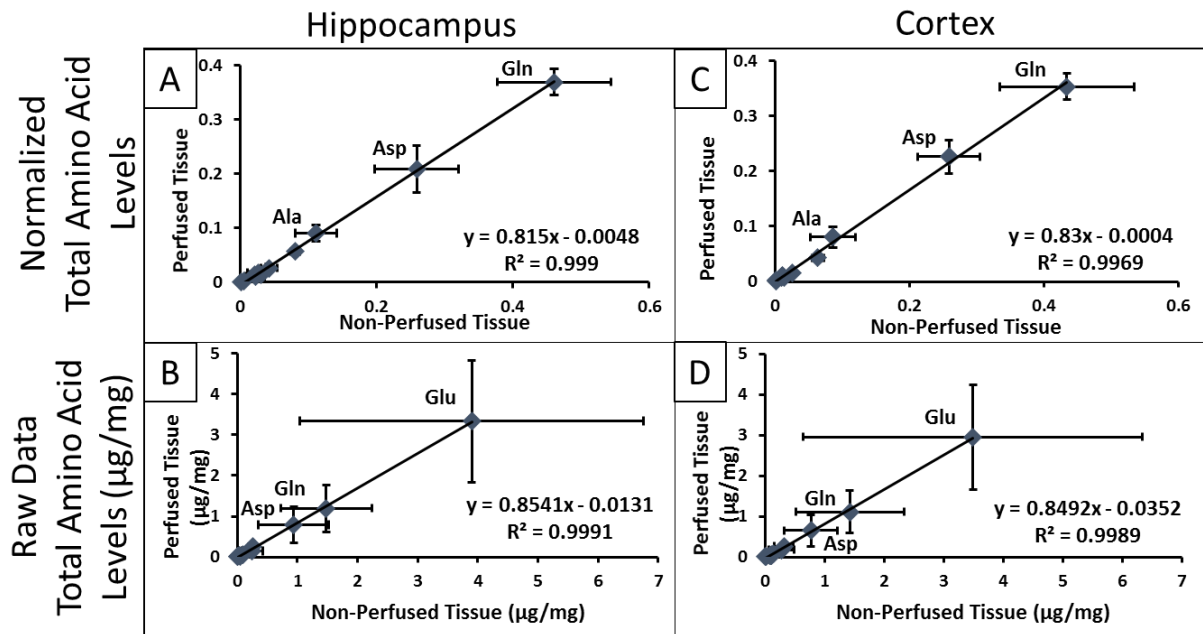


Figure 2-3 Linear plots of the total amino acid levels in perfused and non-perfused samples and normalized data (with respect to glutamic acid) in comparison to raw data.

A) Hippocampus plot of normalized total amino acid levels of perfused tissue vs. non-perfused tissue. B) Hippocampus plot of raw total amino acid levels of perfused tissue vs. non-perfused tissue. C) Cortex plot of normalized total amino acid levels of perfused tissue vs. non-perfused tissue. D) Cortex plot of raw total amino acid levels of perfused tissue vs. non-perfused tissue.

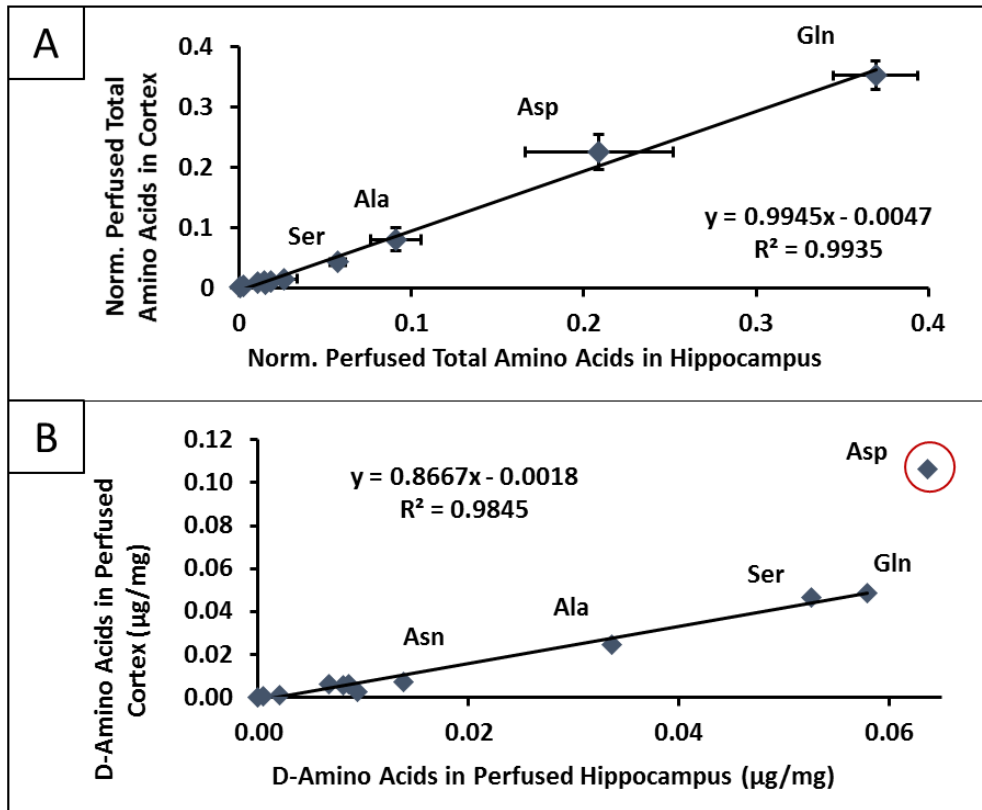


Figure 2-4 A) Comparison of total amino acid levels in the cortex vs. hippocampus. B) Comparison of D-amino acid levels in the cortex vs. hippocampus, and Asp, circled in red, is not included in the calibration. In both plots each data point represent an individual amino acid value that is averaged from N = 7.

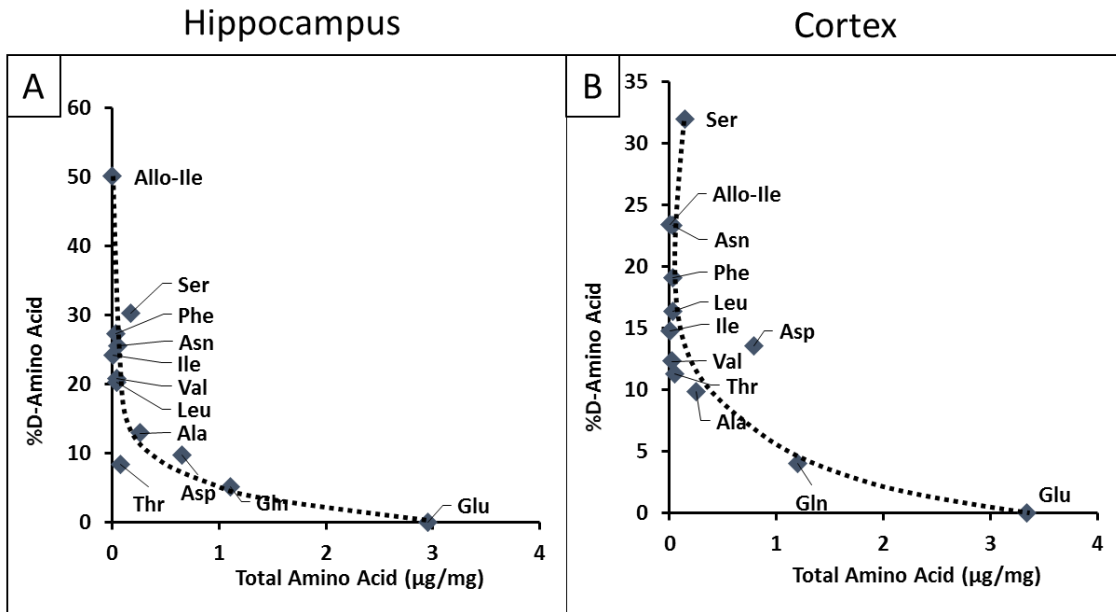


Figure 2-5 A) Plot of hippocampus %D amino acid levels vs. total amino acid levels. B)

Plot of cortex %D amino acid levels vs. total amino acid levels.

In both plots each data point represent an individual amino acid value that is averaged from N = 7.

2.4 Conclusions

This study provides the most complete baseline analysis of L- and D-amino acids in mouse brain tissues to date. Perfusion of brain tissue reduces the variation in brain amino acid levels among mice and suggests that free amino acid data obtained from perfused tissue may give a more accurate measure of cellular and extracellular/extravascular levels. There is little difference in the total amino acid levels in the hippocampus and cortex, but there is an approximate 13% reduction in almost all measured D-amino acid levels in the cortex compared to the hippocampus. An exception is D-aspartic acid, which is 2 times higher in the cortex and has higher blood levels than

all other D-amino acids, thereby making it more available to all tissues. Results suggest that additional processes exist other than DAO and racemases that control broad levels of D-amino acids in brain tissues. Plots of % D-amino acids indicate that there is an approximate inverse relationship between the prevalence of an amino acid and the percentage of its D-enantiomeric form. This suggests that there might be other D-amino acid racemases in mammalian brains that underlie high levels of % D-amino acid values. Total levels of BCAAs are similar in blood compared to hippocampus and cortex tissues, but D-amino acid levels for BCAAs are significantly higher in hippocampus and cortex tissues than blood. A notable result is that glutamic acid, the most prevalent of all free amino acids, had no measurable level of its D-antipode. It is possible that the D-glutamate metabolism is a unidirectional process and not a cycle (i.e., in comparison to the L-glutamate/glutamine cycle). The specific and efficient suppression/removal of D-glutamic acid from the brain is likely to be physiologically important and warrants further investigation.

Chapter 3

Sensitive Analysis of N-blocked Amino Acids Using High-Performance Liquid Chromatography with Paired Ion Electrospray Ionization Mass Spectrometry

Abstract

In this study, a paired ion electrospray ionization (PIESI) mass spectrometry method was developed for sensitive detection of 9-fluorenylmethyl chloroformate (Fmoc)-derivatized amino acids. The structure-optimized ion-pairing reagent was introduced post column to form positively charged complexes which can be detected in the positive ion mode. These complexes are more surface-active than the original analytes, and meanwhile, the intensity of sodium adducts was significantly reduced. The limit of detection of the amino acids obtained with the optimal ion-pairing reagent was 0.5 to 20 pg which was 5 - 100 times lower than the negative mode. In addition, two mass spectrometry platforms - linear ion trap and triple quadrupole - were used to compare the PIEESI improvements. Eventually, the method was applied to successfully detect the level of amino acids in human urine samples with high accuracy and the added benefit of minimizing matrix effects.

3.1 Introduction

Amino acids are one of the most important classes of compounds in nature since they play essential roles as building blocks in proteins as well as metabolic intermediates. [98] They are also involved in other biological pathways, such as transport and storage of nutrients, oxidation protection and regulation of gene expression, and neurotransmission [99, 100]. Abnormal amino acid concentrations can indicate metabolic disorder and can be used as indicators to diagnose disease [101]. Consequently, the sensitive and accurate detection of amino acids are essential in different fields, especially in clinical diagnostics.

Amino acids have been analyzed with gas chromatography (GC), liquid chromatography (LC), and capillary electrophoresis (CE). Enantioseparation of amino acids was also achieved by chiral GC/LC stationary phases or introducing chiral selectors in CE [102, 5, 103, 104, 40, 105, 106]. To achieve improved separation and detection, amino acids were analyzed using MS detection and/or derivatized before analysis [106-109]. Different derivatization reagents have been introduced for amino acids, while the most commonly used ones, such as fluorenylmethyloxycarbonyl chloride (Fmoc-Cl) [110], o-phthalaldehyde (OPA) [111, 112], and 7-fluoro-4-nitrobenzoxadiazole (NBD-F) [113, 114], react with the amino group and leave the carboxyl group free. OPA derivatization is fast but can only react with primary amines, and some of the products were labile and must be analyzed right after derivatization [32]. Fmoc-Cl can react with both primary and secondary amines in a short time with high yield, and the product is quite stable for at least 3 days [110, 115]. In addition to providing a chromophore for UV or fluorescence detection, Fmoc derivatization is also suitable for MS analysis. Fmoc-derivatized amino acids (Fmoc-AAs) and short-chain peptides show 2 orders of magnitude higher ionization efficiency compared to their underivatized analogues in LC-MS analysis [116].

To further enhance the detection sensitivity of Fmoc-AAs with LC-MS, a method based on paired ion electrospray ionization (PIESI) mass spectrometry was developed in this study. PIEI was found to provide ultra-trace level detection sensitivity for anions and some zwitterions (often \leq parts per trillion (ppt) levels) [117-126]. This simple approach introduces low levels of designed synthetic ion-pairing reagents (IPRs) into the sample stream just prior to ESI ($\text{Fmoc-AA}^- + \text{IPR}^{2+} \rightarrow [\text{Fmoc-AA} + \text{IPR}]^+$) [127, 128]. The gas-phase paired ions are then detected in the more sensitive positive ion mode rather than the negative ion mode. The adducts of IPRs and analytes are more surface-active as compared to the original anions and thus show better ionization efficiency with ESI. Furthermore, especially for anions with small molecular weights, the analytes were detected in a higher m/z range with less inherent chemical noise.

In this work, we examined the sensitivity enhancement of 22 (20 proteinogenic and 2 non-proteinogenic) amino acids by using PIEI-MS in both selected ion monitoring (SIM) and selected reaction monitoring (SRM) modes. Different IPRs (symmetrical and unsymmetrical dicationic, tricationic, tetracationic) were examined and compared. Moreover, the optimized PIEI approach was then hyphenated to HPLC for the analysis of amino acids in urine samples.

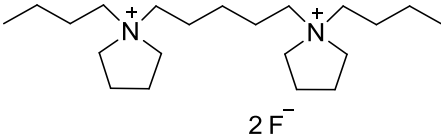
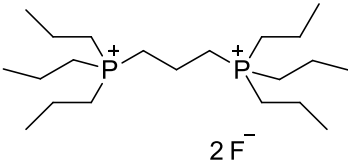
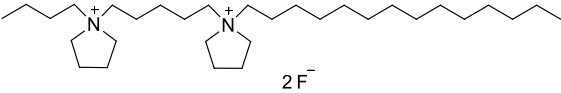
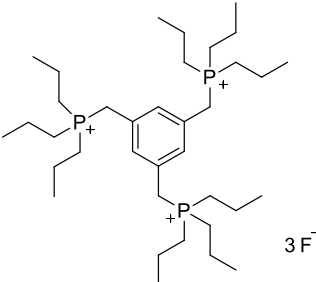
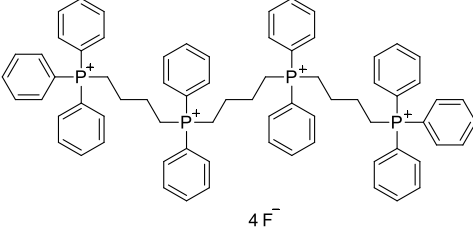
3.2 Experimental

3.2.1 Reagents and materials

The abbreviations and chemical structures of the ion-pairing reagents used in this study are shown in Table 4-1. 1,5-Pentanediy-bis(1-butylpyrrolidinium) difluoride solution, 1,3-propanediy-bis(tripropylphosphonium) difluoride solution, 1-butyl-1-[5-(1-tetradecyl-1-pyrrolidiniumyl)pentyl]pyrrolidinium difluoride, 1,3,5-tris[(tripropylphosphonium)methyl]benzene trifluoride solution, and 1,4-butanediy-

bis[diphenylphosphonium-(1'-4'-butyl-triphenylphosphonium)] tetrafluoride solution were originally developed in our laboratory, and some of them are also commercially available from AZYP, LLC (Arlington, TX, USA). These ion-pairing reagents were initially synthesized in bromide salt form and then ion exchanged to their fluoride form. The amino acid standards [alanine (Ala), γ -aminobutyric acid (GABA), arginine (Arg), asparagine (Asn), aspartic acid (Asp), cysteine (Cys), glutamic acid (Glu), glutamine (Gln), glycine (Gly), histidine (His), isoleucine (Ile), leucine (Leu), lysine (Lys), methionine (Met), phenylalanine (Phe), proline (Pro), serine (Ser), taurine (Tau), threonine (Thr), tryptophan (Trp), tyrosine (Tyr), valine (Val)] and their Fmoc derivatives (9-fluorenylmethyl chloroformate (Fmoc-Cl)), HPLC-MS grade acetonitrile (ACN), and formic acid were purchased from Sigma-Aldrich (St. Louis, MO, USA). Borate buffer was from Waters Corporation (Milford, MA, USA). HPLC-MS water was from Honeywell Burdick and Jackson (Morristown, NJ, USA).

Table 3-1 Abbreviation, exact mass and structure of the ion pairing reagent used in this study

Ion pairing reagent	Abbreviation Exact mass	Structure
1,5-Pentanediy-bis(1-butylpyrrolidinium) difluoride	C ₅ (bpyr) ₂ , 324.4	
1,3-Propanediyl-bis(triethylphosphonium) difluoride	C ₃ (triprp) ₂ , 362.3	
1-Butyl-1-[5-(1-tetradecyl-1-pyrrolidinium)pentyl]pyrrolidinium difluoride	UDC, 464.5	
1,3,5-Tris[(triethylphosphonium)methyl]benzene trifluoride solution	Tristriprp, 597.5	
1,4-Butanediyl-bis[diphenylphosphonium-(1'-4'-butyl-triphenylphosphonium)] tetrafluoride	Tetpp4+, 1062.6	

3.2.2 Paired ion ESI analysis

A scheme of the instrumental setup for the PIESI-MS detection is shown in Figure 3-1. Briefly, a carrier flow consisting of acetonitrile and water (67:33, v/v) was delivered by the binary LC pump at 300 $\mu\text{L}/\text{min}$, while a 40 μM aqueous solution of ion-

pairing reagent was introduced by another pump (Shimadzu LC-6A; Shimadzu, Columbia, MD, USA) at a flow rate of 100 $\mu\text{L}/\text{min}$. The two streams were combined in a low dead volume mixing tee (Thermo Scientific, San Jose, CA, USA). A total flow of acetonitrile/water (50:50, v/v) with 10 μM of ion-pairing reagent was introduced into the MS at a flow rate of 400 $\mu\text{L}/\text{min}$. The continuous use of the non-volatile ion-pairing reagent can result in the contamination of the ion source. To ensure the producibility and accuracy of the analysis results and maintain the optimum performance of the ion source, a mobile phase of 50:50 methanol/water was pumped at a flow rate of 200–400 $\mu\text{L}/\text{min}$ through the sample transfer line, sample tube, and ESI probe for 1 h at the end of each working day until the ion-pairing reagent memory peaks were no longer detected. The spray cone and ion transfer capillary were cleaned weekly according to the manufacturer's instruction. Fmoc amino acids were injected into the HPLC system through a six-port injection valve. As the consequence, positively charged analyte/ion-pairing reagent complexes could be detected by the MS in the positive ion mode. An analytical column was inserted between the mixing device and the injection valve (see Figure 3-1) for the chromatographic separations and sample analysis.

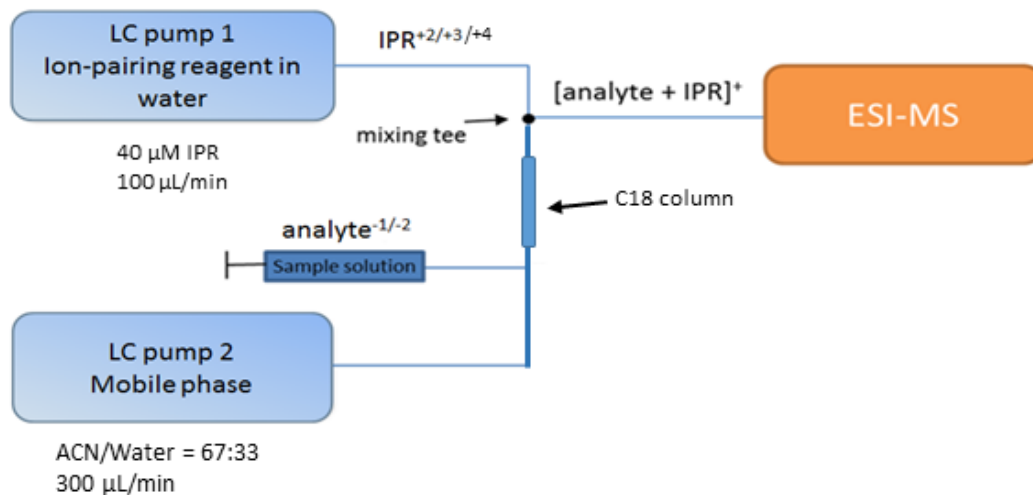


Figure 3-1 The instrument set up of HPLE-PIESI-MS.

3.2.3 Linear ion trap and triple-quadrupole mass spectrometer conditions

The HPLC-MS system used in the study is a Thermo Finnigan LXQ linear ion trap mass spectrometer with an off-axis (45°) Ion Max ESI source, (Thermo Fisher Scientific, San Jose, CA, USA). The MS parameters for the LXQ in the positive ion mode were set as follows: spray voltage (3 kV), capillary voltage (11 V), capillary temperature (350 °C), sheath gas flow (37 arbitrary units (AU)), and the auxiliary gas flow (6 AU). In the SRM mode, the normalized collision energy, the Q value, and the activation time were set at 30, 0.25, and 30 ms, respectively. A Shimadzu LCMS-8040 triple-quadrupole mass spectrometer (Shimadzu, Kyoto, Japan) equipped with an orthogonal ESI source was compared. Operating conditions of the source were performed as follows: ionization voltage (3.5 kV), temperature of desolvation line (250 °C), temperature of heating block (400 °C), nebulizing gas (3 L/min; N₂), and drying gas (15 L/min; N₂), respectively. The voltages at Q1 prebias, collision energies, or Q3 prebias were optimized for each analyte individually.

The signal-to-noise (S/N) ratio was calculated with Xcalibur 2.0 software for the LXQ MS or a LabSolutions system for triple-quadrupole MS. The limit of detection (LOD) was determined at the concentration with a S/N ratio of 3 in five replicated injections for each sample. The PIESI-MS detection was performed in both the SIM mode and SRM mode. In the SIM mode, the m/z of the analyte/ion-pairing reagent complex ion was monitored, while in the SRM mode, the most abundant MS/MS fragment ion from the collision-induced dissociation (CID) was monitored. The injection volume was kept at 5 μL for all the experiments. The LODs obtained in the negative ion mode was used for comparison to the PIESI results. The MS parameters in this mode were optimized also. To have comparable LC conditions, a carrier flow consisting of acetonitrile and water (50:50, v/v) at 400 $\mu\text{L}/\text{min}$ was introduced into the MS directly without using ion-pairing reagent.

3.2.4 Preparation and separation of calibration standards

An internal standard method was used for calibration. The standard stock solution contained 1 $\mu\text{mol}/\text{mL}$ of each amino acid and was further diluted to the desired concentrations: 1, 2, 5, 10, 20, 50, 100, and 200 nmol/mL . To each concentration, 400 μL of amino acid solutions was mixed with 100 μL of 50 nmol/mL norvaline as internal standard (IS). The resulted mixture was derivatized by using the following procedures: 50 μL of borate buffer and 20 μL of sample were added into an autosampler vial, and an aliquot of 5 μL of 0.1 M Fmoc-Cl was added and the mixture was incubated at room temperature for 20 min. Then, 5 μL of 0.8 M 1-aminoadamantane (ADAM) solution was added to quench the reaction. A scheme of the Fmoc derivatization reaction and the structures of each amino acid studied are shown in Figure 3-2. The separation of Fmoc-AA standards was achieved using a gradient method with a C18 stationary phase (Ascentis® Express C18 2.7 μm SPP, 10 cm \times 2.1 mm I.D.). Mobile phase A was

acetonitrile, and mobile phase B was 0.1% formic acid in H₂O, respectively. The flow rate was 0.25 mL/min; the gradient was 30–60% A, 0–19.5 min; 60–95% A, 19.5–20.0 min; and 95% A, 20.0–21.0 min; and the mobile phase went back to 30% A for re-equilibrium of the column for another 10 min. MS data acquisition started with a time delay of 2.5 min.

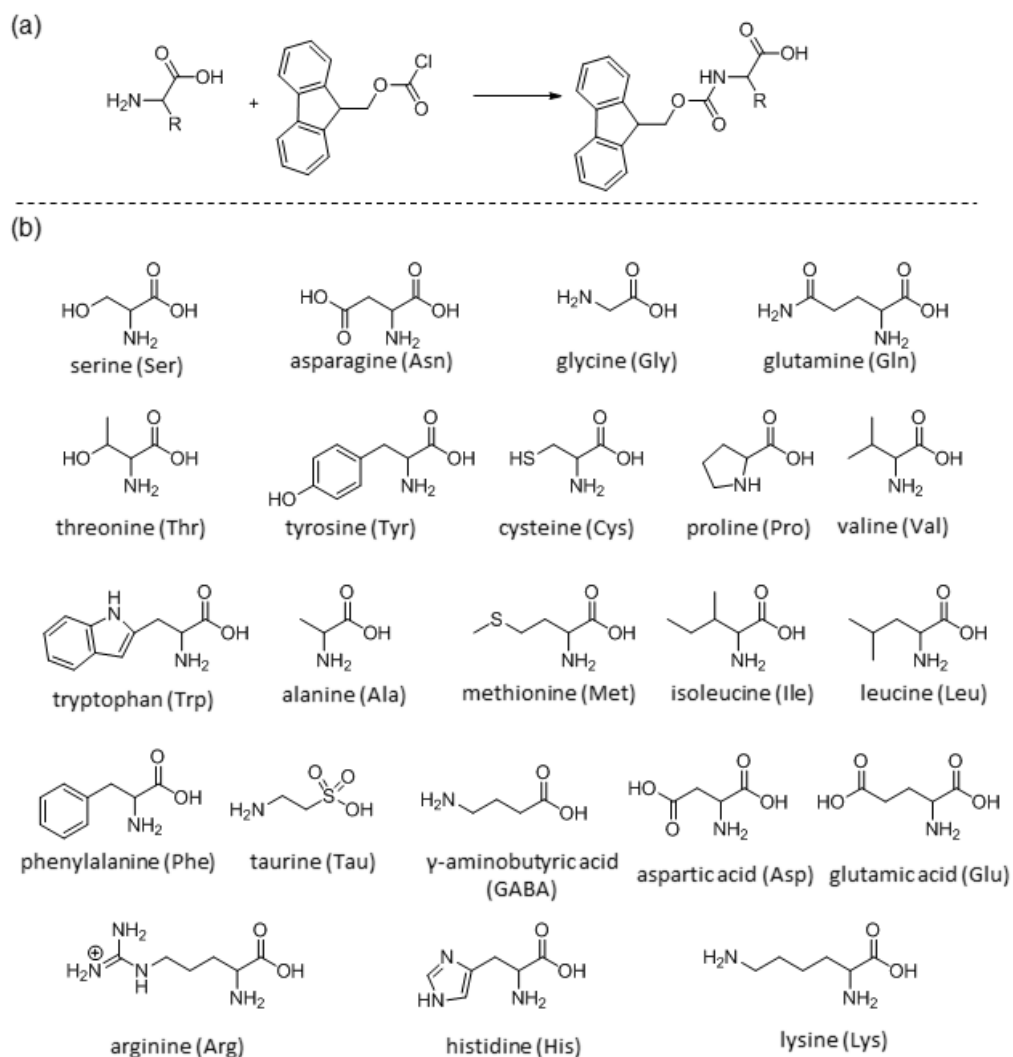


Figure 3-2 (a) Fmoc-derivatization reaction. (b) Structure of all the amino acids studied in this paper.

3.2.5 Urine sample preparation and analysis

Urine samples were obtained from healthy volunteers. For the recovery studies, urine samples were 2 or 10 times diluted with 0.5% formic acid in water. Three aliquots of urine sample were prepared at each dilution factor. One of the samples was non-spiked and used for the analysis of the amino acid content in the urine. The other two samples were spiked with amino acid standards with a final concentration of 2 and 25 nmol/mL. An aliquot of 400 μ L of urine sample was mixed with 100 μ L of IS (three per experimental condition). The mixture was then centrifuged at 13,000 rpm at 4 °C for 15 min to precipitate any protein. The supernatant was collected and filtrated through a filter and stored at – 80 °C until analysis. The resulting samples were processed according to the derivatization protocol described in section “Preparation and separation of calibration standards.” The use of solvent and derivatization reagent dilutes the sample fourfold, so the final dilution factors for the urine are 8 and 40 times. The quantification of the urine sample was accomplished in the PIESI-SIM mode using an internal standard calibration ($R^2 > 0.99$, see section “Preparation and separation of calibration standards”).

3.3 Results and discussion

3.3.1 Mechanism for the improved performance of ion-pairing reagents for Fmoc amino acids

Fmoc-AAs were screened in both the positive and negative ion modes for an initial study. In the positive ion mode, sodium adducts rather than the protonated molecules were detected as the base peaks for the amino acids except for His, Arg, and Lys (an example MS spectrum of Fmoc-Ile is shown in Figure 3-3a). When the sodium adducts were fragmented as precursor ions at MS/MS, insufficient fragmentations were

observed. In the negative ion mode, other than the base peak $[M-H]^-$, a significant deprotonated dimer $[2M-H]^-$ was observed, as shown in Figure 3-3b. As a consequence, in both the positive and negative ion modes, the formation of adducts significantly decreases the intensity of $[Fmoc-AA+H]^+$ or $[Fmoc-AA-H]^-$. ESI conditions could be optimized in order to minimize the formation of the sodium adducts or dimers, but they could not be eliminated. Although these non-covalent adducts can provide information for qualitative analysis, the poor reproducibility of the adducts makes the sensitive and accurate quantitation of low-abundance amino acids highly restricted [129, 130]. It has been reported previously that the ion-pairing reagents used in PIESI shown superior competition versus protons and other small metal cations for anionic sites [131]. So, as expected, when the IPR was infused post column, stable positive charged complexes were formed between the IPR and deprotonated Fmoc-AA anions ($pK_a \approx 2$), as shown in Figure 3-3c. It should be pointed out that the Fmoc-His, Fmoc-Arg, and Fmoc-Lys were detected as $[M+H]^+$ even with the presence of the IPRs, which means there was little association between the basic amino acids and IPR. In this way, all the Fmoc amino acids can be detected simultaneously at the more sensitive positive ion mode. When the Fmoc-Ile complex ion $[C_5(bpyr)_2^{2+} + Fmoc-Ile^-]^+$ was fragmented subsequently, structurally specific product ions were produced (see Figure 3-3d). The mass spectra for each amino acid are shown in Fig. S3 (see ESM). In summary, the utilization of PIESI for Fmoc amino acids overcomes the shortage of common MS approaches in regard to their ionization and fragmentation.

Figure 3-4 shows an example of the S/N improvement when the $C_5(bpyr)_2$ is used as the IPR for the detection of 100 ng/mL of Fmoc-Ile. In the negative SIM mode, no peak was detectable. In the positive SIM mode, only sodium adducts were detected and the S/N was less than 3. In the PIESI-SIM mode, a significant response with S/N 67 was

detected, and the detection at the PIESI-SRM mode further enhanced the detection sensitivity (Figure 3-4).

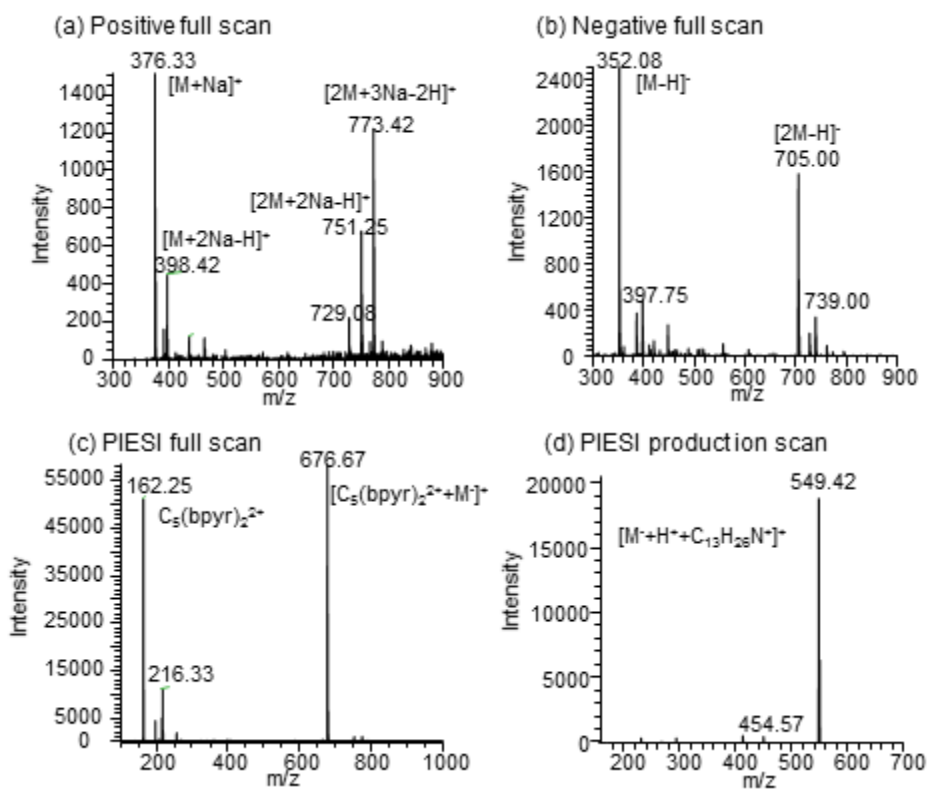


Figure 3-3 | Representative full-scan MS spectra of Fmoc-Ile with and without ion-pairing reagent (IPR).

(a) Positive full scan without IPR. (b) Negative full scan without IPR. (c) PIESI full scan.

(d) PIESI product ion scan when using the m/z 676.7 as precursor. Molecular weight of

Fmoc-Ile = 353. The IPR used in this experiment is 40 μ M $C_5(bpyr)_2$.

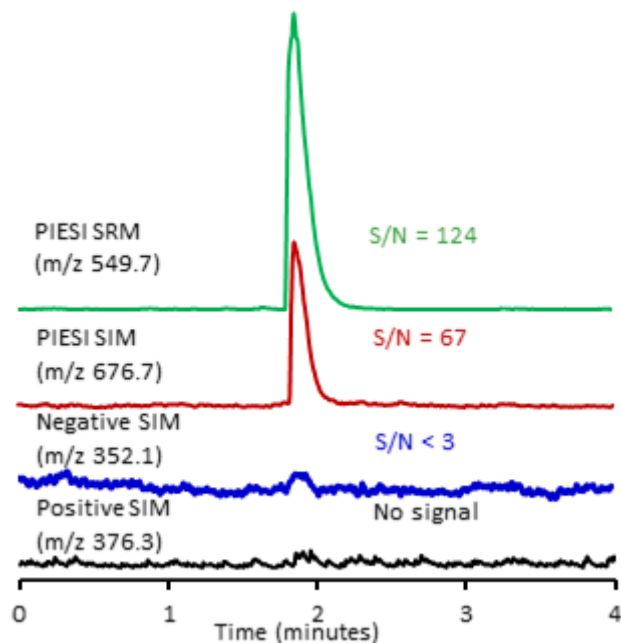


Figure 3-4 Chromatographic profile of signal-to-noise ratio at positive SIM mode, negative SIM mode, PIESI-SIM mode, and PIESI-SRM mode.

Sample injected: 100 ng/mL of Fmoc-Ile. The dicationic ion-pairing reagent used in the PIESI analysis is 40 μM $\text{C}_5(\text{bpyr})_2$.

3.3.2 Selection of the ion-pairing reagent

The overall structure and the nature of the charged moieties of the IPR reagents play essential roles in the selectivity and sensitivity of the PIESI method. In previous studies, the dicationic IPRs provided the best performance for singly charged anions [124, 132]. The tricationic IPRs were shown to have the capability to improve the detection sensitivity for divalent anions [118, 122]. Tetracationic IPRs showed versatility and sensitivity not only to trivalent anions but also to divalent ions and some zwitterions [119-121, 133]. In this work, three dicationic IPRs: $\text{C}_5(\text{bpyr})_2$, $\text{C}_3(\text{triprp})_2$, plus the unsymmetrical IPR (UDC); one tricationic IPR (Tristriprp); and one tetracationic IPR

(Tetpp4+) were chosen as potential IPRs for Fmoc-AA analysis. The structures for all the tested ion-pairing reagents are shown in Table 1. UDC was specifically designed to have a long alkyl chain on one end, contract to its symmetrical analogue. This surface-active IPR provided superior performance to its symmetrical IPR for small inorganic and organic ions owing to enhanced ionization efficiencies [128].

The ESI S/N improvement factor for each individual Fmoc-AA was calculated using the value of the negative SIM mode over the PIESI-SIM/SRM mode. Positive SIM mode was not included in this comparison since the quantitation based on sodium adduct was shown to be much less reproducible and sensitive. To test the sensitivity enhancement for different PIESI reagents, three Fmoc-AAs were evaluated as the test analytes: Fmoc-Leu, Fmoc-Phe, and Fmoc-Glu, because they are aliphatic, aromatic, and acidic amino acids, respectively. No basic amino acid was tested in this study since they did not form a complex as with similarly charged IPRs as verified by the screening results (see section "3.3.1"). As shown in Figure 3-5, the S/N improvement is more substantial for the Fmoc-Leu and Fmoc-Phe than the Fmoc-Glu with the dicationic IPRs. This could be explained by the fact that the Fmoc-Leu and Fmoc-Phe contain one free carboxyl group while the Fmoc-Glu contains two, so the majority of Fmoc-Glu + C₅(bpyr)₂ complexes are uncharged. The tetracationic IPR (Tetpp4+) was superior to the other IPRs for Fmoc-Glu. In contrast, it showed less enhancement than C₅(bpyr)₂ for Fmoc-Leu and Fmoc-Phe because they can form + 3 and + 2 complexes. The UDC did not show better performance than the C₅(bpyr)₂, which may be due to the fact that Fmoc amino acids already have some surface activity. As a result, the C₅(bpyr)₂ and Tetpp4+ performed best for monovalent anionic Fmoc-AA and divalent anionic Fmoc-AA, respectively, so these two IPRs were used for all subsequent studies.

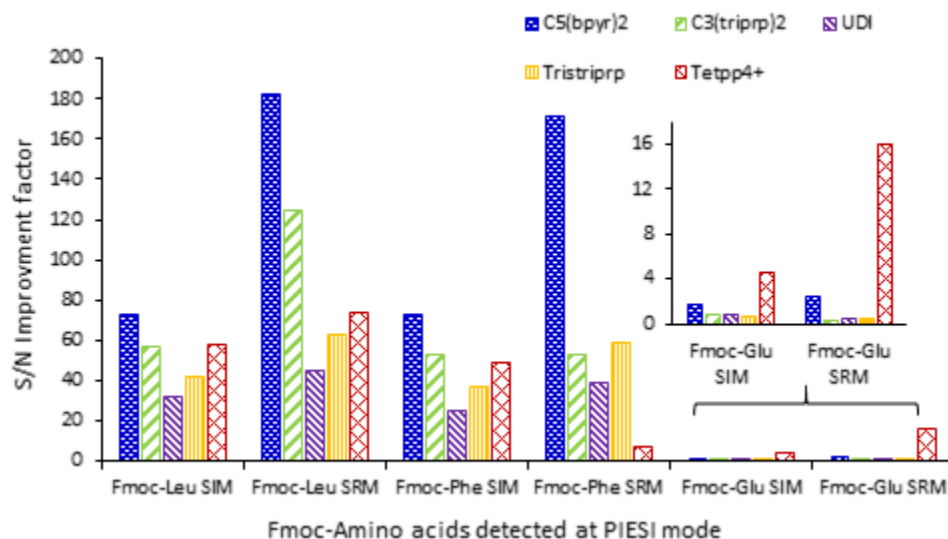


Figure 3-5 The ESI signal-to-noise (S/N) improvement factor for each amino acid is calculated as the S/N value at the PIESI mode over the negative SIM mode.

Concentration of sample = 1 $\mu\text{g/mL}$. Concentration of IPR = 40 μM ; except for UDI with 4 μM . Obtained with the linear ion trap MS analyzer. Refer to Table 1 for the structure of each ion-pairing reagent.

3.3.3 Limit of detection of Fmoc amino acids

Table 2 shows the comparison of the absolute limits of detection for a total of 22 Fmoc amino acids obtained in PIESI modes and the negative ion mode on a linear ion trap mass spectrometer (see "Experimental"). All 22 Fmoc amino acids were detected with LODs from the nanogram to picogram levels in the PIESI mode, which were 10–500 times lower than the LODs obtained in the negative mode. Fmoc-Gly had the lowest LOD value among all the amino acids. This may be due to the smaller size and hydrophilicity of glycine. The SRM of negative mode cannot be conducted because no fragmented signal was detected. The LODs in the SRM mode were evaluated by using the IPR/Fmoc-AA

complex ion as the precursor ion and the most abundant fragment as the daughter ion (Table 3-2). The SRM mode shows improved sensitivity over the SIM mode due to the reduction of background noise.

Table 3-2 Limit of detection values of Fmoc-AAs at negative mode and PIESI SIM/SRM mode obtained with linear ion trap mass analyzer.

Sample	Negative SIM		PIESI SIM		PIESI SRM	
	LOD (pg)	m/z	LOD (pg)	m/z	LOD (pg)	m/z
Ser	250	326	30	650	6.5	523
Asn	450	353	50	677	8.2	550
Gly	800	296	7.5	620	0.8	493
Gln	500	367	50	691	10.0	564
Thr	300	340	25	664	15.0	537
Tyr	500	402	100	726	20.0	599
Cys	700	683	25	1007	7.5	880
Pro	1200	336	15	660	5.0	533
Val	200	338	15	662	2.5	535
Trp	1000	425	20	749	5.0	622
Ala	800	311	12.5	635	5.0	508
Met	250	370	17.5	694	15.0	567
Ile	750	352	12.5	676	2.5	549
Leu	750	352	12.5	676	2.5	549
Phe	400	386	12.5	710	2.5	583
Tau	1200	346	12.5	670	1.0	543
GABA	1000	324	20	648	4.5	521
Asp	125	354	25	473 ^a	12.5	354 ^a
Glu	100	367	25	715 ^a	5.0	604 ^a
Arg ^b			5	397 ^c	1.0	336
His ^b			12.5	378 ^c	2.0	156
Lys ^b			15	600 ^c	2.0	556

a LOD was obtained with the tetracationic ion pairing reagent: 40 μ M Tetpp4+.

b Basic amino acids were not detected at negative mode.

c Detected at [M+H]⁺

3.3.4 Comparison of the performance of PIESI on linear ion trap versus triple-quadrupole mass spectrometer

Linear ion trap MS (LIT-MS) and triple-quadrupole MS (qQq-MS) are the most prevalent tandem mass spectrometer technologies. The fragmentation process (collision-induced dissociation) of analytes can vary considerably between these instruments [134], and the design of the ionization interface and sample introduction system can result in different detection sensitivities. In this study, we have compared the detection limits of these two mass spectrometers for Fmoc-AAs in the PIESI mode (see “Experimental”). Table 3-3 presents the LOD values of each Fmoc amino acid with qQq-MS in negative SIM, PIESI-SIM, and PIESI-SRM mode. The PIESI-SRM and PIESI-SIM generally improve the detection limits 2–10 times compared to the negative mode in qQq-MS for most of the analytes. When comparing the LOD values obtained in the negative SIM mode, the qQq device provides at least an order of magnitude better LODs (Table 3-3) compared to the ion trap (Table 2). This might be due to the improved design of the Shimadzu LC-MS 8040 instrument, which suffers less from corona discharge and background noise in the negative mode. Although the LOD values are instrumentally dependent in the PIESI-SIM/SRM mode, LIT and qQq instruments achieved LODs in the same magnitude which indicates that PIESI-MS is a powerful method in improving the detection sensitivity on both instruments, especially for the cost-effective system LIT-MS.

Table 3-3 Limit of detection values of Fmoc-AAs at negative mode and PIESI SIM/SRM mode obtained with triple quadrupole MS analyzer

Sample	Negative SIM		PIESI SIM		PIESI SRM	
	LOD (pg)	m/z	LOD (pg)	m/z	LOD (pg)	m/z
Ser	15	326	40	650	10	523
Asn	30	353	50	677	2.5	550
Gly	80	296	30	620	7	493
Gln	25	367	50	691	5	564
Thr	30	340	5	664	25	537
Tyr	25	402	5	726	2.5	599
Cys	25	683	5	1007	2.5	880
Pro	50	336	5	660	1	533
Val	30	338	5	662	2.5	535
Trp	27	425	35	749	2.5	622
Ala	50	311	2.5	635	25	508
Met	50	370	5	694	2.5	567
Ile	25	352	10	676	2.5	549
Leu	25	352	12.5	676	2.5	549
Phe	50	386	10	710	30	583
Tau	75	346	22.5	670	5	543
GABA	50	324	25	648	2.5	521
Asp	40	354	5	473 ^a	12	354 ^a
Glu	25	367	20	715 ^a	7.5	604 ^a
Arg ^b			5	397 ^c	1	336
His ^b			30	378 ^c	7.5	156
Lys ^b			15	600 ^c	2	556

^a LOD was obtained with the tetracationic ion pairing reagent: 40 μ M Tetpp4+.

^b Basic amino acids were not detected at negative mode.

^c Detected at [M+H]⁺

3.4 Application

The test of amino acid in urine is used for diagnosis and monitoring of renal function. For example, general elevated levels of amino acids in urine can indicate a disorder in the amino acid transport system resulting from cystinuria and proximal renal tubular dysfunction [135]. In this study, amino acid levels in urine were analyzed using the sensitive PIESI-MS method.

3.4.1 Chromatographic separation of amino acids

A gradient method was developed to simultaneously separate all the 22 Fmoc amino acids using a reversed phase C18 stationary phase. All the amino acids were separated within 22 min (Figure 3-6). The detection was performed in the PIESI mode with the use of $C_5(\text{bpyr})_2$ as an IPR (including Fmoc-Asp and Fmoc-Glu) at full scan mode within the entire run. The total ion chromatogram (TIC) is shown in Figure 3-6, as is the extracted ion chromatogram (EIC) for each amino acid. The presence of each amino acid in urine samples was confirmed in the TIC and EIC according to the identical retention time and its mass spectrum profile as compared to the standard solutions (as shown in Figure 3-7).

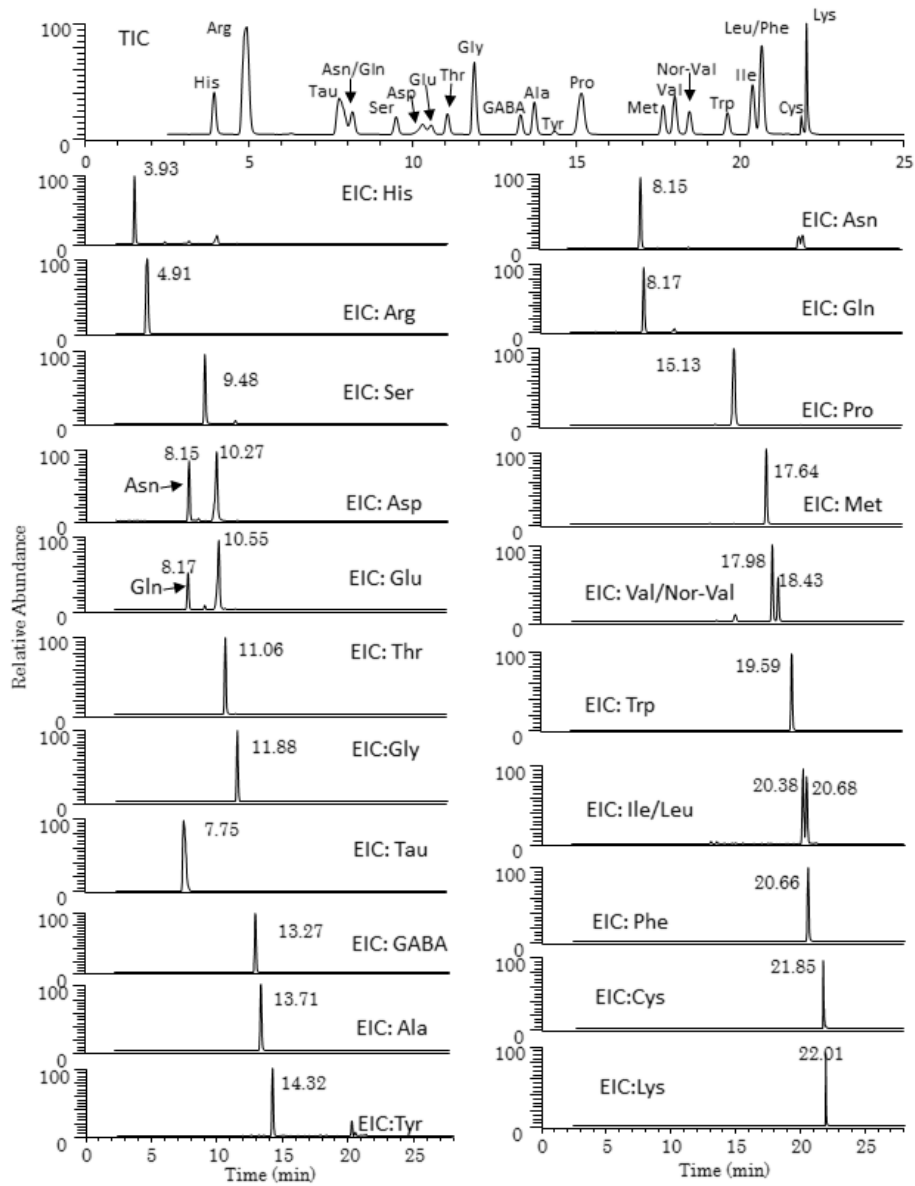


Figure 3-6 Total ion chromatogram (EIC) and extracted ion chromatogram (TIC) of the separation of 22 Fmoc-AAs with HPLC-PIESI-MS.

Column: Ascentis® Express C18 2.7 μ m SPP, 10 cm \times 2.1 mm I.D. Mobile phase A is acetonitrile, and mobile phase B is 0.1% formic acid in H₂O, respectively. Gradient: 30–

60% A, 0–19.5 min; 60–95% A, 19.5–20.0 min; 95% A, 20.0–21.0 min. Flow rate = 0.25 mL/min. MS start delay = 2.5 min

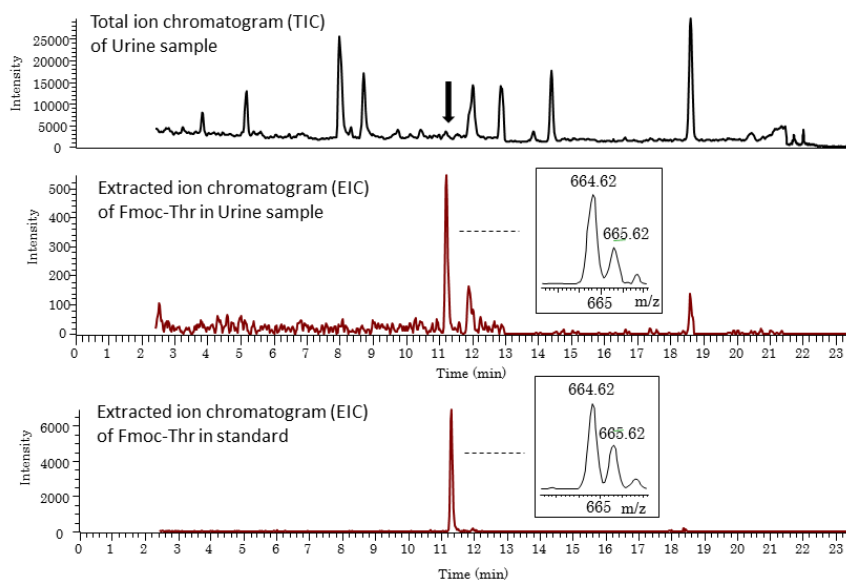


Figure 3-7 HPLC-PIESI-MS analysis of urine sample.

The present of threonine in urine sample (top and middle) was confirmed according to the identical retention time and mass spectrum profile in the EIC of the standard solution (bottom).

3.4.2 Recovery Studies

Our previous study showed that a particular advantage of PIEESI-MS over the negative mode is the ease with which it can reduce matrix effects with minimal dilution in different types of matrices, like groundwater and urine [131]. In this study, dilution factors of 2 and 10 for urine were tested to evaluate the influence of matrix effects. The results are given in Table 3-4 for the low (2 nmol/mL) and high (25 nmol/mL) spiked

concentrations with each dilution factor. The best recovery value ranges from 75 to 116% and from 80 to 109% were obtained at low and high spiked concentrations with a dilution factor of 10. Nevertheless, the low accuracy of the sample with a dilution factor of 2 could be attributed to significant matrix effects. Therefore, a dilution factor of 10 was selected to minimize the matrix effect for further quantitative analysis.

3.4.3 Determination of free amino acids in human urine

The proposed method based on sample dilution and HPLC-PIESI-MS was used to analyze urine samples, and the concentration of each amino acid is shown in Figure 3-8. The results showed that the glycine is the most concentrated amino acid in the urine samples at about 1130 $\mu\text{mol/L}$. Other than that, the urine sample contains a higher level of Lys, Trp, Tyr, Tau, and Ala than the other amino acids (Figure 3-8a). Concerning the profile of the amino acids in the urine sample, most of the values are consistent with the reported concentrations in the literature [136]. The lower concentration of histidine and glutamic acid than the literature value may be due to the age and regional difference of the studied individuals.

Table 3-4 Recovery values at urine sample with different dilution factor.

Values are expressed as percent (%) for each amino acid as a function of the dilution factor and the spiked concentration.

Spiked conc. Sample ^a	Dilution factor							
	2				10			
	Low (2 nmol/mL)		High (25 nmol/mL)		Low (2 nmol/mL)		High (25 nmol/mL)	
	recovery (%)	RSD ^b (%)	recovery (%)	RSD ^b (%)	recovery (%)	RSD ^b (%)	recovery (%)	RSD ^b (%)
Ser	51	6	73	5	83	5	88	5
Asn	83	4	88	5	85	5	92	4
Gly	77	6	86	2	83	4	94	3
Gln	82	7	85	7	80	4	87	2
Thr	77	9	83	2	90	4	92	4
Tyr	51	9	73	4	93	4	85	2
Cys	70	6	71	6	86	6	83	3
Pro	63	5	61	3	82	2	86	2
Val	54	5	71	3	88	3	99	1
Trp	52	8	69	5	113	6	90	4
Ala	77	7	72	4	94	6	91	2
Met	53	3	61	4	84	5	92	2
Ile	48	8	66	4	109	9	109	3
Leu	47	9	72	3	84	7	105	4
Phe	57	8	71	5	84	5	102	2
Tau	82	2	86	1	80	2	87	5
GABA	– ^b	–	–	–	–	–	–	–
Asp	61	4	66	3	–	–	–	–
Glu	55	5	68	5	–	–	–	–
Arg	62	8	65	6	84	3	82	4
His	55	3	64	4	75	4	80	2
Lys	79	4	79	5	116	4	92	4

^a n=3 at each spiked leave

^b Intra-day RSD value

^c Not detectable

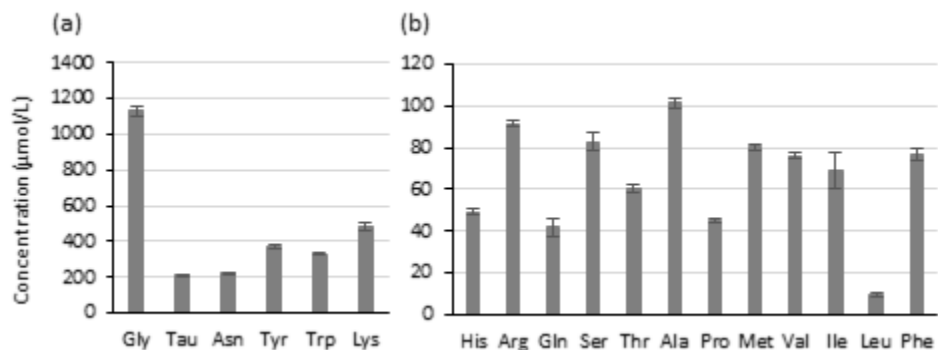


Figure 3-8 Analysis of amino acid concentrations in the urine sample with HPLC-PIESI-MS.

Asp and Glu were not detected. (a) High-concentration amino acids. (b) Low-concentration amino acids

3.5 Conclusions

The proposed PIESI-MS method for detection of Fmoc-derivatized amino acids shows improved detection sensitivity compared to the direct MS positive and negative mode approaches. After testing with different PIESI reagents, it was found that the dicationic IPR produces the best sensitivity enhancements for the neutral amino acids while the tetracationic IPR works best with the two acidic amino acids (Asp and Glu). By applying the optimized ion-pairing reagent, the absolute LOD values in the low picogram levels were obtained with both linear ion trap and triple-quadrupole MS instruments. Simple urine sample preparation consisting of dilution was studied, and good results were obtained with a dilution factor of 10 for both low-level and high-level spiked concentrations. With this methodology, basic, natural, and acidic amino acid concentrations were determined simultaneously with a small volume of human urine. The technique should be applicable for the detection of other anionic metabolites in biological fluids, and further investigation of ultra-trace level of D-amino acid is in progress.

Chapter 4

Variations of L- and D-Amino Acid Levels in the Brain of Wild-Type and Mutant Mice

Lacking D-Amino Acid Oxidase Activity

Abstract

D-amino acids are now recognized to be widely present in organisms and play essential roles in biological processes. Some D-amino acids are metabolized by D-amino acid oxidase (DAO), while D-Asp and D-Glu are metabolized by D-aspartate oxidase (DDO). In this study, levels of 22 amino acids and the enantiomeric compositions of the 19 chiral proteogenic entities have been determined in the whole brain of wild-type ddY mice (ddY/DAO+/+), mutant mice lacking DAO activity (ddY/DAO-/-), and the heterozygous mice (ddY/DAO+/-) using high performance liquid chromatography-tandem mass spectrometry (HPLC-MS/MS). No significant differences were observed for L-amino acid levels among the three strains except for L-Trp which was markedly elevated in the DAO+/- and DAO-/- mice. The question arises as to whether this is an unknown effect of DAO inactivity. The three highest levels of L-amino acids were L-Glu, L-Asp, and L-Gln in all three strains. The lowest L-amino acid level was L-Cys in ddY/DAO+/- and ddY/DAO-/- mice, while L-Trp showed the lowest level in ddY/DAO+/+mice. The highest concentration of D-amino acid was found to be D-Ser, which also had the highest % D value (~ 30%). D-Glu had the lowest % D value (~ 0.1%) in all three strains. Significant differences of D-Leu, D-Ala, D-Ser, D-Arg, and D-Ile were observed in ddY/DAO+/- and ddY/DAO-/- mice compared to ddY/DAO+/+ mice. This work provides the most complete baseline analysis of L- and D-amino acids in the brains of ddY/DAO+/+, ddY/DAO+/-, and ddY/DAO-/- mice yet reported. It also provides the most effective and efficient analytical approach for measuring these analytes in biological samples. This study provides

fundamental information on the role of DAO in the brain and maybe relevant for future development involving novel drugs for DAO regulation.

4.1 Introduction

Amino acids are essential building blocks of proteins in all living organisms. All proteinogenic amino acids can exist in either L- or D-form, except glycine. Only a few decades ago scientists believed L-amino acids were solely relevant in higher organisms, while D-amino acids were thought to be inessential. However, by the mid-20th century, D-Ala was discovered in animal tissue, specifically milkweed bug blood [3]. Additionally, D-Ala and D-Glu were found in the bacterial peptidoglycan components of cell walls [2]. Subsequently, free D-amino acids were detected in plants, invertebrates, vertebrates, and mammals in significant amounts [43, 137, 5, 6, 138]. Moreover, peptides and proteins containing D-amino acids were discovered in various animal tissues [4, 139], and D-pipecolic acid, a non-proteinogenic amino acid, was found in human urine and plasma [48].

Thus, questions arise about the production, regulation, and function of D-amino acids in biological systems. Several free D-amino acids have been found to participate in neurological processes. D-Ser is a co-agonist of the N-methyl-D-aspartate (NMDA) receptor and activates the NMDA receptor together with glutamate [12, 13]. Low D-Ser levels in serum and cerebrospinal fluid have been reported in schizophrenia patients [14]. Also, increased D-amino acid oxidase (DAO) activity has been found in the brain of schizophrenia patients [77]. DAO oxidizes D-Ser to its corresponding imino acid, and this could explain the decreased levels of D-Ser in schizophrenia patients. However, hypofunction of NMDA receptors due to decreased D-Ser levels and its consequence needs further study and evaluation [15]. In addition to D-Ser, D-Ala and D-Asp have been

reported to act as co-agonists of NMDA receptors [16, 17]. NMDA receptor has been shown to be involved in learning and memory processes and decreased D-Asp levels in the brain were suggested to contribute to memory loss in patients with Alzheimer's disease [22, 21]. D-Ser has been found to serve another function as a biomarker for patients with treatment-resistant depression (TRD) who were treated with ketamine. It was found that plasma D-Ser levels were significantly lower in TRD patients who responded to ketamine treatment in comparison to the patients who did not respond to ketamine treatment [58]. Also, it has been found that D-Leu, but not L-Leu, can serve as a unique treatment for terminating ongoing seizures in mice [23]. Additionally, mice lacking Tas1R2/R3, which is a D-amino acid receptor, have been found to be protected against seizures [140]. Recently, it was reported that in NIH Swiss mice the levels of all D-amino acids, except D-Glu, were orders of magnitude higher in the hippocampus and cortex than in blood [141]. The low levels of only D-Glu were in stark contrast to all other proteinogenic amino acids and indicated a specific or unique removal/control mechanism. This further suggests that they can have diverse effects: some essential and others deleterious.

Some endogenous D-amino acid levels in microorganisms, plants, and invertebrates are currently known to be controlled via DAO and D-amino acid racemases. D-amino acid racemases can convert L-amino acids to their corresponding D-amino acids [142]. To date, serine racemase and aspartate racemase have been found in mammalian tissues [7, 69]. DAO, which was first discovered by Krebs in pig kidneys in 1935, is an important enzyme that regulates certain D-amino acid levels in mammals [9]. DAO is a flavoprotein and catalyzes the oxidation of neutral and basic D-amino acids to give α -keto acids and ammonia. Kinetic studies of DAO from yeast, pigs, and humans have determined D-amino acids' specificity for DAO [70, 143]. As expected, increased

levels of D-Ser, D-Pro, D-Ala, and D-Leu have been reported in ddY/DAO^{-/-} mice, which is a naturally-occurring mutant mouse strain [10, 144]. The single point mutation (G541A) in the DAO gene resulted in a non-conservative change in the DAO enzyme, causing the inactivity of DAO in ddY/DAO^{-/-} mice. [145].

Growing evidence indicates that D-amino acids are involved in various diseases. D-amino acid regulating enzymes, *e.g.*, racemases and DAO, could be promising targets for novel drug development. Consequently, a fundamental baseline study of all free proteinogenic L- and D-amino acids is needed to clarify the natural variation and levels of intrinsic L- and D-amino acids following the alteration of DAO activity. This study reports a comprehensive high performance liquid chromatography-tandem mass spectrometry (HPLC-MS/MS) analysis of all free proteinogenic L- and D-amino acids in the brain of wild-type ddY mice (ddY/DAO^{+/+}), mutant mice lacking DAO activity (ddY/DAO^{-/-}), and the heterozygous mice (ddY/DAO^{+/-}). Although they are not chiral, taurine and gamma-amino butyric acid (GABA) also were investigated due to their neurotransmitter activity in the central nervous system (CNS) [146-148].

4.2 Materials and Methods

4.2.1 Chemicals

Amino acid standards, perchloric acid, and ammonium formate were obtained from Sigma-Aldrich (St. Louis, MO). The AccQ-Tag Ultra derivatization kit (AccQ-Tag Ultra reagent powder, AccQ-Tag Ultra borate buffer, and AccQ-Tag Ultra reagent diluent) was purchased from Waters Corporation (Milford, MA, USA). HPLC-MS grade methanol and water were purchased from Sigma-Aldrich, and ultrapure water was obtained from a Milli-Q water system (Millipore, Bedford, MA, USA).

4.2.2 Animals

Male and female ddY mice (a gift from T. Seyfried, Boston College) were housed under a 14 hr light/10 hr dark cycle in a vivarium and were given food and water freely. Successive generations were bred and maintained. Mice lacking D-amino acid oxidase activity were identified by genotyping and were maintained by heterozygote-heterozygote crosses. Male ddY/DAO^{+/+}, ddY/DAO^{+/-}, and ddY/DAO^{-/-} mice were sacrificed at 2-4 months of age by CO₂ exposure in a closed container in the vivarium, followed by decapitation. Detailed procedures for mouse brain dissection and perfusion were described in our previous study [141]. All procedures were approved by the Johns Hopkins Institutional Animal Care and Use Committee. Samples were all stored at -80 °C until analyzed.

4.2.3 Stock solutions and standards

Stock solutions were prepared by dissolving standard amino acids in ultra-pure water. The concentrations of D- and L-amino acid stock solutions were 2 mM and 1 M, respectively. D-norvaline was used as an internal standard (IS) with a concentration of 100 µM. The concentration of the calibration solutions ranged from 0.05 to 20 µM for D-amino acids and 5 to 1000 µM for L-amino acids. Each 1 mL of the calibration solution was mixed with 50 µL of IS. Low, medium and high concentration of quality control (QC) samples were prepared by spiking different amounts of standard solutions including the IS into the matrix (Table S3 & S4, see Electronic Supplemental Material).

4.2.4 Sample preparation and derivatization procedure

AccQ-Tag Ultra derivatization kit was used in all derivatization procedure. Following the protocol provided by the manufacturer, 10 µL of the amino acid solution was mixed with 70 µL of borate buffer and 20 µL of reconstituted AccQ-Tag Ultra reagent (6-aminoquinolyl-*N*-hydroxysuccinimidyl carbamate (AQC), 3 mg/mL in acetonitrile).

The sample was vortexed followed by incubation for 10 min at 55 °C, and 3 µL of the reaction mixture was injected into the HPLC-MS/MS system for analysis. Enantiomers of AQC-amino acids are easily separated and can be detected in the positive mode of LC-MS [34].

Mouse whole brain tissues were homogenized in 1 mL of 0.3 M perchloric acid and 50 µL of IS on ice for 30 s (three 10 s pulses) with a Q-Sonica CL-18 probe (Newtown, CT, USA). The homogenates were incubated on ice for 15 min and centrifuged at 4 °C for 20 min at 13,000 rpm. The supernatant was collected, filtered, and derivatized following the procedure described above.

4.2.5 Instrumentation and chromatographic conditions

HPLC-MS/MS analysis was performed on a LCMS-8040 (Shimadzu Scientific Instruments, Columbia, MD, USA), triple quadrupole spectrometer with electrospray ionization (ESI). Two different chiral stationary phases with opposite enantioselectivity were used for all analyses. A quinine based chiral stationary phase was utilized for the separation and quantification of amino acids. It was prepared in-house utilizing quinine covalently bonded to superficially porous particles (SPP) and slurry packed into a 4.6 x 50 mm i.d. stainless steel column (IDEX Health and Science, Oak Harbor, WA) [38]. A gradient method was used for the chiral separation of amino acids on the quinine column. Mobile phase A was 100 mM ammonium formate and methanol (v:v 10:90; adjust to the apparent pH of 6), and mobile phase B was 50 mM ammonium formate and methanol (v:v 10:90; adjust to the apparent pH of 5). The following gradient was applied: 0 - 4 min, 0 to 100% B; 4 - 15 min, 100% B; 15 - 16 min, 100 – 0% B. The column was re-equilibrated for 9 min before another injection. A TeicoShell column (4.6 x 150 mm, AZYP, LLC) also was used to confirm the peak identity of the amino acids due to its opposite enantioselectivity compared to the quinine column. This chiral stationary phase

is based on macrocyclic glycopeptides [149-151]. Mobile phase A was 5 mM ammonium formate (pH 4), and mobile phase B was acetonitrile. A gradient method for TeicoShell column was applied as following: 0-2 min, 30% to 40% B; 2-15 min, 40% to 50% B; 15-16 min, 50% to 30% B; 16-30 min, 30% B. The flow rate was 0.65 mL/min for both columns, and a splitter was used before the MS. The flow rate directed to the MS was 0.325 mL/min. HPLC-MS/MS was operated in multiple reaction monitoring (MRM) mode using positive electrospray ionization source. The drying gas and nebulizing gas flow rate were 15 L/min and 2 L/min, respectively. The desolvation line and heat block temperatures were 275 °C and 400 °C, respectively. Collision energies and MRM transitions were optimized for each amino acid. Shimadzu LabSolution software was used for data acquisition.

The method was evaluated for linearity, sensitivity, precision, accuracy, and matrix effect according to US Food and Drug Administration (FDA) document for bioanalytical method validation [152]. Detailed method validation procedures and results are shown in the supplementary material (See Electronic Supplementary Material Table S1-S5). To evaluate the statistical significance of differences among the three strains, data was analyzed by one-way analysis of variance (ANOVA). The student's t-test was performed to compare the difference for ddY/DAO^{+/-} vs ddY/DAO^{+/+}, and ddY/DAO^{-/-} vs ddY/DAO^{+/+}. All statistical analyses were carried out using XLSTAT add-on package to Microsoft Excel. *P* values less than 0.05 were considered to have significant differences compared to the wild-type. Literature data for the only six amino acid levels reported in the same mouse strain were found to be comparable to those in this study and were included in Tables 4-1 & 4-2 [10, 153, 154].

Table 4-1 L-Amino acid levels in mice whole brain^a (ng/mg wet tissue)

	ddY/DAO ^{+/+}		ddY/DAO ^{+/-}		ddY/DAO ^{-/-}	
	Range	Average	Range	Average	Range	Average
Asn	21.3 - 81.8	51.5	40.3 - 65.8	47.6	29.6 - 62.2	37.8
Asp^b	410.7 - 1723.8	815.4	364.7 - 1871.6	749.2	345.0 - 1627.4	738.2
Glu	1315.8 - 2062.4	1689.1	1159.1 - 1633.9	1444.1	1267.2 - 1606.9	1411.2
Gln	442.0 - 734.5	588.2	501.5 - 694.8	595.3	492.7 - 657.1	579.3
Gly	52.6 - 73.8	63.2	60.6 - 79.9	68.3	60.9 - 76.0	69.5
Leu^b	5.8 - 16.2	10.5	5.0 - 13.6	9.0	5.9 - 15.9	10.1
Ile	11.7 - 28.3	20.0	14.8 - 27.9	20.7	14.8 - 23.7	19.3
Met	4.0 - 18.1	11.1	11.5 - 18.3	15.0	11.4 - 20.9	15.4
Phe	41.9 - 91.4	66.6	59.4 - 100.6	75.9	54.6 - 94.0	74.3
Pro^b	7.7 - 19.5	11.2	5.5 - 17.0	11.0	5.4 - 12.7	7.7
Thr	109.7 - 195.1	152.4	114.2 - 151.2	133.7	96.4 - 143.3	131.0
Trp^b	1.0 - 5.1	3.8	18.0 - 24.6	21.0	19.7 - 25.5	22.4
Val	19.1 - 37.6	28.4	21.6 - 34.6	25.9	23.9 - 32.5	28.0
Tyr	10.4 - 19.8	15.1	13.8 - 17.8	15.4	11.0 - 19.2	14.9
Ser^b	68.7 - 113.6	88.1	63.3 - 127.4	91.4	70.8 - 119.3	91.1
Ala^b	54.8 - 278.9	113.5	59.8 - 183.1	107.9	88.5 - 169.5	108.2
Lys	111.2 - 180.9	146.0	103.3 - 161.0	129.4	97.3 - 119.4	110.4
His	11.1 - 28.2	19.6	16.4 - 21.1	19.0	13.7 - 30.9	19.8
Arg	108.0 - 222.6	165.3	121.5 - 199.5	148.5	128.6 - 169.5	149.2
Cys	4.8 - 7.2	5.9	5.2 - 7.1	6.1	5.4 - 7.7	6.4
Taurine	483.5 - 657.7	570.6	530.3 - 620.0	573.2	501.9 - 636.7	564.4
GABA	242.1 - 651.6	446.9	345.1 - 573.6	436.1	389.7 - 629.3	536.1

a. Values represent the range and average of amino acid content from five mice (ng/mg wet tissue)

b. Data from previous reports were included for this amino acid [10],[153], & [154]

Table 4-2 D-Amino acid levels in mice whole brain^a (ng/mg wet tissue)

	ddY/DAO ^{+/+}			ddY/DAO ^{+/-}			ddY/DAO ^{-/-}		
	Range	Average	% D ^c	Range	Average	% D ^c	Range	Average	% D ^c
Asn	0.07 - 0.15	0.11	0.21	0.10 - 0.16	0.12	0.27	0.10 - 0.15	0.13	0.35
Asp^b	2.56 - 17.50	6.32	0.77	1.35 - 18.90	6.25	0.82	2.75 - 17.59	6.58	0.88
Glu	0.08 - 0.11	0.10	0.01	0.07 - 0.14	0.09	0.01	0.09 - 0.16	0.11	0.01
Gln	0.62 - 0.77	0.70	0.12	0.52 - 0.62	0.59	0.10	0.59 - 0.65	0.62	0.11
Leu^b	0.03 - 0.09	0.05	0.46	0.34 - 0.65	0.51	5.29	0.49 - 0.74	0.59	5.56
Ile	0.17 - 0.39	0.28	1.36	0.32 - 0.60	0.45	2.33	0.40 - 0.61	0.51	2.62
Met	0.14 - 0.24	0.19	1.67	0.18 - 0.25	0.21	1.43	0.20 - 0.26	0.23	1.54
Phe	0.17 - 0.26	0.22	0.32	0.20 - 0.31	0.24	0.32	0.20 - 0.23	0.22	0.30
Pro^b	0.003 - 0.08	0.02	0.21	0.01 - 0.05	0.02	0.22	0.02 - 0.05	0.03	0.33
Thr	0.16 - 0.27	0.22	0.14	0.20 - 0.28	0.23	0.17	0.21 - 0.29	0.24	0.19
Trp^b	0.25 - 0.34	0.29	7.20	0.26 - 0.35	0.31	1.48	0.29 - 0.31	0.30	1.33
Val	0.04 - 0.06	0.05	0.18	0.04 - 0.06	0.05	0.22	0.04 - 0.07	0.06	0.21
Tyr	0.02 - 0.03	0.03	0.18	0.02 - 0.04	0.03	0.17	0.02 - 0.02	0.02	0.16
Ser^b	21.54 - 30.77	22.11	20.06	18.09 - 34.88	27.41	22.98	24.17 - 38.83	29.90	24.72
Ala^b	0.41 - 1.77	0.81	0.71	3.05 - 7.30	5.07	4.54	4.21 - 8.01	5.40	4.76
Lys	0.13 - 0.32	0.22	0.15	0.21 - 0.30	0.26	0.20	0.21 - 0.36	0.27	0.25
His^d	- - -	-	-	- - -	-	-	- - -	-	-
Arg	5.63 - 7.15	6.39	3.72	9.10 - 10.25	9.77	6.41	9.20 - 10.91	9.86	6.24
Cys	0.11 - 0.27	0.18	2.88	0.12 - 0.23	0.18	2.93	0.11 - 0.23	0.15	2.28

a. Values represent the range and average of amino acid content from five mice (ng/mg wet tissue)

b. Data from previous reports were included for this amino acid [10],[153], & [154]

c. % D = 100*D/(D+L)

d. Not detected, below LOD

4.3 Results and discussion

The concentration and enantiomeric composition of all free proteinogenic amino acids, as well as two achiral neurotransmitters, were investigated in mouse whole brain. HPLC-MS/MS MRM chromatograms of the separation of AQC amino acids are shown in Figure 4-1 and 4-2. Results are shown in Tables 4-1 and 4-2 and summarized in Figure 4-3 and 4-4.

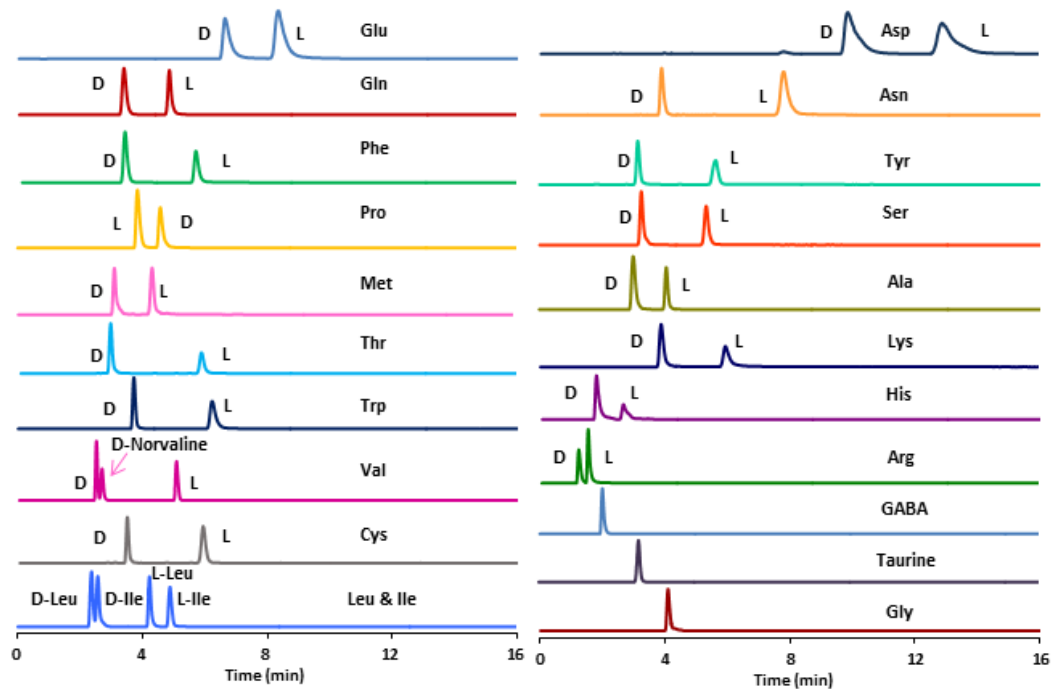


Figure 4-1 HPLC-MS/MS chromatogram of the separation of AQC-amino acid standards on the quinine SPP chiral stationary phase (see Materials and methods for exact conditions). Note the opposite enantioselectivity to that shown in Figure 4-2.

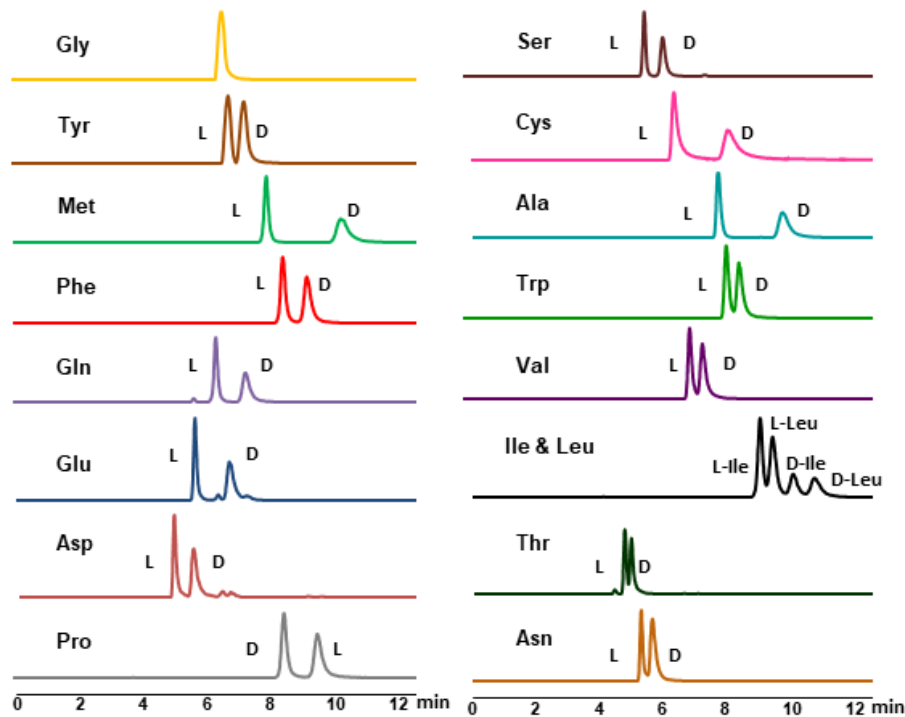


Figure 4-2 HPLC-MS/MS chromatogram of the separation of AQC-amino acid standards on TeicoShell chiral stationary phase (see Materials and methods for exact conditions). Note the opposite enantioselectivity to that shown in Figure 4-1.

4.3.1 L-Amino acid levels in mouse whole brain

The L-amino acid with the highest concentration was L-Glu in all three strains of ddY mice, followed by L-Asp then L-Gln (Figure 4-3). These results are consistent with the literature, in which Glu, Gln, and Asp showed the highest L-amino acid levels in the cortex and hippocampus regions of NIH Swiss mice [141]. The group of L-amino acids with the highest levels (> 400 ng/mg) included L-Glu, L-Asp, L-Gln, taurine, and GABA, all of which play essential roles in the CNS. L-Glu and L-Asp function as excitatory

neurotransmitters, while GABA and taurine function as inhibitory neurotransmitters in mature mice [155-157]. Gln is a precursor of the neurotransmitter amino acids mentioned above [155]. Considering their important functions in neurotransmission, high levels of these amino acids in the brain are not unexpected. Among the ddY/DAO^{+/-} and ddY/DAO^{-/-} mice, L-Cys (~6.3 ng/mg), L-Pro (~9.3 ng/mg), and L-Leu (~9.6 ng/mg) had the three lowest L-amino acid levels. In the ddY/DAO^{+/+} control group, L-Trp had the lowest level (3.8 ng/mg), followed by L-Cys (5.9 ng/mg) and L-Leu (10.5 ng/mg). No significant difference was observed in L-amino acid levels in ddY/DAO^{+/+}, ddY/DAO^{+/-}, and ddY/DAO^{-/-} mice except for L-Trp (Figure 4-3).

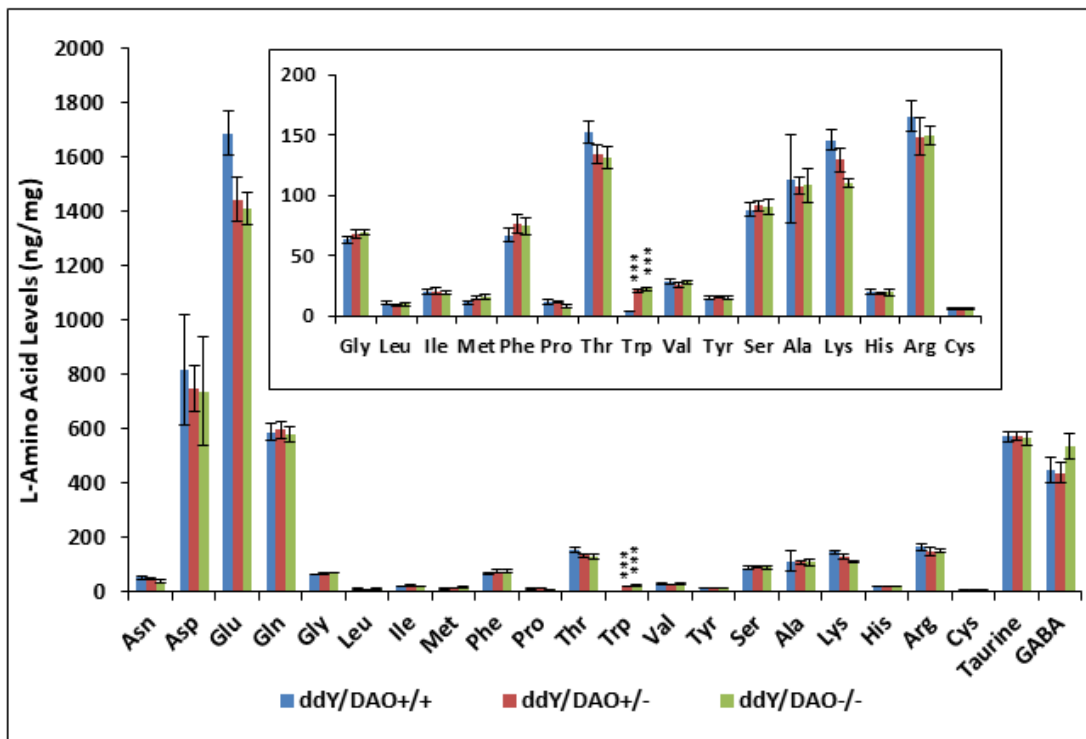


Figure 4-3 L-Amino acid levels in mice whole brain.

Values represent mean \pm SEM (ng/mg) from five mice. *** P < 0.001, significant increase from the values of ddY/DAO^{+/+} mice.

This study is the first report of elevated L-Trp levels in ddY/DAO^{+/-} and ddY/DAO^{-/-} mice compared to ddY/DAO^{+/+} control group. Higher L-Trp levels in the mutant mouse brains may result from either inhibited L-Trp metabolism or enhanced L-Trp transport into the brain. The two major pathways for L-Trp are the kynurenine pathway and serotonin pathway [158]. Mutation of a gene can lead to changes in other systems, and, in this case, mutation of DAO gene may affect the activities of enzymes that convert L-Trp to kynurenine and serotonin, causing the accumulation of L-Trp in mutant mouse brains. Thus, kynurenine and serotonin levels should be investigated in the brain of ddY/DAO^{+/-}, ddY/DAO^{-/-}, and ddY/DAO^{+/+} mice. It could be hypothesized that non-detectable or very low levels of kynurenine and serotonin in the mutant mice brain could indicate abnormal metabolism of L-Trp in DAO mutant mice. Another explanation for the higher L-Trp levels may be the elevated uptake of L-Trp from plasma in mutant mice. L-Trp is transported across the blood-brain barrier via the large neutral amino acid transporters [159]. However, the brain L-Trp level does not solely depend on plasma L-Trp level, but also the ratio of L-Trp to other plasma neutral amino acids sharing the same amino acid transporter [160]. Thus plasma L-Trp levels together with other neutral amino acids, *i.e.*, Tyr, Phe, Leu, Ile, and Val should be investigated in the ddY/DAO^{+/-}, ddY/DAO^{-/-}, and ddY/DAO^{+/+} mice.

Higher L-Trp levels in the brains of mutant mice, if from the elevated uptake of L-Trp, may also lead to higher levels of serotonin. The rate-limiting enzyme on the serotonin pathway, tryptophan hydroxylase, is normally not saturated at brain Trp concentrations [161]. Therefore, serotonin synthesis is dependent on the availability/levels of its precursor, L-Trp, in the brain [159]. If this is true, it may explain the elevated anxiety observed in mice lacking DAO activity [162], since high levels of

serotonin have been found to contribute to anxiety [163]. Investigation of kynurenine and serotonin levels in the blood and brain as well as the common amino acid levels in the blood of the wild-type and mutant ddY mice would be an interesting study and may provide evidence to support these hypotheses. However, the underlying mechanisms through which inactivation of DAO influences other systems remains to be resolved.

4.3.2 *D-amino acid levels in mouse whole brain*

D-amino acids with high concentrations (> 6 ng/mg) are D-Ser, D-Asp, and D-Arg in all three strains (Figure 4-4). Given their essential roles in the CNS and the presence of racemases in mammals, it is not unexpected that high amounts of D-Ser (~ 26 ng/mg) and D-Asp (~ 6 ng/mg) are found in the brain of both wild-type and mutant mice. D-Arg in the CNS can serve as a stimulant or a depressant at different levels, as demonstrated in a previous study, although the exact mechanism remains unclear [164].

Concentrations of D-Tyr, D-Val, D-Pro, and D-Glu are among the lowest in all three strains (< 0.2 ng/mg). In a previous study, the concentration of D-Glu was below detection limits in the cortex and hippocampus of NIH Swiss mice [141]. In this study, D-Glu in ddY mice whole brain is determined using the sensitive HPLC-MS/MS method (See Materials and methods). It was detected, but only at very low levels (~ 0.1 ng/mg) despite the fact that L-Glu is, by far, the most prevalent amino acid in these brain samples. Further, the % D-Glu was 1 to 3 orders of magnitude lower than any other D-amino acid in this study for all three strains (~ 0.01%). Results from this study further support the hypothesis that D-Glu metabolism may be a unidirectional process and not a cycle, like the L-glutamate-glutamine cycle, considering the high abundance of D-Gln and trace amount of D-Glu [141].

Clear differences were observed for some specific D-amino acids levels in ddY/DAO^{+/-} and ddY/DAO^{-/-} mice compared to ddY/DAO^{+/+} mice, see Figure 4-4. D-Leu levels in the brain of ddY/DAO^{+/-} and ddY/DAO^{-/-} mice were twelve times higher than that in ddY/DAO^{+/+} mice ($P < 0.001$). D-Ala levels were increased approximately sevenfold in ddY/DAO^{+/-} and ddY/DAO^{-/-} mice ($P < 0.001$). Significant increases of D-Ser, D-Ile, and D-Arg levels were also observed in the brain of ddY/DAO^{+/-} and ddY/DAO^{-/-} mice. Results are in accordance with the kinetic studies of DAO, in which DAO shows high substrate affinity and catalytic efficiency for the D-amino acids mentioned above [70]. DAO has been reported to be active for D-Pro as well [143], however, no significant differences of D-Pro levels were observed in the whole brain of the three mouse strains. These results can be explained by the previous report from Hamase *et al.* [10]. D-Pro levels increased significantly only in cerebellum and pituitary gland of mice lacking DAO activity, while the majority of the brain regions did not show much difference [10]. Due to the regional distribution of D-Pro in mouse brain, the increase of D-Pro levels in the whole brain of ddY/DAO^{+/-} and ddY/DAO^{-/-} mice are too low to be noticeable. Acidic D-amino acids, D-Asp and D-Glu, are oxidized by D-aspartate oxidase (DDO), but not DAO [8]. Therefore, given the absence of DAO, no difference in the levels of D-Asp and D-Glu among ddY/DAO^{+/+}, ddY/DAO^{+/-}, and ddY/DAO^{-/-} mice were found or expected. Results obtained from the present study are in good agreement with previously reported values for D-Leu, D-Pro, D-Ser, D-Ala, and D-Asp [10, 144, 153].

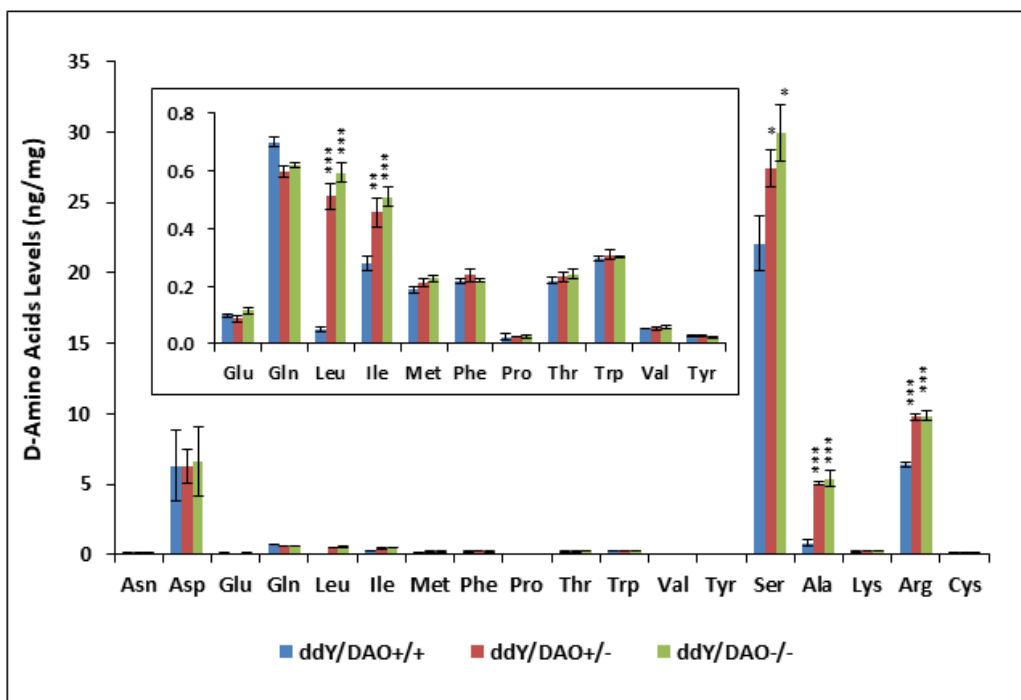


Figure 4-4 D-Amino acid levels in mice whole brain.

Values represent mean \pm SEM (ng/mg) from five mice. * $P < 0.05$, significant increase from the values of ddY/DAO^{+/+} mice; ** $P < 0.01$, significant increase from the values of ddY/DAO^{+/+} mice; *** $P < 0.001$, significant increase from the values of ddY/DAO^{+/+} mice

4.4 Conclusions

In the present investigation, a rapid and sensitive method was established for the simultaneous analysis of amino acid contents and their enantiomeric compositions in mouse brains. This study provides the most complete analysis of L- and D-amino acids in the whole brain of wild-type mice as well as mice lacking DAO activity. There is no difference observed for L-amino acid levels among wild-type and mutant mice except L-Trp. The elevated levels of L-Trp in DAO deficient mice have not been reported

previously and may be a secondary effect of DAO inactivation. DAO did appear to affect a few D-amino acid levels in the brain of mutant mice in this study, including D-Leu, D-Ala, D-Ser, D-Ile, and D-Arg, but not all the D-amino acids.

Altered D-amino acids levels have been reported in varying diseases, suggesting that D-amino acids may be potential biomarkers and have diagnostic values.

Furthermore, regulation of D-amino acid levels via DAO may be a promising approach in the treatment of various diseases. As shown in this study, some D-amino acid levels were affected significantly by altering DAO activity. Inhibition of DAO activity through DAO inhibitors, *e.g.*, 3-methylpyrazole-5-carboxylic acid [165], or application of D-amino acids may improve the conditions caused by insufficient D-amino acids.

Chapter 5

Altered Profiles and Metabolism of L- and D-Amino Acids in Cultured Human Breast Cancer Cells vs. Non-tumorigenic Human Breast Epithelial Cells

Abstract

Herein we describe for the first time the endogenous levels of free L- and D-amino acids in cultured human breast cancer cells (MCF-7) and non-tumorigenic human breast epithelial cells (MCF-10A). D-Asp and D-Ser, which are co-agonists of the N-methyl- D-aspartate (NMDA) receptors, showed significantly elevated levels in MCF-7 cancer cells compared to MCF-10A cells. This may result from upregulated enzymatic racemases. Possible roles of these D-amino acids in promoting breast cancer proliferation by regulating NMDA receptors were indicated. D-Asn may also be able to serve as exchange currency, like specific L-amino acids, for the required uptake of essential amino acids and other low abundance nonessential amino acids which were elevated nearly 60 fold in cancer cells. The relative levels of specific L- and D-amino acids can be used as malignancy indicators (MIs) for the breast cancer cell line in this study. High MIs (>50) result from the increased demands of specific essential amino acids. Very low MIs (<1) result from the increased demands of specific D-amino acids (i.e., D-Ser, D-Asp) or the cellular release of amino acid exchange currency (i.e., L- and D-Asn) used in the upregulated amino acid antiporters to promote cancer cell proliferation.

5.1 Introduction

Cancer is not a single disease, but a group of related diseases and the most fundamental feature of all cancers is uncontrolled proliferation [166]. More than 90 years ago, German physiologist Otto Warburg observed that cancer cells consumed large amounts of glucose compared to normal cells even in the presence of oxygen, which is now known as the Warburg effect [167]. Besides glucose, another principle nutrient supporting the optimal growth of cancer cells is L-glutamine, as first described by Eagle in the 1950s [168]. While many studies have focused on the metabolism of glucose and L-glutamine in cancer, amino acids besides glutamine also are utilized by cancer cells and may play essential roles in cancer cell proliferation. Recently it has been found that N-methyl-D-aspartate (NMDA) receptors that are widely present in the central nervous system (CNS) are not only expressed but functional in a variety of cancer cell lines and tumors, *e.g.*, lung cancer, breast cancer, and esophageal cancer, with functions in regulating cancer cell growth and division [24]. It is known that D-Ser, as well as D-Asp and D-Ala, act as co-agonists of NMDA receptors [13, 16, 17]. This means D-amino acids, which were once thought to be unnatural and superfluous in mammalian systems [6, 5, 169, 141], may play important roles in the metabolism and proliferation of cancer cells. Also, it has been noted in a recent report that non-glutamine amino acids provide abundant nitrogen and carbon for biosynthesis to proliferating cells, while most glucose is converted into lactate and exported from cancer cells [170]. The metabolism and essential roles of many amino acids during cancer cell proliferation may be underestimated or have yet to be considered. Cancer patients are always in a hypermetabolic state, thus enhanced protein synthesis and degradation can result in the altered amino acid concentrations [171]. Indeed, it is well established that specific amino acid transporters are upregulated in cancer cells [172]. Free plasma amino acid profiles

in patients with different types of cancer have been found to differ significantly from those of healthy controls, and the altered amino acid profiles may have great potential for the early detection of cancer [173]. For example, patients with breast cancer, in both early and advanced stages, showed high levels of amino acids in their saliva compared to a healthy control group [171]. The accumulation of specific amino acids in cancer cells, particularly specific D-amino acids, could be potential oncometabolites, which are defined as the metabolites whose abundance increases markedly and are involved in the development of malignancy [174]

To date, almost all the cancer studies regarding amino acids focused only on L-amino acids. Questions about D-amino acids and cancer cells have not been asked or answered. One is whether there is cellular uptake or release of D-amino acids during cancer cell proliferation? Second, do D-amino acids exhibit altered profiles in cancer cells as do L-amino acids, and if so, why? This study is the first report of endogenous levels of free L- and D-amino acids in human breast cancer cells (MCF-7) and non-tumorigenic human breast epithelial cells (MCF-10A). Altered profiles and metabolism of free L- and D-amino acids were determined in cultured MCF-7 cells compared to MCF-10A cells. Also, effects of glucose concentration were studied for MCF-7 cell proliferation and their endogenous L- and D-amino acid levels. Further, a simple test using specific D- and L-amino acid relative levels has been derived and used to produce malignancy indicators (MIs) of cancer cells.

5.2 Materials and methods

5.2.1 Chemicals and reagents

Amino acid standards, perchloric acid, and ammonium formate were obtained from Sigma-Aldrich (St. Louis, MO, USA). The AccQ-Tag Ultra derivatization kit (AccQ-Tag Ultra reagent powder [6-aminoquinolyl-N-hydroxysuccinimide carbamate

(AQC)], AccQ-Tag Ultra borate buffer, and AccQ-Tag Ultra reagent diluent) was purchased from Waters Corporation (Milford, MA, USA). All the cell medium and additives were purchased from Sigma-Aldrich. HPLC-MS grade methanol and water were purchased from Sigma-Aldrich, and ultrapure water was obtained from a Milli-Q water system (Millipore, Bedford, MA, USA).

5.2.2 Cell lines and culture conditions

Human breast cancer cell line (MCF-7) and non-tumorigenic human breast epithelial cells (MCF-10A) were purchased from American Type Culture Collection (ATCC). MCF-7 cells were grown and maintained in normal, or high glucose Dulbecco's Modified Eagle Medium (DMEM) supplemented with 10% fetal bovine serum (FBS), 1% L-glutamine, and 1% penicillin-streptomycin. MCF-10 cells were grown and maintained in Mammary Epithelial Cell Growth Medium (MEGM) that was supplemented with 10% FBS, 100 ng/mL cholera toxin and MEGM kit. All the cells were incubated at 37 °C in a humidified atmosphere of 5% CO₂.

5.2.3 Cell counting

Cells were seeded into 150 x 25 mm cell culture dish grown until 80 to 90% confluency and then split into 9 of 100 x 20 mm cell culture dishes. Triplicate plates were seeded for each experimental condition. Cells were trypsinized and centrifuged at 1000 g for 5 min. The cell pellet was washed twice with phosphate buffer saline (PBS). Cells were counted at the specified time points, *i.e.*, 24 hours, 48 hours, and 72 hours, by conducting the Trypan blue assay using a hemacytometer (Sigma-Aldrich, St. Louis, MO).

5.2.4 Intracellular and extracellular amino acids extraction and analysis

Amino acids were extracted from the cells or cell media with 0.3 M perchloric acid and 100 µM norvaline (internal standard) on ice for 30 s (three 10 s pulses) with a Q-

Sonica CL-18 probe (Newtown, CT, USA). After vigorous vortexing, the samples were centrifuged at 4 °C for 20 min at 13,000 rpm. The supernatant was collected, filtered, and derivatized as previously detailed [175]. In brief, 10 µL of the extract solution was mixed with 70 µL of borate buffer and 20 µL of AQC reagent. The sample was vortexed followed by incubation at 55 °C for 10 min.

High performance liquid chromatography-tandem mass spectrometry (HPLC-MS/MS) analysis was performed on a LCMS-8040 (Shimadzu Scientific Instruments, Columbia, MD, USA), triple quadrupole spectrometer with electrospray ionization (ESI). Two different chiral stationary phases with opposite enantioselectivity were used for all analyses. A Q-Shell column (4.6 x 50 mm), quinine based chiral stationary phase, was prepared in-house and utilized for the separation and quantification of amino acids . A gradient method was used for the chiral separation of amino acids on the Q-Shell column. Mobile phase A was ammonium formate (100 mM)-methanol (10:90, v/v) (pH* 6), and mobile phase B was ammonium formate (50 mM)-methanol (10:90, v/v) (pH* 5). The following gradient was applied: 0 - 4 min, 0 to 100% B; 4 - 15 min, 100% B; 15 - 16 min, 100 - 0% B; 16 - 25 min 100 B%. The second chiral stationary phase was TeicoShell column (4.6 x 150 mm, AZYP, LLC, USA), which was based on macrocyclic glycopeptides. TeicoShell column was used to confirm amino acids peak identity due to its opposite enantioselectivity. For a complex matrix, there is still a chance that an impurity with the same *m/z* and a similar structure is co-eluting with the analyte of interest on one column. Having a second column with different selectivity can separate the impurity that is co-eluting with the analyte on the first column. Indeed this was the case with these samples where L-Hyp overlapped with L-Ile on the Q-Shell column initially but was resolved on the TeicoShell column. Mobile phase A was ammonium formate (5 mM, pH 4), and mobile phase B was acetonitrile. A gradient method for TeicoShell column

was applied as following: 0-2 min, 30% to 40% B; 2-15 min, 40% to 50% B; 15-16 min, 50% to 30% B; 16-30 min, 30% B. The flow rate was 0.65 mL/min for both columns, and a splitter was used before the MS. HPLC-MS/MS was operated in multiple reaction monitoring (MRM) mode using positive ESI source. Collision energies and MRM transitions were optimized for each amino acid. Shimadzu LabSolutions software was used for data acquisition.

Representative chromatograms of the AQC-amino acids in cultured cells are shown in Figure 5-1. Internal standard calibration curve was constructed for each amino acid. The method was evaluated for linearity, sensitivity, precision, accuracy, and matrix effect according to US Food and Drug Administration document for bioanalytical method validation. Detailed procedures for method optimization and validation were described previously [175], and results were shown in. The method developed here is a rapid and sensitive separation method that can complete the analysis of 39 amino acids including L- and D-enantiomers within 15 min with LODs in the sub-pg level. Also, D-enantiomers elute before their corresponding L-enantiomers on Q-Shell column, which is favorable for the quantification of D-amino acids in biological samples due to the lack of interference from the corresponding L-amino acids.

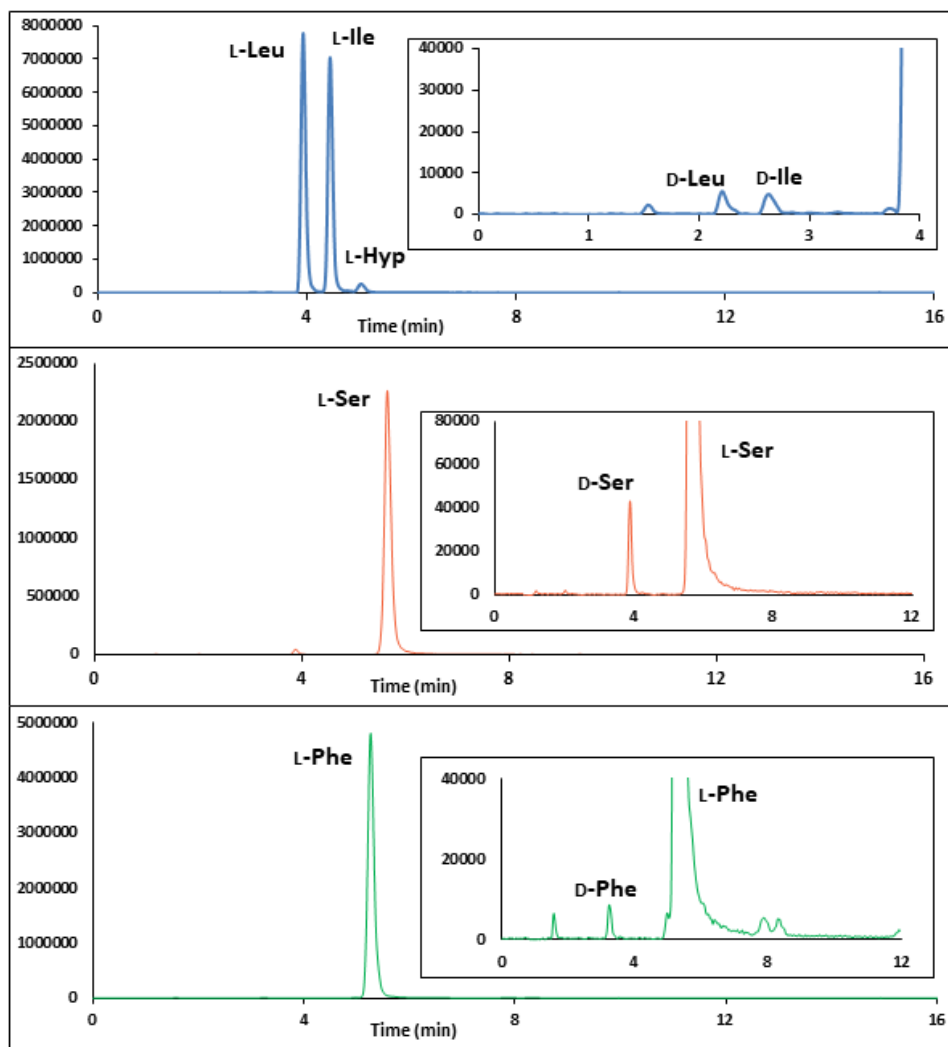


Figure 5-1 Representative chromatograms of AQC derivatized amino acids in MCF-7 cancer cells after 48-hour growth in high glucose medium

The starting amino acid levels of uncultured media (prior to any cell growth) were determined after serum supplementation. To determine changes in extracellular amino acid levels over time, uncultured medium was included in the analysis. Data were plotted as percent change from the uncultured medium, which was calculated by the following equation:

$$\frac{\text{Amino acid level in the cultured medium} - \text{amino acid level in the uncultured medium}}{\text{Amino acid level in the uncultured medium}} \times 100\%$$

Malignancy indicators (MIs) in were calculated by the following equations:

$$\text{a. L-amino acids} = \frac{\text{Intracellular L-amino acid levels in MCF-7 cells}}{\text{Intracellular L-amino acid levels in MCF-10A cells}}$$

$$\text{b. D-amino acids} = \frac{\text{Intracellular D-amino acid levels in MCF-7 cells}}{\text{Intracellular D-amino acid levels in MCF-10A cells}}$$

$$\text{c. MIs} = \frac{\text{L-amino acids}}{\text{D-amino acids}}$$

Each experimental condition was performed in triplicate. Average and standard deviations for intracellular and extracellular amino acid levels were calculated from parallel triplicate experiments.

5.3 Results and Discussion

5.3.1 Free L-Amino Acid Profiles in MCF-7 and MCF-10A Cells

5.3.1.1 Intracellular and extracellular free L-amino acid levels

Intracellular free L-amino acid levels were determined for MCF-7 and MCF-10A cells after 24-hours, 48-hours, and 72-hours incubation, results are shown in Figure 5-2. The general trends in MCF-7 cells from both high and low glucose media were that L-Gln, Gly, L-Glu, and L-Thr had the highest levels after 72-hour growth, ranging from 418 to 866 nmol/10⁶ cells. L-Hyp, L-Cys, and GABA had the lowest levels, ranging from 2.3 to 12.5 nmol/10⁶ cells. However, different trends of intracellular L-amino acid levels were observed for the non-tumorigenic MCF-10A cells. L-Glu, L-Asp, and L-Asn showed the highest levels in MCF-10A cells after 72-hour growth, ranging from 37 to 73 nmol/10⁶ cells. L-Met, GABA, and L-Lys showed the lowest levels which ranged from 1.2 to 4.0 nmol/10⁶ cells. L-Asn had the third highest level in MCF-10A cells (~65 nmol/10⁶ cells), but it was one of the lowest levels of amino acids in MCF-7 cells (~23 nmol/10⁶ cells). Compared to MCF-10A cells, MCF-7 cells with the same incubation time had up to 56

fold higher levels of free L-amino acids except for L-Asn. For example, L-Met levels were around 67 nmol/10⁶ cells in MCF-7 cells and 1.2 nmol/10⁶ cells in MCF-10A cells after a 72-hour growth period (**Fig 5-2C**).

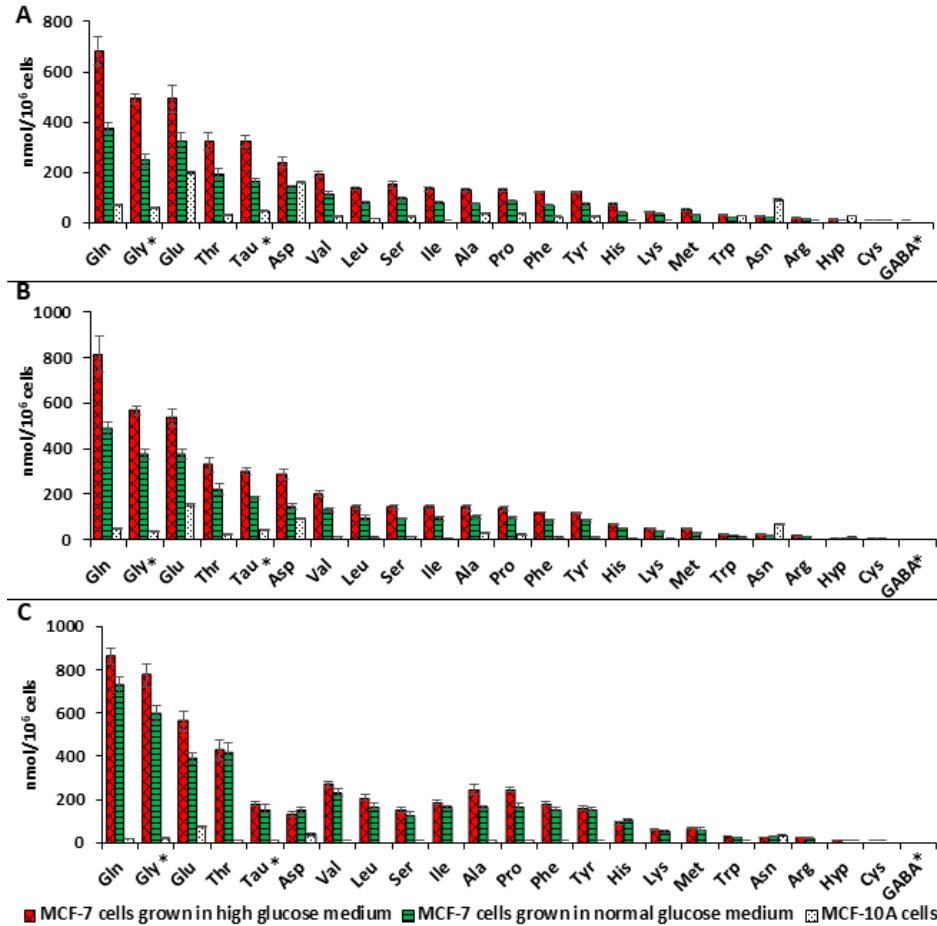


Figure 5-2 Intracellular L-amino acid profiles.

L-Amino acid levels in MCF-7 and MCF-10 cells after (A) 24-hours, (B) 48-hours, and (C) 72-hours growth in the associated medium. Red bars represent MCF-7 cells grown in high glucose medium, green bars represent MCF-7 cells grown in normal glucose medium, and white bars represent MCF-10A cells grown in the MEGM. * indicates non-chiral amino acids.

Extracellular L-amino acid profiles were expressed as percent changes of the amino acid from the uncultured medium (calculated by the equation shown in Materials and methods) and are shown in Figure 5-3. Extracellular profiles of L-amino acids were divided into two categories: essential and nonessential amino acids, due to the general trends observed in each category. The percent change of the nine essential amino acids from uncultured media showed negative values for both MCF-7 and MCF-10A cells, indicating the uptake of these amino acids from the growth media (Figure 5-3A). Regarding nonessential amino acids, as shown in Figure 5-3B, cellular uptake (net removal from the growth media) of L-Ser, L-Gln, L-Arg, L-Tyr, and L-Cys was observed for MCF-7 and MCF-10A cells. Cellular release of L-Ala, L-Pro, and L-Glu was observed in both cells lines. Cellular uptake of L-Asp and Gly were observed for MCF-7 cells, but cellular release of L-Asp and Gly was shown for MCF-10A cells. On the other hand, the release of L-Asn was detected for MCF-7 cells, but the uptake of L-Asn was detected for MCF-10A cells.

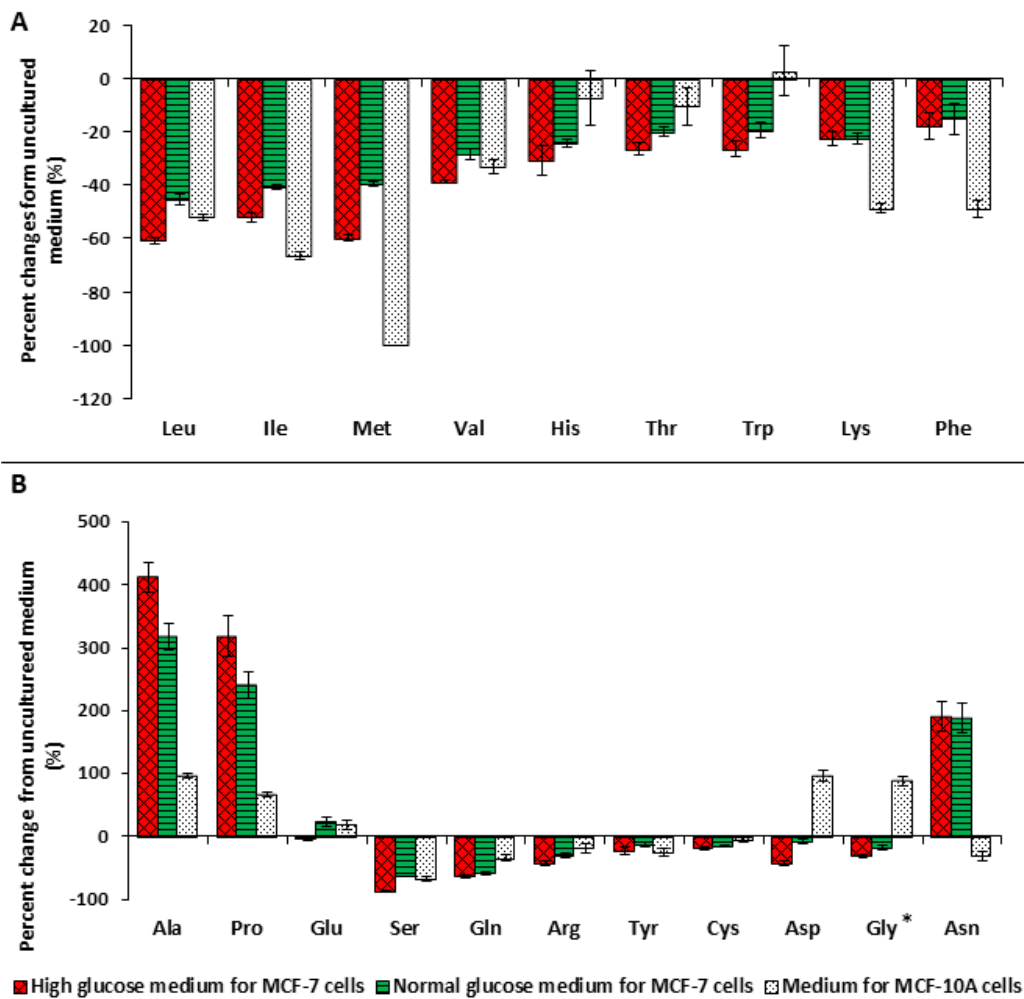


Figure 5-3 Extracellular L-amino acid profiles.

Changes of (A) essential amino acid, (B) non-essential amino acid levels in the media with MCF-7 cells (red: high glucose medium; green: normal glucose medium) and MCF-10A cells (white: MEGM). Values are shown as percent change of L-amino acid in the medium after 72-hours incubation from the uncultured medium, with negative bars indicating cellular consumption and positive bars indicating production. * indicates non-chiral amino acids.

5.3.1.2 Altered L-amino acid profiles and metabolism for MCF-7 breast cancer cells

Cancer cells require higher amounts of amino acids and glucose to fulfill the metabolic demands associated with proliferation [166]. Significant increases of Pro, Thr, Glu, Phe, Trp, Met, Asp, Ser, Gln, Leu, His, Val, and Lys have been reported in the saliva from breast cancer patients compared to healthy controls [171]. In our study, L-amino acid concentrations were found to be up to 56 times higher in MCF-7 breast cancer cells compared to non-tumorigenic MCF-10A cells in both high and normal glucose media (Figure 5-2). Intracellular high levels of L-amino acids could be one of the reasons that elevated levels of L-amino acids are observed in the saliva and plasma of breast cancer patients.

Cellular uptake of all essential amino acids was anticipated, as essential amino acids cannot be synthesized in mammalian cells and must be acquired from the growth media (Figure 5-3). On the other hand, the net flux of nonessential amino acids was unknown. Although they can be produced in mammalian cells from glycolysis, glutaminolysis, or the TCA cycle, extracellular nonessential amino acids can be readily utilized by the cells to reduce the biosynthetic burden on the cells [176]. In this study, cellular uptake of Gly and L-Asp, two nonessential amino acids, was detected for MCF-7 cells. In contrast, release of Gly and L-Asp were observed for MCF-10A cells, suggesting metabolic differences between MCF-7 and MCF-10A cells. Gly can be synthesized from L-Ser, and both are involved in one-carbon metabolism providing methyl groups for the biosynthesis of nucleotides and cofactors [177]. Although the uptake of L-Ser was seen in both MCF-7 and MCF-10A cell lines, recent evidence suggested that cancer cells were more reliant upon the uptake of extracellular Ser. It has been reported that depletion of exogenous L-Ser reduced cancer cell proliferation by affecting nucleotide synthesis [178]. Additionally, cancer cells have shown upregulated activity of the enzymes involved in L-

Ser and Gly synthesis [179]. Downregulation of argininosuccinate synthase 1 (ASS1), using L-Asp as a substrate, has been reported in cancer cells [180]. Decreased ASS1 activity leads to the elevated L-Asp levels in cancer cells, allowing L-Asp to be used for nucleotide biosynthesis and to support cancerous proliferation [180]. Nonessential amino acids, specifically Gly, L-Ser, and L-Asp could be promising targets in cancer therapy, as they become necessary for cancer cell proliferation [181].

5.3.2 Free D-amino acid profiles in MCF-7 and MCF-10A cells

5.3.2.1 Intracellular and extracellular free D-amino acid levels

Intracellular free D-amino acid profiles were determined in both MCF-7 and MCF-10A cells (Figure 5-4). D-Asp, D-Ser, and D-Glu had the highest levels in both cell lines, although they were 2 to 22 fold higher in MCF-7 breast cancer cells. Unlike the trend of L-amino acid levels observed between the two cell lines, MCF-7 did not always exhibit higher levels of D-amino acids compared with MCF-10A cells. Some D-amino acid levels were higher in MCF-7 cells, *i.e.*, D-Asp, D-Ser, D-Asn, D-Ala, D-Thr, and D-Tyr. Others showed higher levels in MCF-10A cells, *i.e.*, D-Val, D-Leu, D-Pro, D-Lys, and D-Trp, while a few had similar levels in both cell lines (Figure 5-4). It is noteworthy that D-Pro, D-Lys, and D-Trp were found only in MCF-10A cells and only after 72-hour growth. MCF-10A cells showed higher percentages of D-enantiomers for almost all the amino acids, except D-Asp and D-Asn (Figure 5-5).

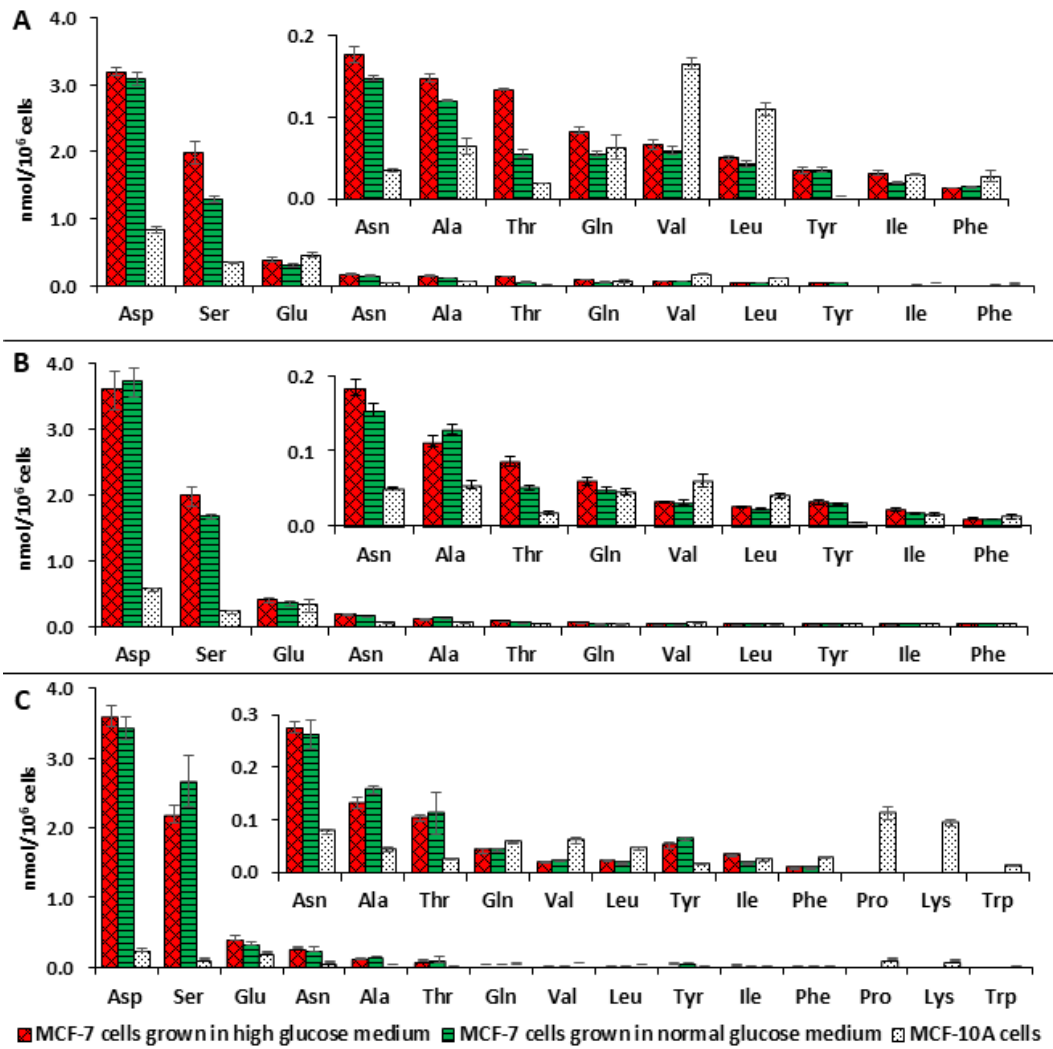


Figure 5-4 Intracellular D-amino acid profiles.

D-Amino acid levels in MCF-7 and MCF-10 cells after (A) 24-hours, (B) 48-hours, and (C) 72-hours growth in the associated medium. Red bars represent MCF-7 cells grown in high glucose medium, green bars represent MCF-7 cells grown in normal glucose medium, and white bars represent MCF-10A cells grown in the MEGM.

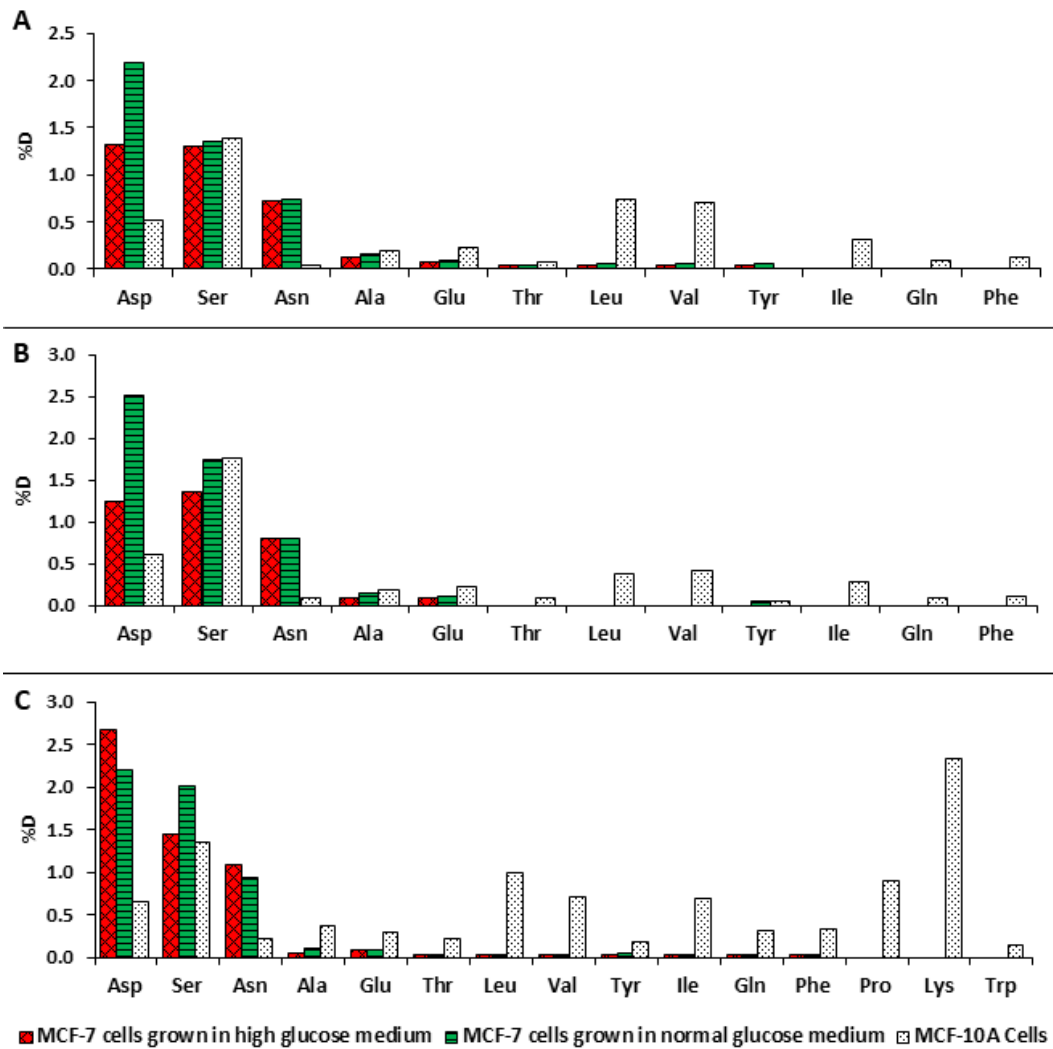


Figure 5-5 Intracellular percent D-amino acid levels.

Intracellular % D-Amino acids in MCF-7 and MCF-10 cells after (A) 24-hours, (B) 48-hours, and (C) 72-hours growth in their associated medium. Red bars represent MCF-7 cells grown in high glucose medium, green bars represent MCF-7 cells grown in normal glucose medium, and white bars represent MCF-10A cells grown in the MEGM.

Extracellular (*i.e.*, growth media) free D-amino acid profiles were determined for MCF-7 and MCF-10A cells as shown in Figure 5-6. Cellular uptake of all D-amino acids was found in MCF-10A cells except for D-Ser and D-Lys. Concerning MCF-7 breast cancer cells, cellular uptake was observed for D-Leu, D-Asp, D-Gln, D-Ala, D-Tyr, and D-Val, while cellular release was observed for D-Asn, D-Arg, D-Thr, and D-Ser. Surprisingly, MCF-7 cells exhibited net uptake of D-Ile, D-Glu, D-Phe, and D-Lys when grown at high glucose condition, but these amino acids were released from the MCF-7 cells at the normal glucose condition.

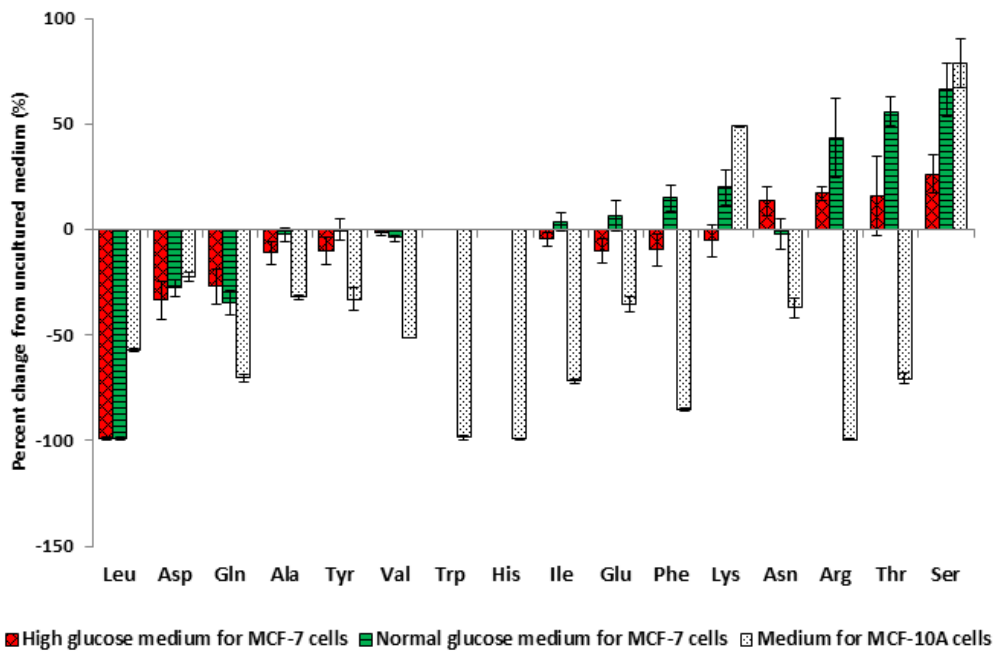


Figure 5-6 Extracellular D-amino acid profiles.

Percent changes of D-amino acids in the media with MCF-7 cells (red: high glucose medium; green: normal glucose medium) and MCF-10A cells (white: MEGM). Values are shown as percent change of L-amino acid in the medium after 72-hours incubation from the uncultured medium, with negative bars indicating cellular consumption and positive bars indicating production.

5.3.2.2 Altered D-amino acid profiles and metabolism for MCF-7 breast cancer cells

Low percentages of most D-amino acids were observed in MCF-7 compared to MCF-10A cells. It was mostly due to the high levels of L-amino acids in MCF-7 cells, as the corresponding D-amino acid levels were not much different between these two cell lines (Figures 5-4 and 5-5). However, significantly high amounts of D-Asp and D-Ser were determined in MCF-7 breast cancer cells, *i.e.*, 3 to 22 times higher than in MCF-10A cells. High levels of intracellular D-Asp may be caused by the absorption of D-Asp from extracellular sources (*i.e.*, uptake of D-Asp was observed, Figure 5-6) or the biosynthesis of D-Asp by aspartate racemase or a combination of both [182]. Given the fact that D-Ser levels were increased in the growth media after cell incubation (Figure 5-6), biosynthesis of D-Ser by serine racemase may occur in the cultured cells and then released into the growth medium [183].

Questions arise as to whether the higher intracellular levels indicate an important or unique function of D-Asp and D-Ser for MCF-7 breast cancer cells. Besides the essential roles in the CNS, NMDA receptors have been implicated in regulating cancer cell growth and division [24]. It has been demonstrated that MCF-7 breast cancer cells expressed functional NMDA receptors with NR1 and NR2 subunits, and blockage of NMDA receptors with antagonists inhibited proliferation and reduced viability of cultured MCF-7 cells [184]. Interestingly, it has been determined that D-Ser binds to NMDA receptor NR1 subunits at the glycine binding site, and D-Asp binds to NMDA receptor NR2 subunits at the glutamate binding site [13, 16, 17]. As co-agonists of NMDA receptors, high levels of D-Asp and D-Ser as shown in our work may be required or at least beneficial for MCF-7 breast cancer cell proliferation since activation of NMDA receptors in breast cancer cells is important for maintaining cell growth and viability. As

they have shown increased availability and have selectively accumulated in MCF-7 breast cancer cells, D-Asp and D-Ala could be potential oncometabolites for breast cancer. Further, accumulation of specific D-amino acids in cancer cells may be the consequences of upregulated racemases, as the presence of Ser racemase and Asp racemase has been reported in mammals [182, 183]. Although further investigation and validation are needed for the proposed potential oncometabolites and the possible upregulated racemases for breast cancer, this study provides a new approach for breast cancer diagnosis.

D-Amino acids were found in MCF-7 and MCF-10A cells as well as in the cultured and uncultured media. Changes in extracellular D-amino acid levels were detected, indicating the release or uptake of D-amino acids by MCF-7 and MCF-10A cells (Figure 5-6). Our results demonstrated that the transfer of D-amino acids occurred between cells and growth media. Amino acids are hydrophilic molecules and cannot cross the cell membrane without the aid of amino acid transporters. It has been reported that most of the transporters show high stereoselectivity, and only a few transporters have been shown to transport D-amino acids, *e.g.*, LAT1, ASCT1, ASCT2, ATB⁰⁺, and EAAT [185-187]. They have shown selectivity to D-Leu, D-Ser, D-Met, D-Phe, and D-Asp. Cellular release of D-Ser (observed in our study) through the less stereoselective amino acid transporters is likely to be important in regulating extracellular levels of D-Ser, which activate NMDA receptors and further affects breast cancer cell proliferation. It has been determined that cancer cells express some amino acid transporters at high levels to satisfy their increased demand for amino acids [172]. Interestingly, all the transporters mentioned above have been shown to be upregulated in cancer cells. This further supports the possibility that altered D-amino acid profiles may be a metabolic adaptation to breast cancer cell proliferation. Thus, reducing the availability of the potential

oncometabolites, D-Asp and D-Ser, to breast cancer cells could be a possible anticancer strategy. Future studies could explore more on the inhibition of the enzymes/pathways that produce D-Asp and D-Ser, and interference with the upregulated amino acid transporters in cancer cells that show selectivity for these D-amino acids. Another notable result was that D-Thr, D-Tyr, and D-Ala also were elevated in MCF-7 cells. Although it has been reported that D-Ala can also bind to NMDA receptor, the presence of Ala racemases have not been confirmed in mammals. Concerning D-Thr and D-Tyr, there are no studies concerning their presence and functions for breast cancer cells to our knowledge. Our results suggest that it may be worthy of exploring the roles of D-Thr, D-Tyr, and D-Ala during cancer cell proliferation.

5.3.3 L-Asn and D-Asn may both serve as exchange currency during breast cancer cell proliferation

Amino acid transporters carry out not only net transport of amino acids (*i.e.*, symporters, substrates travel in the same direction), but also obligatory amino acid exchange (*i.e.*, antiporters), which means uptake of one amino acid via this transporter is obligatorily coupled to the export of another amino acid [187]. A recent study indicated that depletion of intracellular and/or extracellular L-Asn in breast cancer cells impaired the uptake of extracellular amino acids, especially L-Ser, L-Arg, and L-His, and reduced cancer cell proliferation [188]. However, the function of D-Asn for cancer cell proliferation was not investigated. In the present study, cellular uptake of L-Ser, L-Arg, and L-His was observed for MCF-7 breast cancer cells (Figure 5-3). In addition, cellular release of both L-Asn and D-Asn was observed for MCF-7 breast cancer cells, but not for MCF-10A cells (Figures 5-3 and 5-6). Our results support and further suggest that intracellular L-Asn, together with D-Asn, exchanges with extracellular amino acids, especially L-Ser, L-Arg, and L-His, to promote cancer cell proliferation [188]. Asn, L- and D-enantiomers, may

serve as exchange currency for the uptake of essential amino acids and/or low abundance nonessential amino acids that are required by cancer cells during proliferation.

5.3.4 Malignancy indicators may be used to indicate the presence of cancer

The question arises, as to whether the substantially altered levels of D- and L-amino acids in cancer cells can be used to provide a sensitive and reliable index to identify malignancy? A relatively simple malignancy indicator (MI) comparing the ratio of each L-amino acid in cancer vs. noncancerous cell line and divided by the analogous ratio of D-amino acid, are given in Table 5-1 (see Materials and methods for calculations). Clearly, there are three notable features which are: 1) increased demands of specific L-amino acids contribute to a high MI; 2) increased demands of specific D-amino acids contributes to low MIs, and 3) designated cellular release of specific L- and D-amino acids contribute to low MI. Gln, Phe, Ile, Val, and Leu show high MI due the significant elevated levels of L-enantiomers but decreased levels of D-enantiomers in MCF-7 breast cancer cells. Low MI values are determined for Asn, Asp, and Ser, and how these elevated D-amino acids contribute to low MIs were discussed above.

Table 5-1 Malignancy indicators for breast cancer

	L-amino acids ^a	D-amino acids ^b	Malignancy Indicator (MI) ^c
Asn	0.8	3.4	0.2
Asp	4.0	14.0	0.3
Ser	15.0	22.0	0.7
Glu	5.4	1.6	3.4
Ala	13.7	3.6	3.8
Tyr	16.8	4.2	4.0
Thr	35.9	4.4	8.2
Trp ^d	2.7	0.07	> 39 ^d
Gln	41.0	0.8	51
Phe	18.0	0.3	60
Ile	46.0	0.7	66
Val	27.0	0.4	68
Leu	36.0	0.4	90
Pro ^d	13.6	0.03 ^d	> 450 ^d
Lys ^d	12.9	0.01 ^d	> 1300 ^d

Results in this table were obtained from MCF-7 breast cancer cells grown in normal glucose condition vs. MCF-10A cells after 72-hours incubation. Calculations for: L-amino acids^a, D-amino acids^b, and Malignancy Indicator^c are given in the Materials and methods. ^d indicates that this D-amino acid was detected only in MCF-10A cells, but not in MCF-7 breast cancer cells. In these cases, the limit of detection (LOD) for these D-amino acids was used to estimate a MI value.

5.3.5 Effect of glucose concentration on MCF-7 cell proliferation and amino acid levels

Cell media with different glucose concentrations (i.e., 5 mM and 25 mM) were examined for the effect of glucose level on cancer cell proliferation. Cell number and free

amino acid levels were measured for MCF-7 cells with different growth times, i.e., 24-hours, 48-hours, and 72-hours (S4, S5, S7, S8, S10, S11, and S25 Tables). As expected, the proliferation of MCF-7 cells increased when the glucose concentration in the medium was increased from 5.5 mM to 25mM at 72 hours (Fig S3). MCF-7 cells grown in high glucose medium showed higher levels of free L-amino acids compared to those grown in normal glucose medium (Figure 5-2). For instance, L-Gln levels in MCF-7 cells grown in high glucose and normal glucose condition were 681 nmol/10⁶ cells and 377 nmol/10⁶ cells, respectively, after 24-hour incubation (Figure 5-2A). However, the trends of intracellular L-amino acid levels for MCF-7 cells were similar despite the glucose concentration in the medium (Figure 5). L-Gln, Gly, and L-Glu were the three amino acids with the highest levels, and the three L-amino acids with the lowest levels were always GABA, L-Cys, and L-Hyp in MCF-7 cells regardless of the growth media. Concerning D-amino acids, most of them did not show significant changes in MCF-7 cells when the glucose levels were changed in the medium (Figure 5-4). The exceptions were D-Thr and D-Ser, which were higher in MCF-7 cells grown in high glucose conditions, especially after 24-hour growth.

5.4 Conclusions

The altered intracellular and extracellular free L-amino acid profiles determined in MCF-7 breast cancer cells, demonstrate the metabolic differences between the breast cancer cells and non-tumorigenic breast cells. Significantly high intracellular L-amino acids levels may contribute to the elevated levels of L-amino acids that are observed in the saliva and plasma of breast cancer patients. Our data indicate that cellular uptake and release of specific D-amino acids occur during cancer cell proliferation. It is clear that D-amino acids also have altered profiles in cancer cells. Specific D-amino acids showed

significantly altered levels in cancer cells compared to non-tumorigenic cells. In particular, two D-amino acids, D-Ser and D-Asp, had elevated levels and could be potential oncometabolites for breast cancer via selective accumulation in MCF-7 breast cancer cells. Elevated levels of D-Ser and D-Asp in MCF-7 breast cancer cells may result from upregulated enzymatic racemases. Like specific L-amino acids, D-amino acids may also be able to serve as exchange currency to drive the uptake of essential and/or low abundance nonessential amino acids required by the cancer cells. A simple index using specific L- and D-amino acid relative levels has been derived and used to produce malignancy indicator (MI) of cancer. High MIs (>60) result from the increased demands of specific essential amino acids (*i.e.*, L-Leu, L-Ile, L-Val, and L-Phe) and L-Gln that functions like “essential” amino acids for cancer cells during proliferation. Very low MIs (<1) result from the increased demands of specific D-amino acids (*i.e.*, D-Ser, D-Asp) or the cellular release of amino acid exchange currency (*i.e.*, L- and D-Asn) to promote cancer cell proliferation. Such a simple and fast technique based on both high and low MI values may be used to predict/estimate the development of malignancy and perhaps in the future, early diagnosis of breast cancer. Though we have yet to explore this, it is conceivable that different cancers will each have a unique combination of MIs for a specific set of AAs, something akin to a fingerprint, which could be used for broad range cancer detection.

Chapter 6

Simultaneous Identification of the Isomeric Amino Acid Residues in β -Amyloid: A Remarkable Piece of the Alzheimer's Puzzle

Abstract

Although the underlying cause of Alzheimer's disease (AD) is not known, the extracellular deposition of β -amyloid ($A\beta$) was considered as a hallmark of AD brains. Evidence has shown the occurrence of isomerization/racemization of Asp and Ser in $A\beta$, which may contribute to the neurodegeneration in AD patients. Herein, we have developed the first high-throughput profiling technique of all 20 potential $A\beta$ peptide epimers containing Asp, isoAsp, and Ser isomers using high performance liquid chromatography-tandem mass spectrometry (HPLC-MS/MS).

Introduction

Alzheimer's disease (AD), the most common cause of dementia [189], is a neurodegenerative disease characterized by progressive degeneration of brain tissue [190, 191]. The exact cause of the degeneration has yet to be elucidated, but one of the prime suspects is the extracellular deposition of β -amyloid ($A\beta$) [192]. $A\beta$ is a proteolytically cleaved section of a larger protein called amyloid precursor protein (APP) [193]. It is noteworthy that there is a distinction between $A\beta$ and amyloid plaques. $A\beta$ is a normal peptide generated throughout life although its normal function remains unclear [191]. While amyloid plaques are the insoluble accumulation of $A\beta$ between nerve cells and are the neuropathological hallmark of AD [191]. Recent studies have shown that there is a difference in $A\beta$ between normal elderly people and AD patients [194]. N-terminal truncation of $A\beta$ was significantly more prevalent in AD patients. The molecular composition, rather than the amount, of $A\beta$ was thought to be more associated with neuronal toxicity. Furthermore, racemization and isomerization of Asp and Ser, have been detected in $A\beta$ and thought to contribute to AD [195-199]. The amount of isomerized or racemized amino acid residues in $A\beta$ are significantly higher in AD patients compared to the normal aging populations [196].

Ser occurs in two positions in $A\beta$, Ser8 and Ser26. Little is known about the exact mechanism of D-Ser formation in $A\beta$. Limited studies have shown that approximately 4-9% of Ser exists as D-Ser in the HCl hydrolyzed $A\beta$ peptides from AD patients [195]. The relative ratios of L- to D-Ser at the two positions have not been determined. Moreover, the percentage values of D-Ser reported previously were obtained after HCl hydrolysis, which causes an inherent amount of racemization (estimated 2% error) [195, 200]. It is theorized that racemization at

Ser26 is more toxic as studies have shown that Ser26 racemization leads to non-degradable A β peptide fragments in rats [197, 199].

Asp occurs in three places in A β : Asp1, Asp7, and Asp23. There is evidence of isomerization and racemization of Asp in A β at every position in AD patients [195, 201]. Isomerization and racemization of Asp spontaneously occurs through a cyclic succinimide intermediate resulting in L/D-Asp or L/D-isoAsp [139]. As the racemization/isomerization of Asp leads to four possible permutations, the concurrent analysis of all isomers is desired to better characterize the brain of AD patients. The prevailing consensus is that the isomerization and/or racemization of Asp and Ser either structurally destabilizes A β , leading to misfolding or impairs the likelihood of proper degradation [202]. Indeed, peptides/proteins containing D-amino acids appear to be more resistant to enzymatic degradation in living systems [203-205].

The identification and detection of isomerization and/or racemization products in A β is challenging for several reasons. First, isomerization and racemization do not change the mass of peptides, therefore it cannot be discriminated by a single stage of MS. Second, the isomerization or racemization of a single amino acid residue in a lengthy peptide may not significantly vary chemical properties of the peptide, thus increasing the difficulty of chromatographic separation. Finally, the low abundance of these epimer peptides requires a sensitive detection method for both qualitative and quantitative analysis. Even with the challenges stated many analytical and bioanalytical approaches have been proposed in the investigation of isomeric residues in A β [206-209].

The conventional methods used to quantify D-amino acids involved acid hydrolysis and chiral derivatization followed by reverse-phase liquid

chromatography [195]. As noted earlier, acid hydrolysis induces racemization and cannot detect the presence of isoAsp linkages. Immunohistochemistry involving the use of tailored antibodies has also shown success at the detection of isomerized Asp and Ser, but the methods are not quantitative [196].

MS-based fragmentation techniques have been applied to identify the isomerization of Asp in peptides, including low energy collision induced dissociation [210, 211], electron transfer/capture dissociation [212, 213], and radical-directed dissociation [214], as they generate diagnostic fragment ions for the Asp and isoAsp containing peptides. However, inconsistent results regarding the fragmentation pattern for peptides containing Asp isomers have been reported, which may due to the dependency of peptide sequence and instruments [212].

Combination methods using LC-MS and enzymatic reactions also show promise [207]. This method involves the use of trypsin in combination with three other enzymes: endoproteinase Asp-N (cleavage at N-terminal L-Asp), protein L-isoaspartyl methyltransferase (methylation of L-isoAsp), and D-aspartic acid endopeptidase (cleavage at C-terminal D-Asp). The resulting peptides were then applied to LC-MS for identification. However, the identification of D-Asp was not always successful with D-aspartic acid endopeptidase as reaction conditions need further optimization for complete digestion [207].

Ion mobility spectrometry (IMS) coupled with MS has also been of great interest in the study of isomers separation [215-218]. However, peptides containing Asp and isoAsp were not able to be resolved using conventional IMS-MS due to the low resolution. Recently, Smith's group have designed a new IMS platform-structures for lossless ion manipulations (SLIM), which enables long IMS pathlength to achieve the separation of A β peptides containing L/D-Asp and L/D-

isoAsp [209]. While the SLIM platform alone is a fast analysis method, coupling LC to SLIM is desired to increase detection sensitivity and provide better separation in complex biological samples [219]. In addition, only the isomerization of Asp residues in A β has been studied, and the separation was achieved for only four potential A β peptide epimers.

To better characterize the presence and ratio of Asp and Ser isomers simultaneously in the brain of AD patients, better and faster analytical methods are needed. Our approach for the separation and identification of A β peptide epimers uses trypsin digestion in combination with chiral HPLC stationary phases and MS/MS as the detection method. Unlike previously reported methods, simultaneous detection and quantification of L/D-Ser, L/D-Asp and L/D-isoAsp isomers for all positions in A β are possible. This present method does not use HCl digestion, thus avoids possible racemization and leaves isoAsp linkages intact. Moreover, HPLC-MS/MS is a simple yet quantitative platform that is easily accessible. The theoretical digestion of A β by trypsin produces four peptide groups (Group D was not studied as it does not contain Asp or Ser residues). The amino acid sequence of the potential tryptic A β peptide epimers containing Asp and Ser are shown in Table 1. In total, there are 20 possible peptide combinations containing Asp and Ser isomers. This is the first report of comprehensive separation of A β epimers containing isomeric Asp and Ser residues at every position.

Table 6-1 Amino acid sequence of the three groups of A β peptide epimers with Asp and Ser isomeric residues

Aβ (1-5) Group A	A1: {L-Asp}AEFR	A2: {D-Asp}AEFR
	A3: {L-isoAsp}AEFR	A4: {D-isoAsp}AEFR
Aβ (6-16) Group B	B1: H{L-Asp}{L-Ser}GYEVHHQK	B2: H{D-Asp}{L-Ser}GYEVHHQK
	B3: H{L-Asp}{D-Ser}GYEVHHQK	B4: H{D-Asp}{D-Ser}GYEVHHQK
	B5: H{L-isoAsp}{L-Ser}GYEVHHQK	B6: H{L-isoAsp}{D-Ser}GYEVHHQK
	B7: H{D-isoAsp}{L-Ser}GYEVHHQK	B8: H{D-isoAsp}{D-Ser}GYEVHHQK
Aβ (17-28) Group C	C1: LVFFAE{L-Asp}VG{L-Ser}NK	C2: LVFFAE{D-Asp}VG{L-Ser}NK
	C3: LVFFAE{L-Asp}VG{D-Ser}NK	C4: LVFFAE{D-Asp}VG{D-Ser}NK
	C5: LVFFAE{L-isoAsp}VG{L-Ser}NK	C6: LVFFAE{L-isoAsp}VG{D-Ser}NK
	C7: LVFFAE{D-isoAsp}VG{L-Ser}NK	C8: LVFFAE{D-isoAsp}VG{D-Ser}NK

6.1 Experimental

6.1.1 Materials and chemicals

All tryptic β -amyloid (A β) peptide standards were purchased from Peptide 2.0 (Chantilly, VA, USA) at > 98% purity. Ammonium formate and formic acid were obtained from Sigma-Aldrich (St. Louis, MO, USA). HPLC-MS grade methanol and water were purchased from Sigma-Aldrich and ultrapure water was obtained from a Milli-Q water system (Millipore, Bedford, MA, USA). All the peptide standards were prepared in methanol and water (50:50) at the concentration of 1 mg/mL.

6.1.2 Instruments and stationary phases

Initial screening work for the separation and characterization of A β peptide standards was performed on a 1220 Infinity II HPLC instrument (Agilent Technologies, Santa Clara, CA, US). Among all the stationary phases screened, three chiral stationary phases have shown promising results: modified Q-Shell-1, modified Q-Shell-2, and NicoShell chiral stationary phases which were provided by AZYP, LLC (Arlington, TX, USA). Thus, the separation conditions of A β peptide epimers were further optimized on these chiral stationary phases.

HPLC-MS/MS analysis was performed on LCMS-8060 (Shimadzu Scientific Instruments, Columbia, MD, USA), triple quadrupole spectrometer with electrospray ionization (ESI). The drying gas and nebulizing gas flow rate were 10 L/min and 2 L/min, respectively; the desolvation line temperature and heat block temperature were 275 °C and 400 °C, respectively. HPLC-MS/MS was operated in multiple reaction monitoring (MRM) mode with positive ESI source. Peptide fragmentation ions were further confirmed on LCMS-IT-TOF (Shimadzu Scientific Instruments), ion trap and time-of-flight mass spectrometer with ESI. Collision energies and MRM transitions were optimized for each peptide group. Shimadzu LabSolution software was used for data acquisition.

6.2 Results and discussion

Peptide epimers are diastereomers and can be separated on reverse phase columns, however, better separations of peptide epimers have been achieved on chiral stationary phases [220, 221]. The optimized separations for potential trypsin digested A β peptide epimers are shown in Figure 6-1, 6-2, and 6-3. All separations were achieved on chiral HPLC stationary phases using MS compatible mobile phases. It is important to note that the separation windows do not overlap when the three peptide groups are analyzed simultaneously. For example, the separation of A β (1-5) Group A peptide epimers was achieved on modified Q-shell chiral stationary phase within 7 min. Under the same separation condition, Group B peptides elute at dead volume, while Group C peptides retain longer than 7 min. Thus, there is no interference between the three groups during analysis.

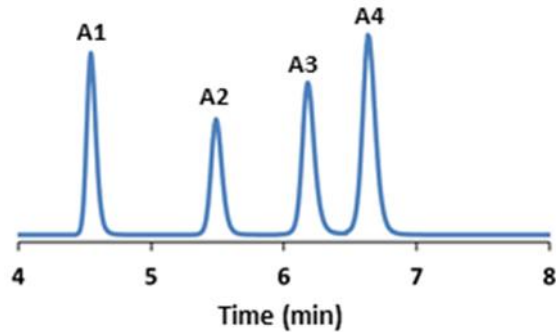


Figure 6-1 Separation of A β (1-5) peptide epimers on modified Q-Shell chiral stationary phase (3 x 150 mm, 2.7 μ m).

Condition: 5/95 methanol/5 mM ammonium formate (pH 3.0), 0.3 mL/min, 23 °C. Group B peptides elute at dead volume while Group C peptides are retained for much longer compared to Group A.

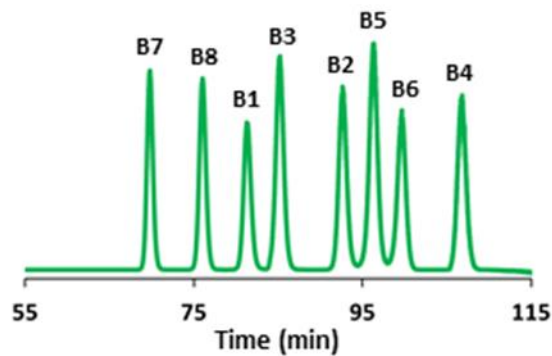


Figure 6-2 Separation of A β (6-16) peptide epimers on NicoShell chiral stationary phase (3 x 150 mm, 2.7 μ m).

Condition: 35/65 acetonitrile/10 mM ammonium formate (pH 4.5), 0.2 mL/min, 45 °C.

Group A and C peptides elute before Group B peptides.

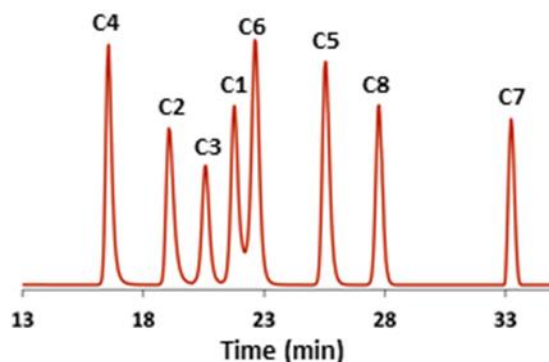


Figure 6-3 Separation of A β (7-28) peptide epimers on modified Q-Shell chiral stationary phase (3 x 150 mm, 2.7 μ m).

Condition: 85/15 methanol/5 mM ammonium formate (pH 3.5), 0.2 mL/min, 10 °C. Group A and B peptides elute around dead volume.

The HPLC-UV method has been successfully transferred to HPLC-MS/MS to improve detection sensitivity. HPLC-MS/MS was operated in multiple reaction monitoring (MRM) mode with positive ESI source. Improved limit of detections for the A β peptides are in the range of 40 to 250 pg. Collision energies and MRM transitions were optimized for each peptide group, results are summarized in Table 6-2.

Table 6-2 Results of MRM optimization and LODs for tryptic A β peptides on LCMS-8060

	Precursor (m/z)	Product (m/z)	Q1 (V)	CE	Q3 (V)	LODs (pg)
Group A Aβ (1-5)	637.5 (M ⁺¹)	322.2(y ₂ ion)	-32	32	-15	40
	637.5 (M ⁺¹)	522.0 (y ₄ ion)	-32	31	-26	-
Group B Aβ (6-16)	669 (M ⁺²)	110.2 (H ion)	-32	48	-19	250
	669 (M ⁺²)	253.3 (b ₂ ion)	-32	27	-24	-
Group C Aβ (17-28)	663.5 (M ⁺²)	1113.3 (y ₁₀ ion)	-32	24	-32	55
	663.5 (M ⁺²)	185.4 (a ₂ ion)	-32	23	-18	-

6.3 Conclusions

In conclusion, we have developed the first comprehensive analytical platform that allows for the separation and quantification of all 20 possible A β peptide epimers containing isomeric Asp and Ser residues. The ability to fully resolve 20 of the A β peptide epimers is extremely valuable for characterizing the Asp and Ser isomerization/racemization in A β from biological samples. This method can help answer questions about which position is more abundant in D-Ser in A β , which has not yet been reported. In addition, there is little investigation whether isomerization/racemization of one position enhances the likelihood of alterations at other positions. Our method allows for the investigations of correlations between the isomerization and racemization of different positions when studying AD patients. In the future, we will examine brain tissues and plasma samples from AD patients using this simple and high-throughput analytical platform. We expect that characterization of these Asp and Ser isomers in A β from AD patients will contribute to a better understanding of the etiology of the disease.

Chapter 7

General Summary

Chapter 2 discusses a highly selective and sensitive heart-cutting two-dimension HPLC separation method for the chiral analysis of amino acids and its application for mouse tissue and blood samples. This is the most comprehensive baseline study of L- and D-amino acids in mouse brain tissues and blood. Two mouse brain regions were investigated in this study: the hippocampus and cortex. The effect of perfusion on amino acid levels was also evaluated for the first time. It was found that blood amino acid levels, both total amino acids (L- plus D-) and D-amino acids, were lower than those in cortex and hippocampus. Perfusion of blood reduced the variation of amino acid levels from mouse to mouse. However, it may also lead to some loss of amino acids. Total amino acid levels were similar in mouse cortex and hippocampus; however, the regional distribution of D-amino acids was observed. A 13% reduction of D-amino acid levels were found in cortex compared to hippocampus, except for D-Asp. The most notable result from this study was that Glu, the most prevalent of all free amino acids studied, had no detectable level of D-Glu.

Chapter 3 described a novel application of paired ion electrospray ionization (PIESI) for the sensitive detection of Fmoc-derivatized amino acids. Ion-pairing reagents were introduced post column to form positively charged complexes, which were more surface active and can be detected in the positive mode. Various PIEESI reagents were evaluated for the detection of Fmoc-amino acids, including symmetrical dicationic, tricationic, tetracationic, and unsymmetrical dicationic ion pairing reagents. The detection limits for the Fmoc-amino acids were improved up to 100 times with the optimal ion pairing reagents using the PIEESI platform compared to the negative ESI-MS mode. LODs obtained with the optimal ion-pairing reagents ranged from 0.5 to 20 pg. Eventually, this

method was applied successfully for the simultaneous analysis of 20 amino acid levels in human urine samples within 23 min with high sensitivity, high accuracy and reduced matrix effects.

A mass spectrometry compatible separation method for L- and D-amino acids was developed on quinine and teicoplanin-based chiral stationary phases with triple quadrupole MS as detection method. Quinine and teicoplanin chiral stationary phases showed the opposite selectivity for the amino acid enantiomers, which aided in confirming peak identities. This currently developed HPLC-MS/MS method showed better separation, high sensitivity, improved selectivity, and reduced analysis time. This novel HPLC-MS/MS platform was applied for the analysis of L- and D-amino acid levels in more complex matrices: mouse whole brain and human cancer cells. The results from these two studies were presented in Chapter 4 and Chapter 5, respectively.

In Chapter 4, L- and D-amino acid levels were determined in the whole brain of wild-type ddY mice (ddY/DAO^{+/+}), mutant mice lacking DAO activity (ddY/DAO^{-/-}), and the heterozygous mice (ddY/DAO^{+/-}). L-Glu, L-Asp, and L-Gln showed the highest levels in all three mice strains. No significant differences in L-amino acid levels were determined within the three mice strains, except for L-Trp. L-Trp showed significantly elevated levels in ddY/DAO^{+/-} and ddY/DAO^{-/-} mice compared to wild-type ddY/DAO^{+/+} mice, which has not been reported previously. The question arises as to whether this is an unknown effect of DAO knockout. Further studies will be needed to answer this question. D-Ser showed the highest %D value (~30%), whereas D-Glu had the lowest % D value (~0.1%) in all three strains. Significantly high levels of specific D-amino acids, *i.e.* D-Leu, D-Ala, D-Ser, D-Arg, and D-Ile, were observed in the mutant mice lack DAO activity compared to wild-type mice. These results were in good agreement with previously reported values.

Chapter 5 described the intracellular and extracellular profiles for L- and D-amino acids in human breast cancer (MCF-7) vs non-tumorigenic breast cells (MCF-10A) for the first time. MCF-7 cancer cells always showed higher levels of L-amino acids, except for L-Asn. In addition, D-Asp and D-Ser exhibited markedly elevated levels in MCF-7 cancer cells than MCF-10A cells, which may be potential oncometabolites. Alterations in the intracellular and extracellular L- and D-amino acid profiles indicated the metabolic differences between breast cancer cells and non-tumorigenic breast cells.

Chapter 6 described the first comprehensive analytical platform for the separation of all 20 possible β -amyloid peptide epimers containing Asp, isoAsp and Ser isomers using HPLC-MS/MS. The separations of three groups of peptide epimers were achieved on modified Q-Shell and NicoShell chiral stationary phases. Isomerization and racemization of Asp and Ser residues have been reported in β -amyloid peptides from Alzheimer's patients, which was suggested to contribute to Alzheimer's disease. Using this simple and high-throughput analytical method, all the possible Asp, isoAsp, and Ser isomers in β -amyloid peptides can be determined simultaneously in the brain of Alzheimer's patients.

This dissertation focused on three analytical techniques for the analysis of amino acids in biological samples: heart-cutting 2D-HPLC, PIESI-MS, and HPLC-MS/MS. These established analytical methods have efficiently separated L- from D-amino acids, and peptide epimers containing D-amino acids with good sensitivity and accuracy, which can be used for future study of D-amino acids in various biological samples. In the future, we will examine brain tissues and plasma samples from Alzheimer's patients to characterize the β -amyloid peptides, and we hope this could contribute to a better understanding of the etiology of the disease.

Appendix A

Publication Information and Contributing Authors

Chapter 2. A manuscript published in ACS Chemical Neuroscience and reprinted with permission from American Chemical Society. Choyce A. Weatherly, Siqi Du, Curran Parpia, Polan T. Santos, Adam L. Hartman, Daniel W. Armstrong, 2017,8, 1251-1261. DOI: [org/10.1021/acscemneuro.6b00398](https://doi.org/10.1021/acscemneuro.6b00398)

Chapter 3. A manuscript published in Analytical and Bioanalytical Chemistry. Yadi Wang, Siqi Du, Daniel W. Armstrong, 2018, 410: 4725. DOI: [10.1007/s00216-018-0901-5](https://doi.org/10.1007/s00216-018-0901-5).

Chapter 4. A manuscript published in Analytical and Bioanalytical Chemistry Siqi Du, Yadi Wang, Choyce A. Weatherly, Kylie Holden, Daniel W. Armstrong, 2018, 410: 2971. DOI: [10.1007/s00216-018-0979-9](https://doi.org/10.1007/s00216-018-0979-9)

Chapter 5. A manuscript published in Journal of Pharmaceutical and Biomedical Analysis. Siqi Du, Yadi Wang, Nagham Alatrash, Choyce A. Weatherly, Daipayan Roy, Frederick M. MacDonnell, Daniel W. Armstrong 2019, 164, 421-429. DOI: [10.1016/j.jpba.2018.10.047](https://doi.org/10.1016/j.jpba.2018.10.047).

Chapter 6. A manuscript submitted to Chemical Communication. Siqi Du, Elizabeth R. Readell, Michael Wey, Daniel W. Armstrong, 2019

Appendix B
Copyright and Permissions

SPRINGER NATURE LICENSE TERMS AND CONDITIONS

Oct 28, 2019

This Agreement between 700 Planetarium Place, CPB 114 ("You") and Springer Nature ("Springer Nature") consists of your license details and the terms and conditions provided by Springer Nature and Copyright Clearance Center.

License Number	4697691510304
License date	Oct 28, 2019
Licensed Content Publisher	Springer Nature
Licensed Content Publication	Analytical and Bioanalytical Chemistry
Licensed Content Title	Sensitive analysis of N-blocked amino acids using high-performance liquid chromatography with paired ion electrospray ionization mass spectrometry
Licensed Content Author	Yadi Wang, Siqi Du, Daniel W. Armstrong
Licensed Content Date	Jan 1, 2018
Licensed Content Volume	410
Licensed Content Issue	19
Type of Use	Thesis/Dissertation
Requestor type	academic/university or research institute
Format	print and electronic
Portion	full article/chapter
Will you be translating?	no
Circulation/distribution	1 - 29
Author of this Springer Nature content	yes
Title	ADVANCES IN LIQUID CHROMATOGRAPHY AND LIQUID CHROMATOGRAPHY MASS SPECTROMETRY FOR THE CHIRAL ANALYSIS OF AMINO ACIDS AND DIFFERENTIATION OF ISOMERIC AMINO ACID RESIDUES IN PEPTIDE/PROTEINS FROM COMPLEX MATRICES
Institution name	University of Texas at Arlington
Expected presentation date	Nov 2019
Order reference number	5
Requestor Location	Siqi Du Siqi Du Chemistry and Biochemistry Department University of Texas at Arlington ARLINGTON, TX 76019 United States Attn: Siqi Du
Total	0.00 USD
Terms and Conditions	

**SPRINGER NATURE LICENSE
TERMS AND CONDITIONS**

Oct 28, 2019

This Agreement between 700 Planetarium Place, CPB 114 ("You") and Springer Nature ("Springer Nature") consists of your license details and the terms and conditions provided by Springer Nature and Copyright Clearance Center.

License Number	4697440232895
License date	Oct 28, 2019
Licensed Content Publisher	Springer Nature
Licensed Content Publication	Analytical and Bioanalytical Chemistry
Licensed Content Title	Variations of l- and d-amino acid levels in the brain of wild-type and mutant mice lacking d-amino acid oxidase activity
Licensed Content Author	Siqi Du, Yadi Wang, Choyce A. Weatherly et al
Licensed Content Date	Jan 1, 2018
Licensed Content Volume	410
Licensed Content Issue	12
Type of Use	Thesis/Dissertation
Requestor type	academic/university or research institute
Format	print and electronic
Portion	full article/chapter
Will you be translating?	no
Circulation/distribution	1 - 29
Author of this Springer Nature content	yes
Title	ADVANCES IN LIQUID CHROMATOGRAPHY AND LIQUID CHROMATOGRAPHY MASS SPECTROMETRY FOR THE CHIRAL ANALYSIS OF AMINO ACIDS AND DIFFERENTIATION OF ISOMERIC AMINO ACID RESIDUES IN PEPTIDE/PROTEINS FROM COMPLEX MATRICES
Institution name	University of Texas at Arlington
Expected presentation date	Nov 2019
Order reference number	2
Requestor Location	Siqi Du Chemistry and Biochemistry Department 700 Planetarium Place, CPB 114 ARLINGTON, TX 76019 United States Attn: Siqi Du

References

1. Vickery HB, Schmidt CLA. The History of the Discovery of the Amino Acids. *Chem Rev.* 1931;9:169-318.
2. Stevens CM, Halpern PE, Gigger RP. Occurrence of D-Amino Acids in Some Natural Materials. *J Biol Chem.* 1951;190:705-10.
3. Auclair JL, Patton RL. On the Occurrence of D-Alanine in the Haemolymph of the Milkweed Bug, *Oncopeltus Fasciatus*. *Rev Can Biol.* 1950;9:3-8.
4. Kreil G. D-Amino Acids in Animal Peptides. *Annu Rev Biochem.* 1997;66:337-45.
5. Armstrong DW, Duncan JD, Lee SH. Evaluation of D-Amino Acid Levels in Human Urine and in Commercial L-Amino Acid Samples. *Amino Acids.* 1991;1:97-106.
6. Armstrong DW, Gasper M, Lee SH, Zukowski J, Ercal N. D-Amino Acid Levels in Human Physiological Fluids. *Chirality.* 1993;5:375-8.
7. Wolosker H, Sheth KN, Takahashi M, Mothet JP, Brady RO, Jr., Ferris CD et al. Purification of Serine Racemase: Biosynthesis of the Neuromodulator D-Serine. *Proc Natl Acad Sci U S A.* 1999;96:721-5.
8. D'Aniello A, D'Onofrio G, Pischetola M, D'Aniello G, Vetere A, Petrucelli L et al. Biological Role of D-Amino Acid Oxidase and D-Aspartate Oxidase. Effects of D-Amino Acids. *J Biol Chem.* 1993;268:26941-9.
9. Krebs HA. Metabolism of Amino-Acids: Deamination of Amino-Acids. *Biochem J.* 1935;29:1620-44.
10. Hamase K, Inoue T, Morikawa A, Konno R, Zaitzu K. Determination of Free D-Proline and D-Leucine in the Brains of Mutant Mice Lacking D-Amino Acid Oxidase Activity. *Anal Biochem.* 2001;298:253-8.
11. Morikawa A, Hamase K, Inoue T, Konno R, Zaitzu K. Alterations in D-Amino Acid Levels in the Brains of Mice and Rats after the Administration of D-Amino Acids. *Amino Acids.* 2007;32:13-20.
12. Schell MJ, Brady RO, Jr., Molliver ME, Snyder SH. D-Serine as a Neuromodulator: Regional and Developmental Localizations in Rat Brain Glia Resemble Nmda Receptors. *J Neurosci.* 1997;17:1604-15.
13. Mothet JP, Parent AT, Wolosker H, Brady RO, Jr., Linden DJ, Ferris CD et al. D-Serine Is an Endogenous Ligand for the Glycine Site of the N-Methyl-D-Aspartate Receptor. *Proc Natl Acad Sci U S A.* 2000;97:4926-31.
14. Bendikov I, Nadri C, Amar S, Panizzutti R, De Miranda J, Wolosker H et al. A Csf and Postmortem Brain Study of D-Serine Metabolic Parameters in Schizophrenia. *Schizophr Res.* 2007;90:41-51.
15. Hashimoto K, Fukushima T, Shimizu E, Komatsu N, Watanabe H, Shinoda N et al. Decreased Serum Levels of D-Serine in Patients with Schizophrenia:

- Evidence in Support of the N-Methyl-D-Aspartate Receptor Hypofunction Hypothesis of Schizophrenia. *Arch Gen Psychiatry*. 2003;60:572-6.
16. Tsai GE, Yang P, Chang Y-C, Chong M-Y. D-Alanine Added to Antipsychotics for the Treatment of Schizophrenia. *Biological Psychiatry*. 2006;59:230-4.
 17. Errico F, Nistico R, Napolitano F, Mazzola C, Astone D, Pisapia T et al. Increased D-Aspartate Brain Content Rescues Hippocampal Age-Related Synaptic Plasticity Deterioration of Mice. *Neurobiol Aging*. 2011;32:2229-43.
 18. Fisher GH, D'Aniello A, Vetere A, Padula L, Cusano GP, Man EH. Free D-Aspartate and D-Alanine in Normal and Alzheimer Brain. *Brain Res Bull*. 1991;26:983-5.
 19. Geddes JW, Chang-Chui H, Cooper SM, Lott IT, Cotman CW. Density and Distribution of Nmda Receptors in the Human Hippocampus in Alzheimer's Disease. *Brain Res*. 1986;399:156-61.
 20. Greenamyre JT, Penney JB, D'Amato CJ, Young AB. Dementia of the Alzheimer's Type: Changes in Hippocampal L-[3h]Glutamate Binding. *J Neurochem*. 1987;48:543-51.
 21. Newcomer JW, Farber NB, Olney JW. Nmda Receptor Function, Memory, and Brain Aging. *Dialogues in Clinical Neuroscience*. 2000;2:219-32.
 22. D'Aniello A, Lee JM, Petrucelli L, Di Fiore MM. Regional Decreases of Free D-Aspartate Levels in Alzheimer's Disease. *Neurosci Lett*. 1998;250:131-4.
 23. Hartman AL, Santos P, O'Riordan KJ, Stafstrom CE, Hardwick JM. Potent Anti-Seizure Effects of D-Leucine. *Neurobiol Dis*. 2015;82:46-53.
 24. Deutsch SI, Tang AH, Burket JA, Benson AD. Nmda Receptors on the Surface of Cancer Cells: Target for Chemotherapy? *Biomedicine & pharmacotherapy = Biomedecine & pharmacotherapie*. 2014;68:493-6.
 25. Kirschner DL, Green TK. Separation and Sensitive Detection of D-Amino Acids in Biological Matrices. *J Sep Sci*. 2009;32:2305-18.
 26. Kitagawa F, Otsuka K. Recent Progress in Capillary Electrophoretic Analysis of Amino Acid Enantiomers. *J Chromatogr B*. 2011;879:3078-95.
 27. Schaeper JP, Sepaniak MJ. Parameters Affecting Reproducibility in Capillary Electrophoresis. *Electrophoresis*. 2000;21:1421-9.
 28. Zahradníčková H, Hušek P, Šimek P. Gc Separation of Amino Acid Enantiomers Via Derivatization with Heptafluorobutyl Chloroformate and Chirasil-L-Val Column. *J Sep Sci*. 2009;32:3919-24.
 29. Ilisz I, Péter A, Lindner W. State-of-the-Art Enantioseparations of Natural and Unnatural Amino Acids by High-Performance Liquid Chromatography. *TrAC, Trends Anal Chem*. 2016;81:11-22.
 30. Agrafiotou P, Sotiropoulos S, Pappa-Louisi A. Direct Rp-Hplc Determination of Underivatized Amino Acids with Online Dual Uv Absorbance, Fluorescence, and Multiple Electrochemical Detection. *J Sep Sci*. 2009;32:949-54.

31. Desai MJ, Armstrong DW. Analysis of Native Amino Acid and Peptide Enantiomers by High-Performance Liquid Chromatography/Atmospheric Pressure Chemical Ionization Mass Spectrometry. *J Mass Spectrom.* 2004;39:177-87.
32. Uutela P, Ketola RA, Piepponen P, Kostianen R. Comparison of Different Amino Acid Derivatives and Analysis of Rat Brain Microdialysates by Liquid Chromatography Tandem Mass Spectrometry. *Anal Chim Acta.* 2009;633:223-31.
33. Salazar C, Armenta JM, Shulaev V. An Uplc-Esi-Ms/Ms Assay Using 6-Aminoquinolyl-N-Hydroxysuccinimidyl Carbamate Derivatization for Targeted Amino Acid Analysis: Application to Screening of Arabidopsis Thaliana Mutants. *Metabolites.* 2012;2:398-428.
34. Pawlowska M, Chen S, Armstrong DW. Enantiomeric Separation of Fluorescent, 6-Aminoquinolyl-N-Hydroxysuccinimidyl Carbamate, Tagged Amino Acids. *J Chromatogr A.* 1993;641:257-65.
35. Armstrong DW. Macrocyclic Antibiotics as a New Class of Chiral Selectors for Liquid Chromatography. *Anal Chem (Wash).* 1994;66:1473-84.
36. Berthod A, Liu Y, Bagwill C, Armstrong DW. Facile Liquid Chromatographic Enantioresolution of Native Amino Acids and Peptides Using a Teicoplanin Chiral Stationary Phase. *J Chromatogr A.* 1996;731:123-37.
37. Cavazzini A, Nadalini G, Dondi F, Gasparrini F, Ciogli A, Villani C. Study of Mechanisms of Chiral Discrimination of Amino Acids and Their Derivatives on a Teicoplanin-Based Chiral Stationary Phase. *J Chromatogr A.* 2004;1031:143-58.
38. Patel DC, Breitbach ZS, Yu J, Nguyen KA, Armstrong DW. Quinine Bonded to Superficially Porous Particles for High-Efficiency and Ultrafast Liquid and Supercritical Fluid Chromatography. *Anal Chim Acta.* 2017;963:164-74.
39. Vauquelin LN, Robiquet PJ. The Discovery of a New Plant Principle in *Asparagus Sativus*. *Ann Chim.* 1806;57:88.
40. Armstrong DW, Gasper MP, Lee SH, Ercal N, Zukowski J. Factors Controlling the Level and Determination of D-Amino Acids in the Urine and Plasma of Laboratory Rodents. *Amino Acids.* 1993;5:299-315.
41. Gal J. Louis Pasteur, Language, and Molecular Chirality. I. Background and Dissymmetry. *Chirality.* 2011;23:1-16.
42. Greenstein JP, Birnbaum SM, Otey MC. Optical and Enzymatic Characterization of Amino Acids. *J Biol Chem.* 1953;204:307-21.
43. Corrigan JJ. D-Amino Acids in Animals. *Science.* 1969;164:142-9.
44. Cline DB. On the Determination of the Physical Origin of Homochirality in Life. *Comments Nucl Part Phys.* 1997;22:131.
45. Aswad DW. Determination of D-Aspartate and L-Aspartate in Amino-Acid Mixtures by High-Performance Liquid-Chromatography after Derivatization with a Chiral Adduct of O-Phthaldialdehyde. *Anal Biochem.* 1984;137:405-9.

46. D'Aniello A. D-Aspartic Acid: An Endogenous Amino Acid with an Important Neuroendocrine Role. *Brain Res Rev.* 2007;53:215-34.
47. Dunlop DS, Neidle A, McHale D, Dunlop DM, Lajtha A. The Presence of Free D-Aspartic Acid in Rodents and Man. *Biochem Biophys Res Commun.* 1986;141:27-32.
48. Armstrong DW, Zukowski J, Ercal N, Gasper M. Stereochemistry of Pimelic Acid Found in the Urine and Plasma of Subjects with Peroxisomal Deficiencies. *J Pharm Biomed Anal.* 1993;11:881-6.
49. Janecka A, Fichna J, Janecki T. Opioid Receptors and Their Ligands. *Curr Top Med Chem.* 2004;4:1-17.
50. Heck SD, Siok CJ, Krapcho KJ, Kelbaugh PR, Thadeio PF, Welch MJ et al. Functional Consequences of Posttranslational Isomerization of Ser(46) in a Calcium-Channel Toxin. *Science.* 1994;266:1065-8.
51. Bathena SP, Huang J, Epstein AA, Gendelman HE, Boska MD, Alnouti Y. Rapid and Reliable Quantitation of Amino Acids and Myo-Inositol in Mouse Brain by High Performance Liquid Chromatography and Tandem Mass Spectrometry. *Journal of Chromatography B-Analytical Technologies in the Biomedical and Life Sciences.* 2012;893:15-20.
52. Lu X, Lu J, Liu C-W, Zhao S-L. Determination of D-Aspartic Acid and D-Glutamic Acid in Midbrain of Parkinson's Disease Mouse by Reversed Phase High Performance Liquid Chromatography. *Chinese Journal of Analytical Chemistry.* 2007;35:1151-4.
53. D'Aniello S, Somorjai I, Garcia-Fernandez J, Topo E, D'Aniello A. D-Aspartic Acid Is a Novel Endogenous Neurotransmitter. *FASEB J.* 2011;25:1014-27.
54. Fuchs SA, Berger R, Klomp LW, de Koning TJ. D-Amino Acids in the Central Nervous System in Health and Disease. *Mol Genet Metab.* 2005;85:168-80.
55. Hashimoto A, Nishikawa T, Hayashi T, Fujii N, Harada K, Oka T et al. The Presence of Free D-Serine in Rat Brain. *FEBS Lett.* 1992;296:33-6.
56. Nagata Y, Horiike K, Maeda T. Distribution of Free D-Serine in Vertebrate Brains. *Brain Res.* 1994;634:291-5.
57. Hashimoto A, Kumashiro S, Nishikawa T, Oka T, Takahashi K, Mito T et al. Embryonic Development and Postnatal Changes in Free D-Aspartate and D-Serine in the Human Prefrontal Cortex. *J Neurochem.* 1993;61:348-51.
58. Moaddel R, Luckenbaugh DA, Xie Y, Villasenor A, Brutsche NE, Machado-Vieira R et al. D-Serine Plasma Concentration Is a Potential Biomarker of (R,S)-Ketamine Antidepressant Response in Subjects with Treatment-Resistant Depression. *Psychopharmacology (Berl).* 2015;232:399-409.
59. Hamase K, Morikawa A, Ohgusu T, Lindner W, Zaitsev K. Comprehensive Analysis of Branched Aliphatic D-Amino Acids in Mammals Using an Integrated

- Multi-Loop Two-Dimensional Column-Switching High-Performance Liquid Chromatographic System Combining Reversed-Phase and Enantioselective Columns. *J Chromatogr A*. 2007;1143:105-11.
60. Hamase K, Miyoshi Y, Ueno K, Han H, Hirano J, Morikawa A et al. Simultaneous Determination of Hydrophilic Amino Acid Enantiomers in Mammalian Tissues and Physiological Fluids Applying a Fully Automated Micro-Two-Dimensional High-Performance Liquid Chromatographic Concept. *J Chromatogr A*. 2010;1217:1056-62.
61. Gage GJ, Kipke DR, Shain W. Whole Animal Perfusion Fixation for Rodents. *J Visualized Exp*. 2012:3564.
62. Sasabe J, Suzuki M, Imanishi N, Aiso S. Activity of D-Amino Acid Oxidase Is Widespread in the Human Central Nervous System. *Frontiers in synaptic neuroscience*. 2014;6:14-.
63. Masuda A, Dohmae N. Amino Acid Analysis of Sub-Picomolar Amounts of Proteins by Precolumn Fluorescence Derivatization with 6-Aminoquinolyl-N-Hydroxysuccinimidyl Carbamate. *Biosci Trends*. 2011;5:231-8.
64. Mangas A, Covenas R, Bodet D, Geffard M, Aguilar LA, Yajeya J. Immunocytochemical Visualization of D-Glutamate in the Rat Brain. *Neuroscience*. 2007;144:654-64.
65. Han H, Miyoshi Y, Koga R, Mita M, Konno R, Hamase K. Changes in D-Aspartic Acid and D-Glutamic Acid Levels in the Tissues and Physiological Fluids of Mice with Various D-Aspartate Oxidase Activities. *J Pharm Biomed Anal*. 2015;116:47-52.
66. Chugh BP, Lerch JP, Yu LX, Pienkowski M, Harrison RV, Henkelman RM et al. Measurement of Cerebral Blood Volume in Mouse Brain Regions Using Micro-Computed Tomography. *NeuroImage*. 2009;47:1312-8.
67. Friedman M. *D-Amino Acids in Chemistry, Life Sciences, and Biotechnology*. 2011.
68. Wolosker H, Blackshaw S, Snyder SH. Serine Racemase: A Glial Enzyme Synthesizing D-Serine to Regulate Glutamate-N-Methyl-D-Aspartate Neurotransmission. *Proceedings of the National Academy of Sciences of the United States of America*. 1999;96:13409-14.
69. Kim PM, Duan X, Huang AS, Liu CY, Ming GL, Song H et al. Aspartate Racemase, Generating Neuronal D-Aspartate, Regulates Adult Neurogenesis. *Proc Natl Acad Sci U S A*. 2010;107:3175-9.
70. Pollegioni L, Piubelli L, Sacchi S, Pilone MS, Molla G. Physiological Functions of D-Amino Acid Oxidases: From Yeast to Humans. *Cell Mol Life Sci*. 2007;64:1373-94.
71. Moreno S, Nardacci R, Cimini A, Ceru MP. Immunocytochemical Localization of D-Amino Acid Oxidase in Rat Brain. *J Neurocytol*. 1999;28:169-85.

72. Ono K, Shishido Y, Park HK, Kawazoe T, Iwana S, Chung SP et al. Potential Pathophysiological Role of D-Amino Acid Oxidase in Schizophrenia: Immunohistochemical and in Situ Hybridization Study of the Expression in Human and Rat Brain. *J Neural Transm.* 2009;116:1335-47.
73. Horiike K, Tojo H, Arai R, Nozaki M, Maeda T. D-Amino-Acid Oxidase Is Confined to the Lower Brain-Stem and Cerebellum in Rat-Brain - Regional Differentiation of Astrocytes. *Brain Res.* 1994;652:297-303.
74. Schell MJ, Cooper OB, Snyder SH. D-Aspartate Localizations Imply Neuronal and Neuroendocrine Roles. *Proceedings of the National Academy of Sciences of the United States of America.* 1997;94:2013-8.
75. Zaar K, Kost HP, Schad A, Volkl A, Baumgart E, Fahimi HD. Cellular and Subcellular Distribution of D-Aspartate Oxidase in Human and Rat Brain. *J Comp Neurol.* 2002;450:272-82.
76. Dixon M, Kleppe K. D-Amino Acid Oxidase .2. Specificity Competitive Inhibition and Reaction Sequence. *Biochim Biophys Acta.* 1965;96:368-&.
77. Madeira C, Freitas ME, Vargas-Lopes C, Wolosker H, Panizzutti R. Increased Brain D-Amino Acid Oxidase (DaaO) Activity in Schizophrenia. *Schizophrenia Research.* 2008;101:76-83.
78. Meldrum BS. Glutamate as a Neurotransmitter in the Brain: Review of Physiology and Pathology. *J Nutr.* 2000;130:1007S-15S.
79. Daikhin Y, Yudkoff M. Compartmentation of Brain Glutamate Metabolism in Neurons and Glia. *J Nutr.* 2000;130:1026S-31S.
80. Shen J, Petersen KF, Behar KL, Brown P, Nixon TW, Mason GF et al. Determination of the Rate of the Glutamate Glutamine Cycle in the Human Brain by in Vivo C-13 Nmr. *Proceedings of the National Academy of Sciences of the United States of America.* 1999;96:8235-40.
81. Wilson WE, Koeppe RE. The Metabolism of D- and L- Glutamic Acid in the Rat. *The Journal of biological chemistry.* 1961;236:365.
82. Pow DV, Crook DK. Direct Immunocytochemical Evidence for the Transfer of Glutamine from Glial Cells to Neurons: Use of Specific Antibodies Directed against TheD-Stereoisomers of Glutamate and Glutamine. *Neuroscience.* 1996;70:295-302.
83. Liang Q, Liu H, Xing H, Jiang Y, Zhang T, Zhang A-H. High-Resolution Mass Spectrometry for Exploring Metabolic Signatures of Sepsis-Induced Acute Kidney Injury. *Rsc Advances.* 2016;6:29863-8.
84. Gorgievskihrisoho M, Colombo JP, Bachmann C. Stimulation of Tryptophan Uptake into Brain Microvessels by D-Glutamine. *Brain Res.* 1986;367:395-7.
85. Davis JL, Cherkin A. D-Glutamine Produces Seizures and Retrograde-Amnesia in the Chick. *Pharmacol Biochem Behav.* 1981;15:367-9.
86. Wolosker H. Nmda Receptor Regulation by D-Serine: New Findings and Perspectives. *Mol Neurobiol.* 2007;36:152-64.

87. Schell MJ. The N-Methyl D-Aspartate Receptor Glycine Site and D-Serine Metabolism: An Evolutionary Perspective. *Philosophical Transactions of the Royal Society B-Biological Sciences*. 2004;359:943-64.
88. D'Aniello A, Di Fiore MM, Fisher GH, Milone A, Seleni A, D'Aniello S et al. Occurrence of D-Aspartic Acid and N-Methyl-D-Aspartic Acid in Rat Neuroendocrine Tissues and Their Role in the Modulation of Luteinizing Hormone and Growth Hormone Release. *FASEB J*. 2000;14:699-714.
89. D'Aniello A, Di Cosmo A, Di Cristo C, Annunziato L, Petrucelli L, Fisher G. Involvement of D-Aspartic Acid in the Synthesis of Testosterone in Rat Testes. *Life Sci*. 1996;59:97-104.
90. Topo E, Soricelli A, Di Maio A, D'Aniello E, Di Fiore MM, D'Aniello A. Evidence for the Involvement of D-Aspartic Acid in Learning and Memory of Rat. *Amino Acids*. 2010;38:1561-9.
91. Errico F, Nistico R, Di Giorgio A, Squillace M, Vitucci D, Galbusera A et al. Free D-Aspartate Regulates Neuronal Dendritic Morphology, Synaptic Plasticity, Gray Matter Volume and Brain Activity in Mammals. *Transl Psychiatry*. 2014;4:e417.
92. Wang WF, Liu G, Yamashita K, Manabe M, Kodama H. Characteristics of Prolinase against Various Iminodipeptides in Erythrocyte Lysates from a Normal Human and a Patient with Prolidase Deficiency. *Clinical Chemistry and Laboratory Medicine*. 2004;42:1102-8.
93. Estin C, Vernadakis A. Primary Glial Cells and Brain Fibroblasts: Interactions in Culture. *Brain Res Bull*. 1986;16:723-31.
94. Matthews DE, Ben-Galim E, Haymond MW, Bier DM. Alloisoleucine Formation in Maple Syrup Urine Disease: Isotopic Evidence for the Mechanism. *Pediatr Res*. 1980;14:854-7.
95. Wendel U, Langenbeck U, Seakins JWT. Interrelation between the Metabolism of L-Isoleucine and L-Allo-Isoleucine in Patients with Maple Syrup Urine Disease. *Pediatric Research*. 1989;25:11-4.
96. Oeckl P, Ferger B. Analysis of Hydroxylation and Nitration Products of D-Phenylalanine for in Vitro and in Vivo Radical Determination Using High-Performance Liquid Chromatography and Photodiode Array Detection. *J Chromatogr B*. 2009;877:1501-8.
97. Iumatov EA, Sarychev EI, Kozlovskii, II, Mineeva MF, Demidov VM, Morozov IS et al. [Enhanced Resistance to Emotional Stress through the Use of D-Phenylalanine]. *Zhurnal vysshei nervnoi deiatelnosti imeni I P Pavlova*. 1991;41:156-61.
98. Berg JM, Tymoczko JL, L. S. *Biochemistry*. New York: W H Freeman; 2002.
99. Wu G. *Amino Acids: Metabolism, Functions, and Nutrition*. *Amino Acids*. 2009;37:1-17.

100. Poncet N, Taylor PM. The Role of Amino Acid Transporters in Nutrition. *Curr Opin Clin Nutr Metab Care*. 2013;16:57-65.
101. Schwartz JH. Neurotransmitters A2 - Ramachandran, V.S. *Encyclopedia of the Human Brain*. New York: Academic Press; 2002. p. 601-11.
102. Armstrong DW, Gasper M, Lee SH, Zukowski J, Ercal N. D-Amino Acid Levels in Human Physiological Fluids. *Chirality*. 1993;5:375-8.
103. Brückner H, Haasmann S, Friedrich A. Quantification of D-Amino Acids in Human Urine Using Gc-Ms and Hplc. *Amino Acids*. 1994;6:205-11.
104. Armstrong DW, Zukowski J, Ercal N, Gasper M. Stereochemistry of Pipecolic Acid Found in the Urine and Plasma of Subjects with Peroxisomal Deficiencies. *J Pharm Biomed Anal*. 1993;11:881-6.
105. Armstrong DW, Rundlett KL, Chen J-R. Evaluation of the Macrocyclic Antibiotic Vancomycin as a Chiral Selector for Capillary Electrophoresis. *Chirality*. 1994;6:496-509.
106. Desai MJ, Armstrong DW. Analysis of Native Amino Acid and Peptide Enantiomers by High-Performance Liquid Chromatography/Atmospheric Pressure Chemical Ionization Mass Spectrometry. *J Mass Spectrom*. 2004;39:177-87.
107. Molnár-Perl I. Quantitation of Amino Acids and Amines in the Same Matrix by High-Performance Liquid Chromatography, Either Simultaneously or Separately. *J Chromatogr A*. 2003;987:291-309.
108. Desai MJ, Armstrong DW. Analysis of Derivatized and Underivatized Theanine Enantiomers by High-Performance Liquid Chromatography/Atmospheric Pressure Ionization-Mass Spectrometry. *Rapid Commun Mass Spectrom*. 2004;18:251-6.
109. Weatherly CA, Du S, Parpia C, Santos PT, Hartman AL, Armstrong DW. D-Amino Acid Levels in Perfused Mouse Brain Tissue and Blood: A Comparative Study. *ACS Chem Neurosci*. 2017;8:1251-61.
110. Einarsson S, Josefsson B, Lagerkvist S. Determination of Amino Acids with 9-Fluorenylmethyl Chloroformate and Reversed-Phase High-Performance Liquid Chromatography. *J Chromatogr A*. 1983;282:609-18.
111. Lindroth P, Mopper K. High Performance Liquid Chromatographic Determination of Subpicomole Amounts of Amino Acids by Precolumn Fluorescence Derivatization with O-Phthaldialdehyde. *Anal Chem*. 1979;51:1667-74.
112. Graser TA, Godel HG, Albers S, Földi P, Fürst P. An Ultra Rapid and Sensitive High-Performance Liquid Chromatographic Method for Determination of Tissue and Plasma Free Amino Acids. *Anal Biochem*. 1985;151:142-52.
113. Watanabe Y, Imai K. Pre-Column Labelling for High-Performance Liquid Chromatography of Amino Acids with 7-Fluoro-4-Nitrobenzo-2-Oxa-1,3-Diazole and Its Application to Protein Hydrolysates. *J Chromatogr A*. 1982;239:723-32.

114. Imai K, Watanabe Y. Fluorimetric Determination of Secondary Amino Acids by 7-Fluoro-4-Nitrobenzo-2-Oxa-1,3-Diazole. *Anal Chim Acta*. 1981;130:377-83.
115. Bank RA, Jansen EJ, Beekman B, te Koppele JM. Amino Acid Analysis by Reverse-Phase High-Performance Liquid Chromatography: Improved Derivatization and Detection Conditions with 9-Fluorenylmethyl Chloroformate. *Anal Biochem*. 1996;240:167-76.
116. Gartenmann K, Kochhar S. Short-Chain Peptide Analysis by High-Performance Liquid Chromatography Coupled to Electrospray Ionization Mass Spectrometer after Derivatization with 9-Fluorenylmethyl Chloroformate. *J Agric Food Chem*. 1999;47:5068-71.
117. Soukup-Hein RJ, Remsburg JW, Dasgupta PK, Armstrong DW. A General, Positive Ion Mode ESI-MS Approach for the Analysis of Singly Charged Inorganic and Organic Anions Using a Dicationic Reagent. *Anal Chem*. 2007;79:7346-52.
118. Soukup-Hein RJ, Remsburg JW, Breitbach ZS, Sharma PS, Payagala T, Wanigasekara E et al. Evaluating the Use of Tricationic Reagents for the Detection of Doubly Charged Anions in the Positive Mode by ESI-MS. *Anal Chem*. 2008;80:2612-6.
119. Dodbiba E, Breitbach ZS, Wanigasekara E, Payagala T, Zhang X, Armstrong DW. Detection of Nucleotides in Positive-Mode Electrospray Ionization Mass Spectrometry Using Multiply-Charged Cationic Ion-Pairing Reagents. *Anal Bioanal Chem*. 2010;398:367-76.
120. Dodbiba E, Xu C, Payagala T, Wanigasekara E, Moon MH, Armstrong DW. Use of Ion Pairing Reagents for Sensitive Detection and Separation of Phospholipids in the Positive Ion Mode LC-ESI-MS. *Analyst*. 2011;136:1586-93.
121. Zhang X, Wanigasekara E, Breitbach ZS, Dodbiba E, Armstrong DW. Evaluation of Tetracationic Salts as Gas-Phase Ion-Pairing Agents for the Detection of Trivalent Anions in Positive Mode Electrospray Ionization Mass Spectrometry. *Rapid Commun Mass Spectrom*. 2010;24:1113-23.
122. Warnke MM, Breitbach ZS, Dodbiba E, Wanigasekara E, Zhang X, Sharma P et al. The Evaluation and Comparison of Trigonal and Linear Tricationic Ion-Pairing Reagents for the Detection of Anions in Positive Mode ESI-MS. *J Am Soc Mass Spectrom*. 2009;20:529-38.
123. Breitbach ZS, Berthod A, Huang K, Armstrong DW. Mass Spectrometric Detection of Trace Anions: The Evolution of Paired-Ion Electrospray Ionization (PESI). *Mass Spectrom Rev*. 2016;35:201-18.
124. Breitbach ZS, Warnke MM, Wanigasekara E, Zhang X, Armstrong DW. Evaluation of Flexible Linear Tricationic Salts as Gas-Phase Ion-Pairing Reagents for the Detection of Divalent Anions in Positive Mode ESI-MS. *Anal Chem*. 2008;80:8828-34.

125. Guo H, Dolzan MD, Spudeit DA, Xu C, Breitbach ZS, Sreenivasan U et al. Sensitive Detection of Anionic Metabolites of Drugs by Positive Ion Mode Hplc-Piesi-Ms. *Int J Mass spectrom.* 2015;389:14-25.
126. Guo H, Riter LS, Wujcik CE, Armstrong DW. Quantitative Analysis of Dicamba Residues in Raw Agricultural Commodities with the Use of Ion-Pairing Reagents in Lc-Esi-Ms/Ms. *Talanta.* 2016;149:103-9.
127. Breitbach ZS, Wanigasekara E, Dodbiba E, Schug KA, Armstrong DW. Mechanisms of Esi-Ms Selectivity and Sensitivity Enhancements When Detecting Anions in the Positive Mode Using Cationic Pairing Agents. *Anal Chem.* 2010;82:9066-73.
128. Xu C, Guo H, Breitbach ZS, Armstrong DW. Mechanism and Sensitivity of Anion Detection Using Rationally Designed Unsymmetrical Dications in Paired Ion Electrospray Ionization Mass Spectrometry. *Anal Chem.* 2014;86:2665-72.
129. Lopes NP, Stark CBW, Gates PJ, Staunton J. Fragmentation Studies on Monensin a by Sequential Electrospray Mass Spectrometry. *Analyst.* 2002;127:503-6.
130. Grimalt S, Pozo ÓJ, Marín JM, Sancho JV, Hernández F. Evaluation of Different Quantitative Approaches for the Determination of Noneasily Ionizable Molecules by Different Atmospheric Pressure Interfaces Used in Liquid Chromatography Tandem Mass Spectrometry: Abamectin as Case of Study. *J Am Soc Mass Spectrom.* 2005;16:1619-30.
131. Guo H, Breitbach ZS, Armstrong DW. Reduced Matrix Effects for Anionic Compounds with Paired Ion Electrospray Ionization Mass Spectrometry. *Anal Chim Acta.* 2016;912:74-84.
132. Remsburg JW, Soukup-Hein RJ, Crank JA, Breitbach ZS, Payagala T, Armstrong DW. Evaluation of Dicationic Reagents for Their Use in Detection of Anions Using Positive Ion Mode Esi-Ms Via Gas Phase Ion Association. *J Am Soc Mass Spectrom.* 2008;19:261-9.
133. Xu C, Pinto EC, Armstrong DW. Separation and Sensitive Determination of Sphingolipids at Low Femtomole Level by Using Hplc-Piesi-Ms/Ms. *Analyst.* 2014;139:4169-75.
134. Vatansever B, Lahrichi SL, Thiocone A, Salluce N, Mathieu M, Grouzmann E et al. Comparison between a Linear Ion Trap and a Triple Quadruple Ms in the Sensitive Detection of Large Peptides at Femtomole Amounts on Column. *J Sep Sci.* 2010;33:2478-88.
135. Macchi FD, Shen FJ, Keck RG, Harris RJ. Amino Acid Analysis, Using Postcolumn Ninhydrin Detection, in a Biotechnology Laboratory. In: Cooper C, Packer N, Williams K, editors. *Amino Acid Analysis Protocols.* Totowa, NJ: Humana Press; 2000. p. 9-30.

136. Glew RH, Melah G, El-Nafaty AI, Brandt Y, Morris D, VanderJagt DJ. Plasma and Urinary Free Amino Acid Concentrations in Preeclamptic Women in Northern Nigeria. *Clin Chim Acta*. 2004;342:179-85.
137. Robinson T. D-Amino Acids in Higher Plants. *Life Sci*. 1976;19:1097-102.
138. Kullman JP, Chen X, Armstrong DW. Evaluation of the Enantiomeric Composition of Amino Acids in Tobacco. *Chirality*. 1999;11:669-73.
139. Ollivaux C, Soyeux D, Toullec J-Y. Biogenesis of D-Amino Acid Containing Peptides/Proteins: Where, When and How? *J Pept Sci*. 2014;20:595-612.
140. Holden K, Hartman AL. D-Leucine: Evaluation in an Epilepsy Model. *Epilepsy & Behavior*. 2018;78:202-9.
141. Weatherly CA, Du S, Parpia C, Santos PT, Hartman AL, Armstrong DW. D-Amino Acid Levels in Perfused Mouse Brain Tissue and Blood: A Comparative Study. *ACS Chem Neurosci*. 2017;8:1251-61.
142. Yoshimura T, Esak N. Amino Acid Racemases: Functions and Mechanisms. *J Biosci Bioeng*. 2003;96:103-9.
143. Sacchi S, Caldinelli L, Cappelletti P, Pollegioni L, Molla G. Structure-Function Relationships in Human D-Amino Acid Oxidase. *Amino Acids*. 2012;43:1833-50.
144. Morikawa A, Hamase K, Inoue T, Konno R, Niwa A, Zaitso K. Determination of Free D-Aspartic Acid, D-Serine and D-Alanine in the Brain of Mutant Mice Lacking D-Amino-Acid Oxidase Activity. *J Chromatogr B*. 2001;757:119-25.
145. Sasaki M, Konno R, Nihio M, Niwa A, Yasumura Y, Enami J. A Single-Base-Pair Substitution Abolishes D-Amino-Acid Oxidase Activity in the Mouse. *Biochimica et Biophysica Acta (BBA) - Molecular Basis of Disease*. 1992;1139:315-8.
146. Huxtable RJ. Physiological Actions of Taurine. *Physiol Rev*. 1992;72:101-63.
147. Kontro P, Marnela KM, Oja SS. Gaba, Taurine and Hypotaurine in Developing Mouse Brain. *Acta physiologica Scandinavica Supplementum*. 1984;537:71-4.
148. Petroff OA. Gaba and Glutamate in the Human Brain. *Neuroscientist*. 2002;8:562-73.
149. Armstrong DW, Liu Y, Ekborgott KH. A Covalently Bonded Teicoplanin Chiral Stationary Phase for Hplc Enantioseparations. *Chirality*. 1995;7:474-97.
150. Karlsson C, Karlsson L, Armstrong DW, Owens PK. Evaluation of a Vancomycin Chiral Stationary Phase in Capillary Electrochromatography Using Polar Organic and Reversed-Phase Modes. *Anal Chem*. 2000;72:4394-401.
151. Péter A, Vékes E, Armstrong DW. Effects of Temperature on Retention of Chiral Compounds on a Ristocetin a Chiral Stationary Phase. *J Chromatogr A*. 2002;958:89-107.

152. US-FDA. Guidance for Industry-Bioanalytic Method Validation. 2001.
153. Miyoshi Y, Hamase K, Tojo Y, Mita M, Konno R, Zaitso K. Determination of D-Serine and D-Alanine in the Tissues and Physiological Fluids of Mice with Various D-Amino-Acid Oxidase Activities Using Two-Dimensional High-Performance Liquid Chromatography with Fluorescence Detection. *J Chromatogr B*. 2009;877:2506-12.
154. Suzuki S, Mori A. Regional Distribution of Tyrosine, Tryptophan, and Their Metabolites in the Brain of Epileptic El Mice. *Neurochem Res*. 1992;17:693-8.
155. Albrecht J, Sidoryk-Wegrzynowicz M, Zielinska M, Aschner M. Roles of Glutamine in Neurotransmission. *Neuron glia biology*. 2010;6:263-76.
156. Wu J-Y, Prentice H. Role of Taurine in the Central Nervous System. *J Biomed Sci*. 2010;17:S1-S.
157. Okamoto K, Kimura H, Sakai Y. Taurine-Induced Increase of the Cl-Conductance of Cerebellar Purkinje Cell Dendrites in Vitro. *Brain Res*. 1983;259:319-23.
158. Le Floc'h N, Otten W, Merlot E. Tryptophan Metabolism, from Nutrition to Potential Therapeutic Applications. *Amino Acids*. 2011;41:1195-205.
159. Pardridge WM. Blood-Brain Barrier Carrier-Mediated Transport and Brain Metabolism of Amino Acids. *Neurochem Res*. 1998;23:635-44.
160. Fernstrom JD, Wurtman RJ. Brain Serotonin Content: Physiological Regulation by Plasma Neutral Amino Acids. *Science*. 1972;178:414-6.
161. Silber BY, Schmitt JAJ. Effects of Tryptophan Loading on Human Cognition, Mood, and Sleep. *Neurosci Biobehav Rev*. 2010;34:387-407.
162. Pritchett D, Hasan S, Tam SK, Engle SJ, Brandon NJ, Sharp T et al. D-Amino Acid Oxidase Knockout (Dao^{-/-}) Mice Show Enhanced Short-Term Memory Performance and Heightened Anxiety, but No Sleep or Circadian Rhythm Disruption. *Eur J Neurosci*. 2015;41:1167-79.
163. Frick A, Åhs F, Engman J, et al. Serotonin Synthesis and Reuptake in Social Anxiety Disorder: A Positron Emission Tomography Study. *JAMA Psychiatry*. 2015;72:794-802.
164. Navarro E, Alonso SJ, Martin FA, Castellano MA. Toxicological and Pharmacological Effects of D-Arginine. *Basic Clin Pharmacol Toxicol*. 2005;97:149-54.
165. Adage T, Trillat A-C, Quattropani A, Perrin D, Cavarec L, Shaw J et al. In Vitro and in Vivo Pharmacological Profile of As057278, a Selective D-Amino Acid Oxidase Inhibitor with Potential Anti-Psychotic Properties. *European Neuropsychopharmacology*. 2008;18:200-14.
166. Hanahan D, Weinberg Robert A. Hallmarks of Cancer: The Next Generation. *Cell*. 2011;144:646-74.
167. Warburg O, Wind F, Negelein E. The Metabolism of Tumors in the Body *The Journal of General Physiology*. 1927;8:519-30.

168. Eagle H, Oyama VI, Levy M, Horton CL, Fleischman R. The Growth Response of Mammalian Cells in Tissue Culture to L-Glutamine and L-Glutamic Acid. *J Biol Chem.* 1956;218:607-16.
169. Di Fiore MM, Santillo A, Chieffi Baccari G. Current Knowledge of D-Aspartate in Glandular Tissues. *Amino Acids.* 2014;46:1805-18.
170. Hosios AM, Hecht VC, Danai LV, Johnson MO, Rathmell JC, Steinhauser ML et al. Amino Acids Rather Than Glucose Account for the Majority of Cell Mass in Proliferating Mammalian Cells. *Dev Cell.* 2016;36:540-9.
171. Cheng F, Wang Z, Huang Y, Duan Y, Wang X. Investigation of Salivary Free Amino Acid Profile for Early Diagnosis of Breast Cancer with Ultra Performance Liquid Chromatography-Mass Spectrometry. *Clin Chim Acta.* 2015;447:23-31.
172. Bhutia YD, Babu E, Ramachandran S, Ganapathy V. Amino Acid Transporters in Cancer and Their Relevance to "Glutamine Addiction": Novel Targets for the Design of a New Class of Anticancer Drugs. *Cancer Res.* 2015;75:1782-8.
173. Bi X, Henry CJ. Plasma-Free Amino Acid Profiles Are Predictors of Cancer and Diabetes Development. *Nutrition & diabetes.* 2017;7:e249.
174. DeBerardinis RJ, Chandel NS. Fundamentals of Cancer Metabolism. *Science advances.* 2016;2:e1600200.
175. Du S, Wang Y, Weatherly CA, Holden K, Armstrong DW. Variations of L- and D-Amino Acid Levels in the Brain of Wild-Type and Mutant Mice Lacking D-Amino Acid Oxidase Activity. *Anal Bioanal Chem.* 2018;410:2971-9.
176. Vinci V, Parekh SR. *Handbook of Industrial Cell Culture: Mammalian, Microbial, and Plant Cells.* vol Book, Whole. Totowa, N.J: Humana Press; 2003.
177. Labuschagne CF, van den Broek NJ, Mackay GM, Vousden KH, Maddocks OD. Serine, but Not Glycine, Supports One-Carbon Metabolism and Proliferation of Cancer Cells. *Cell reports.* 2014;7:1248-58.
178. Maddocks Oliver D, Labuschagne Christiaan F, Adams Peter D, Vousden Karen H. Serine Metabolism Supports the Methionine Cycle and DNA/Rna Methylation through De Novo Atp Synthesis in Cancer Cells. *Mol Cell.* 2016;61:210-21.
179. Snell K, Natsumeda Y, Weber G. The Modulation of Serine Metabolism in Hepatoma 3924a During Different Phases of Cellular Proliferation in Culture. *Biochem J.* 1987;245:609-12.
180. Rabinovich S, Adler L, Yizhak K, Sarver A, Silberman A, Agron S et al. Diversion of Aspartate in Ass1-Deficient Tumors Fosters De Novo Pyrimidine Synthesis. *Nature.* 2015;527:379-83.
181. Geck RC, Toker A. Nonessential Amino Acid Metabolism in Breast Cancer. *Advances in biological regulation.* 2016;62:11-7.

182. Wolosker H, D'Aniello A, Snyder SH. D-Aspartate Disposition in Neuronal and Endocrine Tissues: Ontogeny, Biosynthesis and Release. *Neuroscience*. 2000;100:183-9.
183. De Miranda J, Santoro A, Engelender S, Wolosker H. Human Serine Racemase: Molecular Cloning, Genomic Organization and Functional Analysis. *Gene*. 2000;256:183-8.
184. North WG, Gao G, Memoli V, Pang RHL, Lynch L. Breast Cancer Expresses Functional Nmda Receptors. *Breast cancer research and treatment*. 2010;122:307-14.
185. Hatanaka T, Huang W, Nakanishi T, Bridges CC, Smith SB, Prasad PD et al. Transport of D-Serine Via the Amino Acid Transporter Atb(0,+) Expressed in the Colon. *Biochem Biophys Res Commun*. 2002;291:291-5.
186. Foster AC, Farnsworth J, Lind GE, Li YX, Yang JY, Dang V et al. D-Serine Is a Substrate for Neutral Amino Acid Transporters Asct1/Slc1a4 and Asct2/Slc1a5, and Is Transported by Both Subtypes in Rat Hippocampal Astrocyte Cultures. *PLoS One*. 2016;11:e0156551.
187. Hyde R, Taylor PM, Hundal HS. Amino Acid Transporters: Roles in Amino Acid Sensing and Signalling in Animal Cells. *Biochem J*. 2003;373:1-18.
188. Krall AS, Xu S, Graeber TG, Braas D, Christofk HR. Asparagine Promotes Cancer Cell Proliferation through Use as an Amino Acid Exchange Factor. *Nature communications*. 2016;7:11457.
189. Blennow K, de Leon MJ, Zetterberg H. Alzheimer's Disease. *Lancet*. 2006;368:387-403.
190. Murphy MP, LeVine H, 3rd. Alzheimer's Disease and the Amyloid-Beta Peptide. *J Alzheimers Dis*. 2010;19:311-23.
191. Gouras GK, Olsson TT, Hansson O. B-Amyloid Peptides and Amyloid Plaques in Alzheimer's Disease. *Neurotherapeutics*. 2015;12:3-11.
192. Duyckaerts C, Delatour B, Potier MC. Classification and Basic Pathology of Alzheimer Disease. *Acta neuropathologica*. 2009;118:5-36.
193. Portelius E, Westman-Brinkmalm A, Zetterberg H, Blennow K. Determination of B-Amyloid Peptide Signatures in Cerebrospinal Fluid Using Immunoprecipitation-Mass Spectrometry. *Journal of Proteome Research*. 2006;5:1010-6.
194. Piccini A, Russo C, Gliozzi A, Relini A, Vitali A, Borghi R et al. Beta-Amyloid Is Different in Normal Aging and in Alzheimer Disease. *J Biol Chem*. 2005;280:34186-92.
195. Roher AE, Lowenson JD, Clarke S, Wolkow C, Wang R, Cotter RJ et al. Structural Alterations in the Peptide Backbone of Beta-Amyloid Core Protein May Account for Its Deposition and Stability in Alzheimer's Disease. *J Biol Chem*. 1993;268:3072-83.

196. Shimizu T, Watanabe A, Ogawara M, Mori H, Shirasawa T. Isoaspartate Formation and Neurodegeneration in Alzheimer's Disease. *Arch Biochem Biophys*. 2000;381:225-34.
197. Kaneko I, Morimoto K, Kubo T. Drastic Neuronal Loss in Vivo by Beta-Amyloid Racemized at Ser(26) Residue: Conversion of Non-Toxic [D-Ser(26)]Beta-Amyloid 1-40 to Toxic and Proteinase-Resistant Fragments. *Neuroscience*. 2001;104:1003-11.
198. Shimizu T, Fukuda H, Murayama S, Izumiyama N, Shirasawa T. Isoaspartate Formation at Position 23 of Amyloid Beta Peptide Enhanced Fibril Formation and Deposited onto Senile Plaques and Vascular Amyloids in Alzheimer's Disease. *J Neurosci Res*. 2002;70:451-61.
199. Kubo T, Kumagae Y, Miller CA, Kaneko I. Beta-Amyloid Racemized at the Ser26 Residue in the Brains of Patients with Alzheimer Disease: Implications in the Pathogenesis of Alzheimer Disease. *J Neuropathol Exp Neurol*. 2003;62:248-59.
200. Armstrong DW, Kullman JP, Chen X, Rowe M. Composition and Chirality of Amino Acids in Aerosol/Dust from Laboratory and Residential Enclosures. *Chirality*. 2001;13:153-8.
201. Kuo YM, Emmerling MR, Woods AS, Cotter RJ, Roher AE. Isolation, Chemical Characterization, and Quantitation of a Beta 3-Pyroglutamyl Peptide from Neuritic Plaques and Vascular Amyloid Deposits. *Biochem Biophys Res Commun*. 1997;237:188-91.
202. Kummer MP, Heneka MT. Truncated and Modified Amyloid-Beta Species. *Alzheimer's Research & Therapy*. 2014;6:28.
203. Tugyi R, Uray K, Ivan D, Fellingner E, Perkins A, Hudecz F. Partial D-Amino Acid Substitution: Improved Enzymatic Stability and Preserved Ab Recognition of a Muc2 Epitope Peptide. *Proc Natl Acad Sci U S A*. 2005;102:413-8.
204. Sievers SA, Karanicolas J, Chang HW, Zhao A, Jiang L, Zirafi O et al. Structure-Based Design of Non-Natural Amino-Acid Inhibitors of Amyloid Fibril Formation. *Nature*. 2011;475:96-100.
205. Garton M, Nim S, Stone TA, Wang KE, Deber CM, Kim PM. Method to Generate Highly Stable D-Amino Acid Analogs of Bioactive Helical Peptides Using a Mirror Image of the Entire Pdb. 2018;115:1505-10.
206. Fujii N, Takata T, Fujii N. Quantitative Analysis of Isomeric (L-Alpha-, L-Beta-, D-Alpha-, D-Beta-) Aspartyl Residues in Proteins from Elderly Donors. *J Pharm Biomed Anal*. 2015;116:25-33.
207. Maeda H, Takata T, Fujii N, Sakaue H, Nirasawa S, Takahashi S et al. Rapid Survey of Four Asp Isomers in Disease-Related Proteins by Lc-Ms Combined with Commercial Enzymes. *Anal Chem*. 2015;87:561-8.

208. Hurtado PP, O'Connor PB. Differentiation of Isomeric Amino Acid Residues in Proteins and Peptides Using Mass Spectrometry. *Mass Spectrom Rev.* 2012;31:609-25.
209. Zheng X, Deng L, Baker ES, Ibrahim YM, Petyuk VA, Smith RD. Distinguishing D- and L-Aspartic and Isoaspartic Acids in Amyloid Beta Peptides with Ultrahigh Resolution Ion Mobility Spectrometry. *Chemical communications (Cambridge, England)*. 2017;53:7913-6.
210. Lehmann WD, Schlosser A, Erben G, Pipkorn R, Bossemeyer D, Kinzel V. Analysis of Isoaspartate in Peptides by Electrospray Tandem Mass Spectrometry. *Protein Sci.* 2000;9:2260-8.
211. Gonzalez LJ, Shimizu T, Satomi Y, Betancourt L, Besada V, Padron G et al. Differentiating Alpha- and Beta-Aspartic Acids by Electrospray Ionization and Low-Energy Tandem Mass Spectrometry. *Rapid Commun Mass Spectrom.* 2000;14:2092-102.
212. Cournoyer JJ, Pittman JL, Ivleva VB, Fallows E, Waskell L, Costello CE et al. Deamidation: Differentiation of Aspartyl from Isoaspartyl Products in Peptides by Electron Capture Dissociation. *Protein Sci.* 2005;14:452-63.
213. Sargaeva NP, Lin C, O'Connor PB. Identification of Aspartic and Isoaspartic Acid Residues in Amyloid Beta Peptides, Including Abeta1-42, Using Electron-Ion Reactions. *Anal Chem.* 2009;81:9778-86.
214. Tao Y, Quebbemann NR, Julian RR. Discriminating D-Amino Acid-Containing Peptide Epimers by Radical-Directed Dissociation Mass Spectrometry. *Anal Chem.* 2012;84:6814-20.
215. Wu C, Siems WF, Klasmeier J, Hill HH. Separation of Isomeric Peptides Using Electrospray Ionization/High-Resolution Ion Mobility Spectrometry. *Anal Chem.* 2000;72:391-5.
216. de Magalhães MTQ, Barbosa EA, Prates MV, Verly RM, Munhoz VHO, de Araújo IE et al. Conformational and Functional Effects Induced by D- and L-Amino Acid Epimerization on a Single Gene Encoded Peptide from the Skin Secretion of *Hypsiboas punctatus*. *PloS one.* 2013;8:e59255-e.
217. Jia C, Lietz CB, Yu Q, Li L. Site-Specific Characterization of (D)-Amino Acid Containing Peptide Epimers by Ion Mobility Spectrometry. *Anal Chem.* 2014;86:2972-81.
218. Li G, DeLaney K, Li L. Molecular Basis for Chirality-Regulated A β Self-Assembly and Receptor Recognition Revealed by Ion Mobility-Mass Spectrometry. *Nature communications.* 2019;10:5038.
219. Nagy G, Kedia K, Attah IK, Garimella SVB, Ibrahim YM. Separation of Beta-Amyloid Tryptic Peptide Species with Isomerized and Racemized L-Aspartic Residues with Ion Mobility in Structures for Lossless Ion Manipulations. 2019;91:4374-80.

220. Zhang B, Soukup R, Armstrong DW. Selective Separations of Peptides with Sequence Deletions, Single Amino Acid Polymorphisms, and/or Epimeric Centers Using Macrocyclic Glycopeptide Liquid Chromatography Stationary Phases. *J Chromatogr A*. 2004;1053:89-99.
221. Wimalasinghe RM, Breitbach ZS, Lee JT, Armstrong DW. Separation of Peptides on Superficially Porous Particle Based Macrocyclic Glycopeptide Liquid Chromatography Stationary Phases: Consideration of Fast Separations. *Anal Bioanal Chem*. 2017;409:2437-47.

Biographical Information

Siqi Du was born in Changchun, China. She received her Bachelor's Degree in Bioengineering from Huaihai Institute of Technology (now Jiangsu Ocean University) in 2013. Siqi Du obtained her Master of Science in Biochemistry at the University of Texas at Arlington under the supervision of Dr. Johnson-Winters in August 2015. The research work was focused on enzyme purification and enzyme kinetics.

She obtained her Ph.D in Analytical Chemistry at The University of Texas at Arlington under the supervision of Prof. Daniel W. Armstrong. Her research focuses on method development and validation for rapid, sensitive and robust analysis of amino acid and peptides in biological systems by using HPLC and LC-MS/MS. She plans to continue her research with Dr. Armstrong as Postdoc.